Report on the CCT Supplementary Comparison S1 of Infrared Spectral Normal Emittance/Emissivity

March 2016

Leonard Hanssen[1,7], B. Wilthan[1,2], Christian Monte[3], Jörg Hollandt[3], Jacques Hameury[4], Jean-Remy Filtz[4], Ferruccio Girard[5], Mauro Battuello[5], Juntaro Ishii[6]

[1] National Institute of Standards and Technology (NIST), Sensor Science Division, Gaithersburg, MD, USA

[2] currently with NIST, Applied Chemical and Materials Division, Boulder, CO, USA

[3] Physikalisch-Technische Bundesanstalt (PTB), Temperature and Synchrotron Divison, Berlin, Germany

[4] Laboratoire National de Métrologie et d'Essais (LNE), Photonics and Energy Division, Trappes, France

[5] Instituto Nazionale di Ricerca Metrologica (INRIM), Division of Metrology for Quality of Life, Torino, Italy

[6] National Metrology Institute of Japan (NMIJ), National Institute of Advanced Industrial Science and Technology (AIST), Tsukuba, Japan

[7] To whom correspondence should be addressed: E-mail: hanssen@nist.gov

ABSTRACT

The National Measurement Institutes (NMIs) of the United States, Germany, France, Italy and Japan, have joined in an inter-laboratory comparison of their infrared spectral emittance scales. This action is part of a series of supplementary inter-laboratory comparisons (including thermal conductivity and thermal diffusivity) sponsored by the Consultative Committee on Thermometry (CCT) Task Group on Thermophysical Quantities (TG-ThQ). The objective of this collaborative work is to strengthen the major operative National Measurement Institutes' infrared spectral emittance scales and consequently the consistency of radiative properties measurements carried out worldwide. The comparison has been performed over a spectral range of 2 μm to 14 μm, and a temperature range from 23 °C to 800 °C. Artefacts included in the comparison are potential standards: oxidized inconel, boron nitride, and silicon carbide. The measurement instrumentation and techniques used for emittance scales are unique for each NMI, including the temperature ranges covered as well as the artefact sizes required. For example, all three common types of spectral instruments are represented: dispersive grating monochromator, Fourier transform and filter-based spectrometers. More than 2000 data points (combinations of material, wavelength and temperature) were compared. Ninety-eight percent (98%) of the data points were in agreement, with differences to weighted mean values less than the expanded uncertainties calculated from the individual NMI uncertainties and uncertainties related to the comparison process.

Keywords: Emittance; Emissivity; Infrared; Standards; Comparison; Spectral.

TABLE OF CONTENTS

1 INTRODUCTION

Infrared emittance is an important property for a wide variety of both thermal and optical applications. These include non-contact temperature measurements for industrial materials processing, energy conservation, structural defect detection, infrared signature detection and reduction, etc. In addition, emittance data is critical for thermal modeling of instrumentation from cryogenic radiometers to spacecraft payloads. A number of the major National Measurement Institutes (NMIs) have developed measurement capabilities and standards to support industrial needs in these areas for accurate emittance measurements. In recent decades, several inter-laboratory comparisons of infrared spectral emittance capabilities of NMIs have been conducted, including the Laboratoire National de Métrologie et d'Essais (LNE) of France, National Physical Laboratory (NPL) of the United Kingdom, the CNR Instituto di Metrologia "G. Colonnetti" (IMGC) of Italy (now the Instituto Nazionale di Ricerca Metrologica (INRIM)), and Physikalisch-Technische Bundesanstalt (PTB) of Germany. All but one of these have been bilateral or involved only two NMIs.[1,2,3] The previous work and comparisons have been important to evaluate the sources of error and develop comprehensive uncertainty budgets and have helped to form a basis upon which to pursue a more comprehensive comparison. The CCT – WG 9 was formed in 2003 to help identify critical thermophysical quantities for which there was a need for comparisons (i.e. in order to strengthen the major NMI's infrared spectral emittance scales in support of radiative properties measurements around the world. The specific quantity being compared is the normal directional spectral emittance[i,ii], defined by:

$$\epsilon(\lambda, T, 0°) = L_\lambda(\lambda, T, 0°)/B_\lambda(\lambda, T, 0°) \quad , \qquad (1)$$

where λ is the wavelength, T is the artefact temperature, $L_\lambda(\lambda,T,0°)$ is the spectral radiance per unit wavelength of the artefact in the normal direction, and $B_\lambda(\lambda,T,0°)$ is the spectral radiance per unit wavelength of the ideal blackbody in the normal direction as given by Planck's Law.

Table 1 shows a list identifying all of the variables contained in this report, along with brief description and locations where they are used.

The comparison was designed to be comprehensive, with the ranges of wavelength (2 μm to 14 μm) and temperature (23 °C to 800 °C) selected to span the NMIs' capabilities to the extent that there would be results from at least two NMIs for each data point. Three materials with a range of emittance values, and being considered as potential standards, were selected for inclusion in the comparison: oxidized Inconel (OxIn), boron nitride (BN), and silicon carbide (SiC).

---

[i] Note that for materials the term "emissivity" is an equivalent term, used perhaps more often than "emittance". However, the pilot laboratory prefers consistency with the terminology of the larger family of properties: transmittance, reflectance and absorptance, reserving the term "emissivity" for use in the description of blackbody sources. Standards dictionaries have not exclusively selected one over the other. For internal consistency, other than in the title, this note, and references, when discussing samples, we use only one term, "emittance", throughout this report.

[ii] From this point on, for simplicity we will assume but not specifically denote the normal direction (0°).

Table 1. List of variables and subscripts

Variable	Description	In Eqn.
ε	Normal directional spectral emittance	(1), (3), (4), (6), (7), (8), (13), (15), (16), (17)
λ	Wavelength	global
T	Temperature	global
L_λ	Spectral radiance of the artefact in the normal direction	(1), (4)
B	Spectral radiance of the ideal blackbody as given by Planck's Law	(1), (2), (3), (6), (10), (11)
ν	Wavenumber	global
L_v	Spectral radiance	(2), (3)
C	Complex spectrum	(2)
ϕ_L	Phase	(2)
V	Radiometric signal	(4)
L	Spectral radiance	(5)
f	Correction factor	(7), (8), (11)
n	Number of participants	(8)
RT	Room temperature	(8)
g	Correction factor	(9), (10), (12)
h	Weighting factor	(9)
ε'	RT-normalized emittance	(7), (9), (10), (12)
ε''	Equivalent emittance for comparison	(10),(12), (13), (14), (15), (16), (17)
τ	Spectral transmittance of filter	(10), (11)
$\Re$	Relative spectral responsivity of the detector	(10), (11)
f_i	Correction factor for LNE values (i=2)	(11)
u	Standard uncertainty	(13), (14), (15), (17)
D	Relative deviations from CRV	(16), (18)
U	Expanded uncertainty for D	(17), (18)
k	Coverage factor for expanded uncertainty	(17)
E	Error function	(18)

Subscript	Description
0	Cold
h	Hot
ambient	Surrounding (room)
s	Sample
r	Reference
c	Central
BB	Blackbody
D	Detector
E	Environment
i, j	Participant number
pre	Before measurements
post	After measurements
k	Filter number
λ_{k1}	Wavelength limit 1 of the region of transmittance of the filter
λ_{k2}	Wavelength limit 2 of the region of transmittance of the filter
CRV	Comparison reference value
adj	Adjusted to cut-off value if criteria is met
cut-off	Lower limit to which uncertainty is adjusted if criteria is met
add	Additional uncertainty components

The original set of participants of the inter-laboratory emittance comparison included the NPL, the National Metrology Institute of Japan (NMIJ), LNE, the National Institute of Standards and Technology (NIST) of the United States, INRIM, with NPL serving as the coordinating pilot laboratory. NPL selected and produced the sets of oxidized Inconel (OxIn) and boron nitride (BN) artefacts, used in the comparison. NPL also developed an initial measurement protocol. Before measurements were begun, however, due to an organizational restructuring, NPL was not able to continue their participation. NIST then took over as the pilot laboratory. NIST produced and distributed a third artefact set of silicon carbide (SiC) and also revised the measurement protocol. At approximately the same time as NPL's withdrawal, the PTB joined the comparison as the fifth participant.

2 DESCRIPTION OF THE COMPARISON

2.1 Participants Parameter Ranges

Due to the variety of instrument designs and methods employed by the participants and detailed in Section 2.3, their ideal artefact sizes are different and incompatible with each other, with the exception of NMIJ and PTB. This meant that different artefacts had to be produced for each participant. It also meant that no participant, including the pilot, would be able to measure all the artefacts at all temperatures. It was possible, however, for the pilot lab (NIST) to measure all artefacts at room temperature (RT), which was done both before and after all other measurements by the other participants. Since PTB joined the comparison after the OxIn and BN artefacts were produced, but before the SiC artefacts were made, a second 45 mm SiC artefact is shown in the photo and was used for PTB. The artefact size for each participant is shown in Table 2.

Table 2. Overview of NMI Emittance Measurement Capabilities.[iii]

Identifier Number	NMI	Wavelength (μm)	Temperature Range (°C)	Spectrometer Type	Artefact Size dia. x thick. (mm)
1	NMIJ	5 to 12	-20 to 100	FTIR	45 x 2
2	LNE	1 to 14	23, 100 to 800	Optical Filters	25 x 10
3	NIST	1 to 20	23 to 900	FTIR	18.5 x 5
4	INRIM	1 to 15	23, 250 to 1000	Monochromator	16 x 2
5	PTB	4 to 40	100 to 250	FTIR	45 x 2

2.2 Standard Artefacts

As stated above, three sets of artefacts were selected and produced for the comparison: BN, OxIn, and SiC. All three materials are nominally stable under heating in air after an appropriate bakeout preparation regime and are under consideration as potential candidate standard reference artefacts. In the past, OxIn has been a NIST (formerly NBS) Standard Reference Material 1440,[4] BN has been extensively studied at NPL,[5] and more recently, SiC has been investigated at NIST.[6]

[iii] Spectral and temperature ranges are nominal. Exact spectral ranges are dependent on sample temperature and emittance.

Production of the artefact sets took place over more than one year. Tests were performed on an initial set of BN and OxIn artefacts produced by NPL. Due to significant variation between samples and initial heat treatment difficulties found after testing, second replacement sets were produced and processed. Although not ideal (Section 2.5.1.1), improvements were deemed sufficient to proceed with the comparison. The SiC artefacts obtained and heat treated by NIST were found to be acceptably uniform and stable. Details of the materials' source, composition, heat treatment, and characterizations are given in Table 3.

Table 3. Description of the Artefact Materials.

Material	**Boron Nitride**	**Oxidized Inconel**				**Silicon Carbide**
Material Details						
Vendor(s)	Goodfellow Ltd. (UK)	Goodfellow Ltd. (UK)				Trex Enterprises (US)
		Vereinigte Deutsche Metallwerke AG (Germany)				
Material Type	Hot Pressed BN	Inconel alloy 600				CVD Process
		Inconel alloy 600				
Material Form (from Vendor)	2 mm sheet ϕ25.4 mm rod	2 mm sheet				N.A.*
		ϕ75 mm rod				
Material Composition (4 most abundant, wt%)	N.A.*	Ni	Cr	Fe	C	N.A.*
		73.0	16.5	9.0	0.7	
		Ni	Cr	Fe	Mn	
		75.4	15.5	8.0	<1	
Sample Machining & Polishing	Agate Ltd. (UK)	NPL Engineering Services (UK) (+ sand blasted)				Trex Enterprises (US)
Artefact Properties						
Density (g/cm^2) (Vendor)	N.A.*	N.A.*				3.18 (±0.04)†
Surface Roughness RMA (µm)**	0.7 – 1.4 (NPL)	2.4 – 4.4 (NPL)				<0.1 (Trex Ent.)
Specular/Diffuse Reflectance (NIST)	95% Diffuse at 2 µm to 80% Specular at 14 µm	Diffuse				Specular
Heat Treatment						
Where	NIST	NPL				NIST
Temperature (°C)	600	980				600 + 900
Duration (h)	30	30				10 + 20
Atmosphere	Air	Air				Air

* N.A. – not available.
† Trex Enterprises
** After heat treatment.

Photos of the artefact sets used in the comparison are shown in Figure 1: BN in (a), OxIn in (b), and SiC in (c). 10 mm diameter x 10 mm thick artefacts, produced for NPL are shown, but were not used in the comparison.

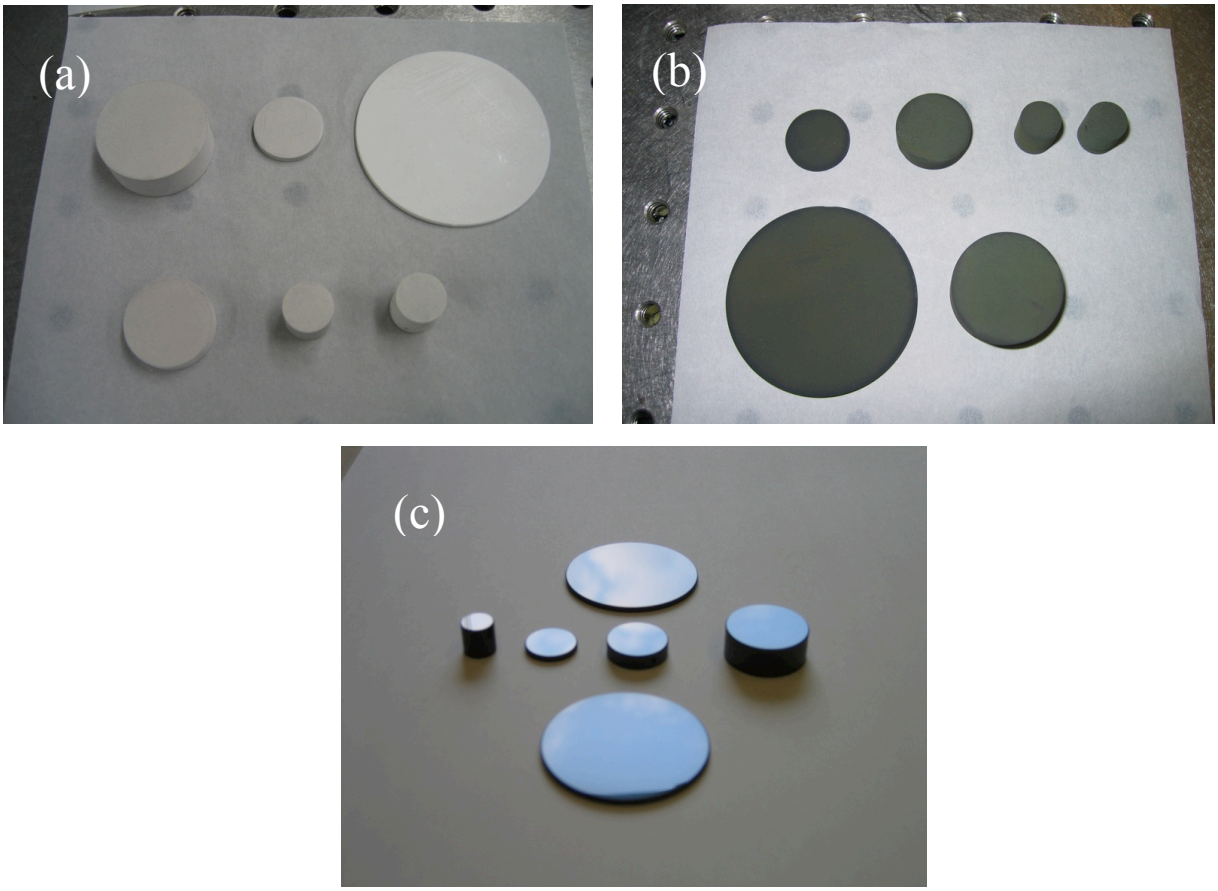

Figure 1. Photos of a) boron nitride, b) oxidized Inconel, and c) silicon carbide artefact sets produced for the comparison. Artefacts for NPL (1 cm dia. x 1 cm thick) are also shown but were not used.

2.3 Comparison Process Schedule

The comparison was carried out in a "star" mode in which the samples are provided by the pilot laboratory and sent out to all the participants at approximately the same time. This was done primarily because of the incompatibility of the measurement systems to a single artefact size, as described above. Other factors, including the overall duration of the comparison and the risk of artefact loss or damage made the star mode preferable. At the start of the measurement campaign, NPL sent the sets of BN and OxIn artefacts to NIST for measurement at room temperature (23 °C) in middle of 2007. Subsequently the artefacts were distributed to the other participants in late 2007. After the change in pilot laboratory, NIST measured the SiC artefacts at room temperature and delivered to participants in early 2008.

Measurements by all the participants were completed, and the artefacts returned to NIST by the end of 2008. NIST completed the repeat room temperature measurements of all artefacts by early 2009. Additional details of the history and process are given in Appendix A, the Technical Protocol.

2.4 Instrument, Method and Uncertainties Descriptions

2.4.1 NMIJ

The NMIJ measurement system employs an FTIR spectrometer, and is designed for normal spectral emittance measurements of opaque solid materials near ambient temperatures.[7] A schematic of the system is shown in Figure 2. A liquid nitrogen cooled photovoltaic mercury cadmium telluride (MCT) detector operated with a current mode preamplifier, which has a high sensitivity and a highly linear response, was used instead of the conventional photoconductive MCT detector operated with a voltage mode preamplifier. In order to reduce the air absorption effect, all optical components including the sample and the reference blackbodies are operated in vacuum. The spectrometer is calibrated against high quality

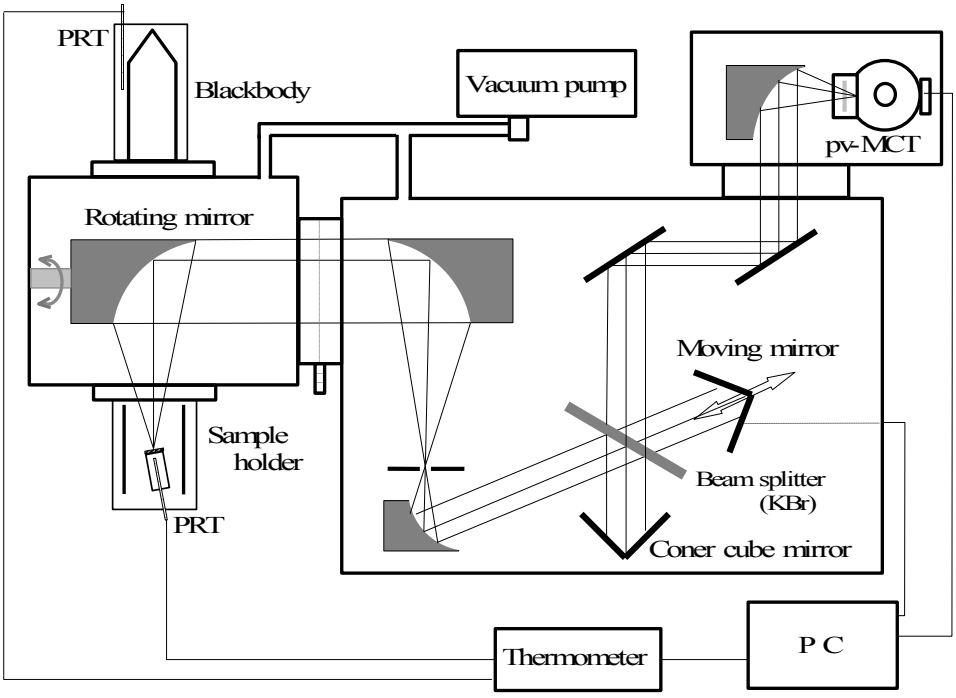

Figure 2. The NMIJ spectral emittance measurement system.

reference blackbodies. An appropriate phase correction technique is used to cancel the phase error caused by the emission from the surroundings.[8] The sample spectral radiance, $L_\nu(\nu)$ is obtained from

$$L_\nu(\nu,T) = \mathrm{Re}\left[\frac{C_\mathrm{s}(\nu)-C_0(\nu)}{C_\mathrm{h}(\nu)-C_0(\nu)}\right]\cdot\left[B_\nu(\nu,T_\mathrm{h})-B_\nu(\nu,T_0)\right]+B_\nu(\nu,T_0)=|L_\nu|\exp(i\phi_\mathrm{L}) \qquad (2)$$

,

where ν is the wavenumber, C are the complex spectra obtained from viewing the sample, s, the cold blackbody, 0, and the hot blackbody, h; B are the ideal blackbody spectral radiances for the hot and cold blackbodies; and ϕ_L is the phase.

$$L_\nu(\nu,T) = \varepsilon(\nu,T_\mathrm{s})\cdot B_\nu(\nu,T_\mathrm{s})+\left[1-\varepsilon(\nu,T_\mathrm{s})\right]\cdot B_\nu(\nu,T_\mathrm{ambient}) \qquad (3)$$

is then solved for $\varepsilon(\nu,T_\mathrm{s})$ to obtain the sample emittance. Refinements are also made that take into account variations in the different regions of the background, which are seen by the sample.

An example uncertainty analysis for the BN sample is shown in Table 4.[9] The same uncertainty analysis was performed for all intercomparison measurements with the resultant

expanded uncertainties (combined uncertainties times $k = 2$) provided. The emittance values and expanded uncertainties, after the processing discussed in Section 2.4, are shown in the results Tables in Appendix A.

Table 4. NMIJ example uncertainty budget for the emittance measurement of the boron nitride sample at 100 °C and 10 μm wavelength, where $\varepsilon = 0.83$. (Relative quantities are shown.)

BN Emittance		Values (%)
Radiation measurement		
Reference blackbody		
Reference platinum resistance thermometer	0.01 K	0.01
Effective emittance of the high temperature reference	0.9996 (±0.0001)	0.06
Stability of the temperature control	0.02 K	0.02
Effective emittance of the liquid nitrogen cooled reference	0.9994	N.S.
Nonlinearity of the spectrometer response		0.28
Size-of-source effect		N.S.
Temperature of the sample surface		
Reference platinum resistance thermometer	0.01 K	0.01
Stability of the temperature control	0.02 K	0.02
Temperature drop (thickness of 1 mm, thermal conductivity of 30 W m^{-1} K^{-1})	0.02 K	0.06
Correction of radiance reflected at sample surface		0.31
Noise on the emittance spectra		0.05
Reproducibility (stdev, 3 days)		0.01
Relative combined standard uncertainty ($\Delta\varepsilon/\varepsilon$)		0.43
Relative expanded uncertainty ($\Delta\varepsilon/\varepsilon$) ($k=2$)		0.86

N.S.: negligibly small.

2.4.2 LNE

LNE uses a custom designed infrared reflectometer to measure the spectral directional hemispherical reflectance of solid materials at ambient temperature.[10] For opaque materials, the spectral directional emittance can be calculated from the measured reflectance. The reflectance can be measured from 0.8 µm to 14 µm in five directions with an angle of 12°, 24°, 36°, 48°, and 60° with respect to the normal to the surface of the sample. The optical arrangement to collect the reflected flux is based on the Coblentz arrangement (hemispherical mirror). Four mirrors cut in a hemisphere are used to collect the flux reflected by the sample. This optical arrangement was chosen to limit the angle of incidence of rays on the detector (38° instead of 90° for the Coblentz arrangement). The final expanded uncertainty (level of confidence 95 %) of the reflectance is estimated to be about 0.03 for wavelengths between 0.8 µm and 10 µm and 0.04 for wavelengths over 10 µm. The uncertainty budget for emittance measurement of a comparison artefact is shown below in Table 5.

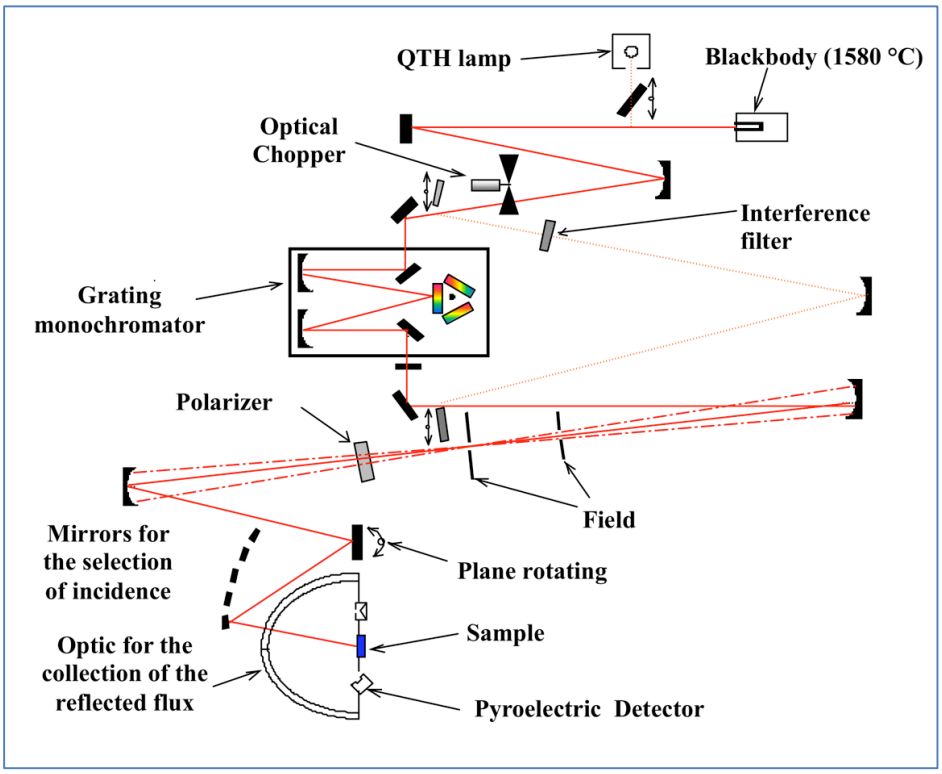

Figure 3. The LNE spectral reflectance measurement system.

An apparatus for the measurement, in the temperature range of 200 °C to 800 °C, of normal spectral emittance of opaque good thermal conductors is shown in Figures 4 and 5, in side and top views, respectively.[11] The direct method based on the comparison of the spectral radiance of the sample with the spectral radiance of a blackbody is used. The apparatus is designed to enable broad control of influencing parameters.

The sample and the reference blackbody are located in a vacuum chamber, which enables measurements either with air or inert atmosphere. The reference blackbody is a V-grooved and oxidized refractory steel cavity heated with an electrical furnace. The temperature is determined by a calibrated type S thermocouple placed at the level of the bottom of the cavity. The thermocouple is calibrated periodically and the spectral radiance of the blackbody is also calibrated periodically by comparison to a portable calibrated blackbody. A temperature-

controlled shield at ambient temperature, located at the ceiling of the chamber, is used to control the background temperature. The shield is coated with a high-emittance black paint. A cold blackbody controlled at a temperature close to the ambient is used for correction of the background radiation. The sample is clamped in a crucible heated by an electrical resistor. Two shielded type S thermocouples are embedded in the sample in two holes drilled parallel to the surface, for determination of the sample surface temperature.

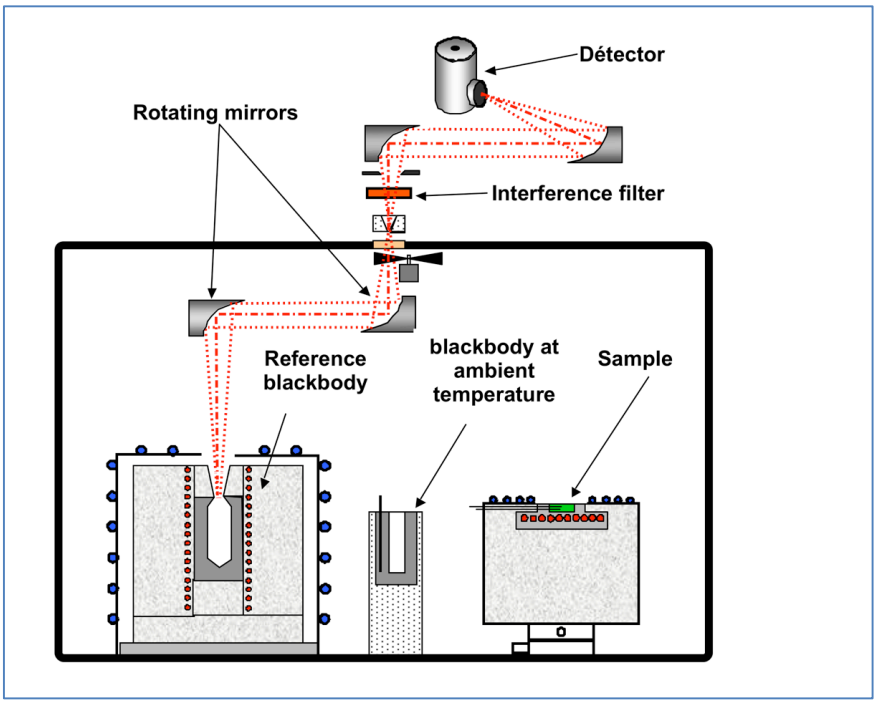

Figure 4. The LNE spectral emittance measurement system, side view.

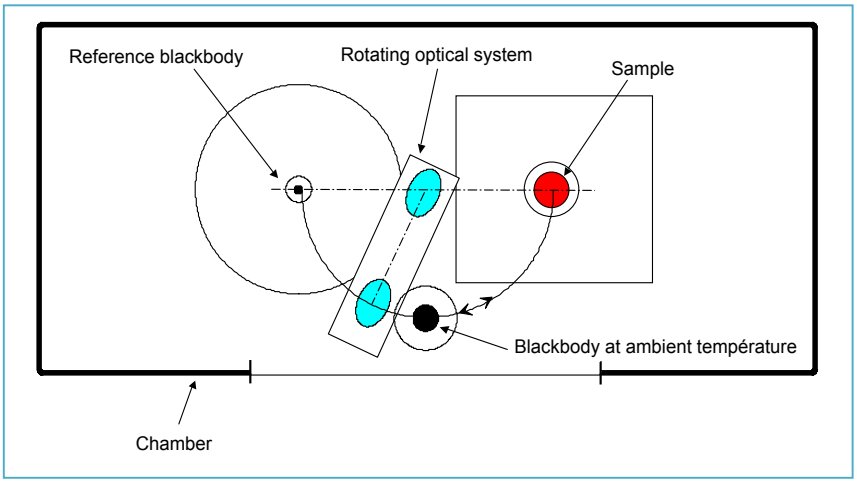

Figure 5. The LNE spectral emittance measurement system, top view.

For the emittance measurement process, radiative signals and temperatures of the reference blackbody, the cold blackbody and the specimen are measured in succession, by rotating the collection optics as shown in Figure 5. The spectral emittance is then calculated using the following formula:

$$\varepsilon(\lambda_c, T_s) = \frac{V_s - V_0}{V_r - V_0} \cdot \frac{L_{\lambda_c}(T_r) - L_{\lambda_c}(T_0)}{L_{\lambda_c}(T_s) - L_{\lambda_c}(T_0)} \quad , \qquad (4)$$

where λ_c is the central wavelength of the filter, V_s, V_r, V_0 are respectively the radiometric signals measured of the sample, the reference blackbody and the cold blackbody, T_s is the surface temperature of the sample, T_r is the reference blackbody temperature, T_0 is the cold blackbody temperature.
The main assumptions of the model are: the linearity of the spectroradiometer response, the stability of the temperature of the chopper blade, the equality between the cold blackbody radiance and the background radiance in the chamber. A listing of the significant uncertainty components for emittance including those contributing to the temperatures used in the emittance calculation is shown in Table 6.

Table 5. LNE uncertainty budget components for the oxidized Inconel sample directional spectral emittance. (Relative quantities are shown.)

Emittance Uncertainty Components	**Sub components**	**Type**	**Value (%)**
Room Temperature Reflectometer (Measurement at 5 µm - Emissivity = 0.772)			
	Sample signal noise	A	0.12
	Reference signal noise	A	0.06
	Nonuniformity of the detector	B	0.6
	Nonlinearity of the detector	B	0.1
	Reflected radiation losses	B	0.09
	Atmospheric absorption	B	0.15
	Collecting mirror reflectance	B	0.6
	Varying reflectance of "incidence mirrors"	B	0.44
	Sample position	B	0.15
	Sample orientation (angle)	B	N.S.
	Effective wavelength defined by the filter	B	N.S.
	Polarization of the incident beam	B	N.S.
Combined type A (k=1)		A	0.13
Combined type B (k=1)		B	1.0
Relative combined standard uncertainty (k=1)			1.0
Relative expanded uncertainty (k=2)			2.1

N.S.: negligibly small.

Table 6. LNE uncertainty budget components for the oxidized Inconel sample directional spectral emittance. (Relative quantities are shown.)

Emittance Uncertainty Components	Sub components	Type	Value (%)
Direct Radiance Technique (Measurement at 350 °C and 3 µm - Emissivity = 0.813)			
	Reproducibility & repeatability of emissivity results	A	0.12
	Sample surface temperature	B	1.2
	Blackbody radiance temperature	B	0.9
	Mean background temperature	B	0.4
	Nonlinearity of the detector	B	0.1
	Variation of atmospheric absorption	B	N.S.
	Effective wavelength defined by the filter	B	N.S.
	Size-of-Source Effect of measurement system	B	0.1
	Sample orientation (angle)	B	N.S.
	Combined type A (k=1)	A	0.12
	Combined type B (k=1)	B	1.6
	Relative combined standard uncertainty (k=1)		1.6
	Relative expanded uncertainty (k=2)		3.2

N.S.: negligibly small.

2.4.3 NIST

The NIST setup of equipment for infrared spectral transmittance and reflectance, including indirect measurement of emittance, is shown in Figure 6. The spectral source is a Digilab FTS-7000[iv] commercial Fourier transform spectrophotometer (FTS). Measurements are performed in one of three configurations: an internal sample compartment for transmittance, an external Infrared Gonio-Reflectometer Transmissometer (IGRT), for angle dependent measurements of specular samples, and the Infrared Reference Integrating Sphere (IRIS) for near-normal (8° incidence) measurements of both specular and diffuse samples. The IRIS is a custom diffuse-gold coated integrating sphere which employs an absolute measurement method to determine the reflectance from which emittance is calculated using Kirchhof's law and energy conservation, and was used for all measurements up to 150 °C.[12,13]

The interface optics consisting of the aperture plate, filter wheel, and polarizers are commonly available to the IRIS and IGRT along with beam steering flat mirrors mounted on translation stages, to select between the instruments. An aperture plate is used to select a spot size and vary the flux levels on the sample. For the comparison measurements, a 10 mm diameter spot size was selected. Using a sample heater with an inserted thermocouple, the comparison artefacts are measured at temperatures from 23 °C to 200 °C.

[iv] Certain commercial equipment, instruments, or materials are identified in this paper to specify the experimental procedure adequately. Such identification is not intended to imply recommendation or endorsement by the National Institute of Standards and Technology, nor is it intended to imply that the materials or equipment identified are necessarily the best available for the purpose.

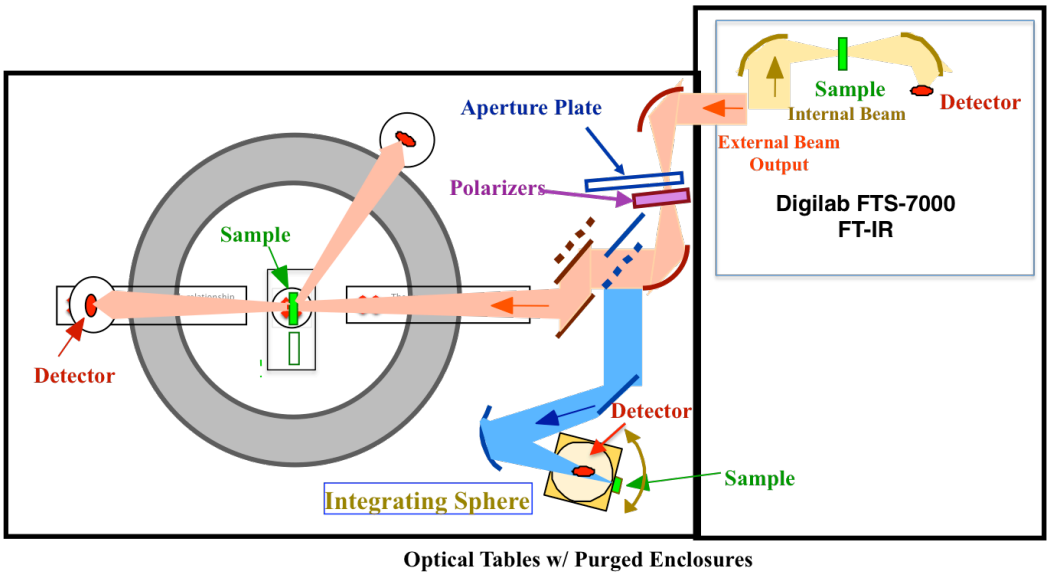

Figure 6. Schematic oft he NIST system used for the artefact reflectance measurements from 23 °C to 200 °C.

A second NIST facility, the Infrared Spectral Emittance System (ISES) is based on the direct measurement of spectral emittance of a material, comparing the spectral radiance of the sample to that of a blackbody at a similar temperature.[14,15] The ISES facility consists of several major subsystems designed to accomplish these requirements. These are shown schematically in Figure 7. Radiation from blackbody reference sources (to the left) is compared with that from a sample (located opposite the blackbodies) via rotation of a selection mirror. The reference source system consists of water, cesium and sodium heat-pipe blackbody sources, with calibrated platinum resistance thermometers (PRTs) traceable to ITS-90, on a motorized translation stage. Looking down, the source selection mirror can also view an ambient temperature stabilized "cold" vertical blackbody source (not shown). The sample system consists of several interchangeable heater mounts and manipulation stages. As the primary means of sample temperature measurement, an integrating sphere reflectometer with a calibrated room temperature reference sample is used. The low scatter interface optics[16] is not shown except for the rotatable mirrors, for source selection and for detector selection. The emitted radiation is measured with an FTS or filter radiometer, as selected by means of the mirror and a translation stage.

NIST employs the sample temperature measurement method developed by INRIM,[17] in which the sample emittance at the desired temperature is obtained from a hemispherical-directional reflectance factor measurement at the wavelength of a narrow-band filter radiometer, and a subsequent relative radiance comparison of the sample and a reference blackbody.[18] Both Si (905 nm) and InGaAs (1550 nm) radiometers are used to cover the temperature range of 150 °C to 1000 °C. Separate InGaAs and Si pyrometers traceable to the ITS-90 can be used to verify the PRT readings with radiance temperature measurements of the blackbodies.

NIST also employs the same measurement method and calculations for emittance as NMIJ, using Equations 2 and 3.

Example uncertainty budgets for sample measurements on both of NIST's systems are shown in Tables 7 and 8. Table 7 shows the emittance uncertainty budget for the directional-hemispherical reflectance measurements using the IRIS sphere with sample heater. Table 8 shows the complete emittance determination for measurements using the ISES system,

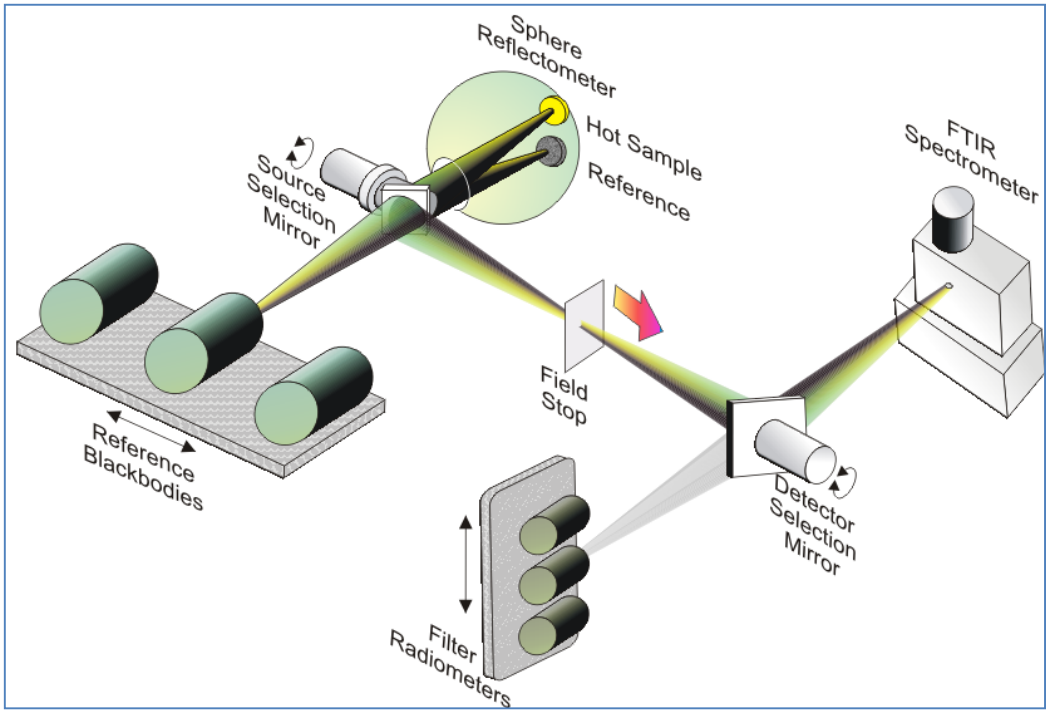

Figure 7. Schematic of the NIST Infrared Spectral Emittance Characterization Facility.

including the components for the sample temperature measurement process as well as the spectral radiance comparison. Each table shows the budget for one combination of artefact, temperature and wavelength.

Table 7. NIST example uncertainty budget for an OxIn artefact, using the IRIS spectral reflectance system at 150 °C and 11 µm wavelength. (Relative quantities are shown.)

Emittance uncertainty components	**Type**	**Value (%)**
Inter-reflections	B	0.01
Detector nonlinearity	B	0.02
Atmospheric absorption variation	B	0.01
Beam flip	B	0.01
Inequivalent sample/reference beam alignment	B	0.01
Retro-reflected light lost out sphere entrance port	B	0.10
Spatial variation of sphere throughput	B	0.31
Errors in sphere mapping	B	0.13
Sphere entrance port overfill	B	N.S.
Sphere sample port overfill	B	0.02
Beam geometry, polarization	B	0.01
Phase errors	B	0.01
Sample uniformity	B	0.10
Sample emitted radiance correction	B	0.10
Combined repeatability & reproducibility	A	0.10
Relative combined standard uncertainty		**0.39**
Relative expanded uncertainty (k = 2)		**0.78**

N.S.: negligibly small.

Table 8. NIST example uncertainty budget for sample spectral emittance of the SiC sample, at 600 °C using the ISES spectral radiance comparison system. (Relative quantities are shown.)

Uncertainty budget of sample spectral emittance		
	Type	**Value (%)**
Sample temperature calibration		
Repeatability of temperature comparison	A	0.05
Sample reflectance		
Repeatability of reflectance comparison	A	0.03
Sample		
Alignment	B	0.19
Temperature	B	N.S.
Reflectance reference		
Calibration	B	0.09
Alignment	B	0.19
Sphere reflectometer	B	0.20
Radiometer calibration		
Calibration at FP	B	0.01
Interpolation	B	0.01
Alignment	B	N.S.
SSE of interface optics	B	0.04
Spectral radiance comparison using FTIR		
Repeatability of spectral radiance comparison	A	0.30
Calibration of room-temperature reference BB		
Temperature	B	0.01
Spectral emissivity	B	0.03
Calibration of reference BB		
Temperature	B	0.01
Spectral emissivity	B	0.03
Nonlinearity of the FT detector	B	0.03
Relative combined standard uncertainty		**0.47**
Relative expanded uncertainty (k = 2)		**0.94**

N.S.: negligibly small.

2.4.4 INRIM

For room temperature emittance, INRIM employs a blackbody reflectometer to characterise reference standards for normal spectral emittance in the spectral range from 1 µm to 15 µm, shown schematically in Figure 8.[19] As compared with previous reflectometers of the same type, this apparatus takes advantage of a heat-pipe device, which greatly improves the temperature uniformity in the blackbody cavity. The measurement method consists of comparing the radiance of a cooled sample, which is held in a heated blackbody cavity, and the radiance of the cavity itself. The ratio of these radiances yields the sample reflectance. The main sources of uncertainty in the measured reflectance originate from: (i) departures from blackbody conditions due to the presence of the sample, apertures and the temperature gradients on the cavity wall; and (ii) emission of the sample due to heating which leads to an overestimate of reflectance.

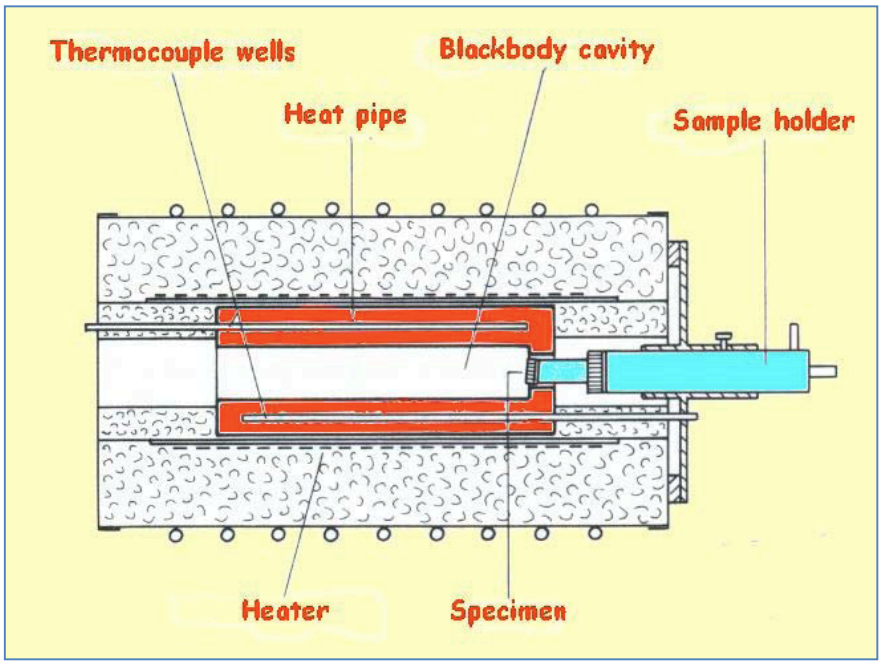

Figure 8. The INRIM Hohlraum spectral reflectance measurement system.

The INRIM system used for sample temperatures above 250 °C is shown in Figures 9 and 10. The hybrid method developed by INRIM and used by NIST (Section 2.3.3), consists of two stages.[17,20] First, a two step process to determine the sample surface temperature: a) measurement of the heated sample reflectance (1 - emittance) using an integrating sphere (Figure 9), and an appropriate narrow wavelength band, with a filter pyrometer; and b) a subsequent relative radiance measurement at the same wavelength, comparing to a reference blackbody (Figure 10). Second (also Figure 10), the relative spectral radiance measurement is made, using a set of filters or monochromator to obtain the sample spectral emittance.

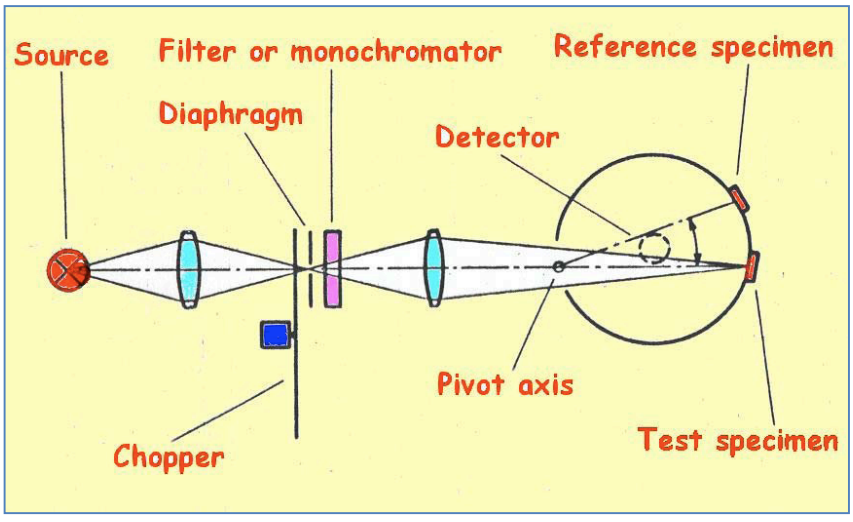

Figure 9. The INRIM spectral emittance measurement system.

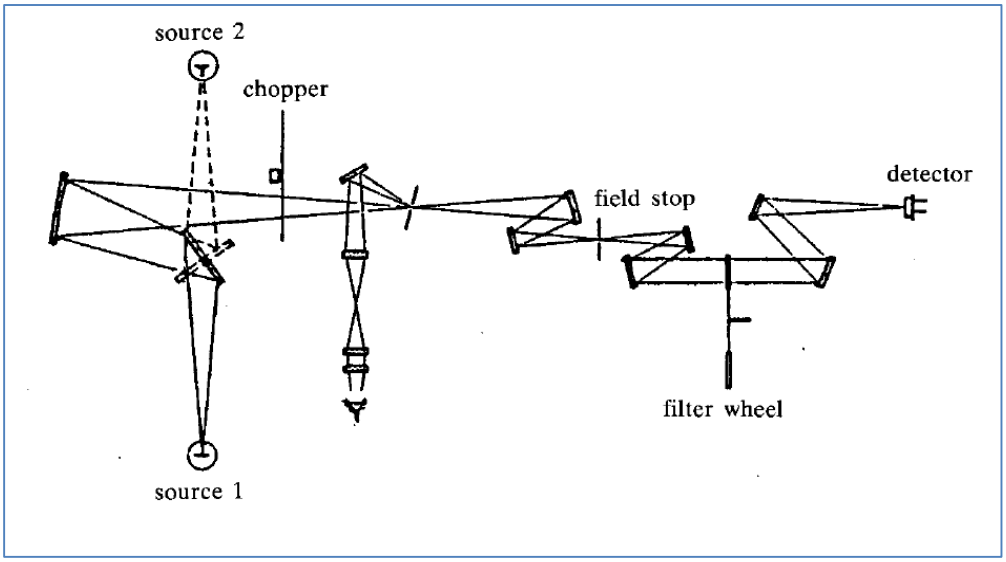

Figure 10. Optical layout of the INRIM spectral radiance measurements, where the sources 1 and 2 correspond to the heated sample, and reference blackbody. The filter wheel was replaced by a monochromator for the intercomparison measurements.

The primary components of uncertainty for INRIM's two measurement systems are listed in Tables 9 and 10.

Table 9. INRIM example uncertainty budget for the Blackbody Reflectometer measurement of the oxidized Inconel sample, directional spectral emittance. (Relative quantities are shown.)

Emittance uncertainty components	**Sub components**	**Type**	**Value (%)**
Room Temperature Blackbody Reflectometer			
(measurements at 3 μm)			
	Signal noise	A	0.50
	Signal repeatability	A	0.50
	Monochromator wavelength scale	B	0.05
	Blackbody reflectometer	B	0.20
	Sample position and rotation angle	B	1.00
Relative combined standard uncertainty			**1.24**
Relative expanded uncertainty (k = 2)			**2.48**

Table 10. INRIM example uncertainty budget for the direct radiance technique measurement of the oxidized Inconel sample directional spectral emittance at 350 °C and 3 μm wavelength. (Relative quantities are shown.)

Emittance uncertainty components	**Sub components**	**Type**	**Value (%)**
Direct Radiance Technique			
Sample Temperature via Integrating Sphere (at 350 °C and 1.6 μm)			
	Signal noise	A	0.1
	Signal repeatability	A	0.1
	Filter radiometer wavelength	B	0.1
	Sample position and rotation angle	B	0.6
	Reference sample reflectance	B	1.0
Spectral Radiance Measurements (at 350 °C and 3 μm)			
	Signal noise	A	0.70
	Signal repeatability	A	0.50
	Sample temperature (from above)	B	0.65
	Monochromator wavelength scale	B	0.12
	Sample position and rotation angle	B	1.00
	Reflected ambient background rad.	B	N.S.
Relative combined standard uncertainty			**1.48**
Relative expanded uncertainty (k = 2)			**2.96**

N.S.: negligibly small.

2.4.5 PTB

The experimental setup for the measurement of the directional spectral emittance in air consists of a Fourier-transform spectrometer, a sample holder with heater inside a spherical enclosure and a reference blackbody, all temperature-stabilized. The sample and the blackbody are alternately positioned in its detection area with the help of a translation stage (Figure 11). Since the emittance of the sample is less than unity, the sample also reflects part of the radiation emitted by the surroundings towards the spectrometer. An isothermal background at a known temperature and with a constant spectral emittance is provided here by the spherical enclosure around the sample. This enables the ambient radiation incident on the sample and, consequently, the emittance of the sample, to be determined from sample and blackbody relative spectral radiance and temperature measurements:[21]

$$Q = \tilde{L}_{\mathrm{s}}\left(T_{\mathrm{s}}\right) / \tilde{L}_{\mathrm{BB}}\left(T_{\mathrm{BB}}\right) \quad \text{and} \quad (5)$$

$$\varepsilon_{\mathrm{s}} = \frac{Q \cdot \left(B\left(T_{\mathrm{BB}}\right) - \varepsilon_{\mathrm{D}} B\left(T_{\mathrm{D}}\right)\right) + \varepsilon_{\mathrm{D}} B\left(T_{\mathrm{D}}\right) - \varepsilon_{\mathrm{E}} B\left(T_{\mathrm{E}}\right)}{B\left(T_{\mathrm{s}}\right) - \varepsilon_{\mathrm{E}} B\left(T_{\mathrm{E}}\right)} \quad , \quad (6)$$

where s denotes the sample, BB the reference blackbody source, D the detector, and E the environment. The significant sources of uncertainty, which form the uncertainty budget, are listed in Table 11.[22] These include instrumentation factors, temperature measurements, and thermal properties affecting the sample and enclosure temperatures.

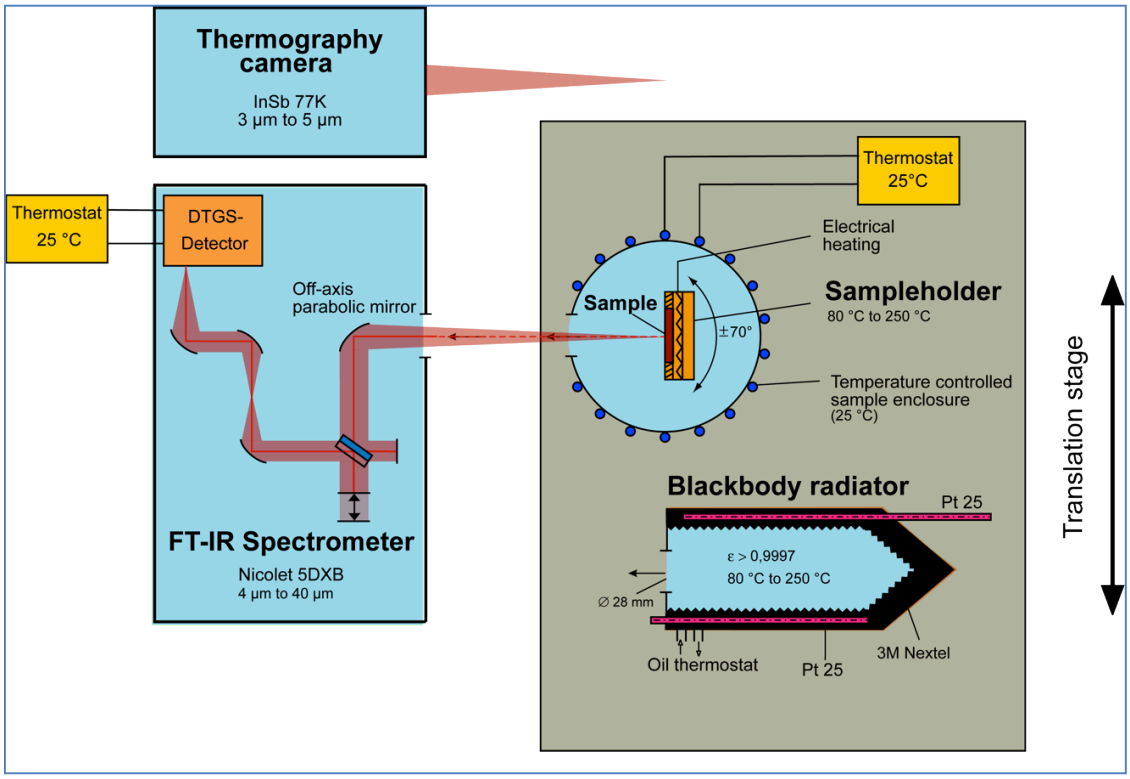

Figure 11. The PTB spectral emittance measurement system.

An example of the major uncertainty components and the resultant combined standard uncertainty is shown in Table 11. In addition the contributions of the sample surface temperature, the blackbody temperature, the detector temperature and the repeatability of the measured signal are shown.

The values of the uncertainty components are given with their absolute values and the respective units. This is because the sample surface temperature is not determined by an analytical expression but rather as a result of several nested iterative calculations, solving the equations describing the heat flow through the sample and the convective loss from the sample surface. Following the *Supplement 1 of the GUM*[23], the uncertainties of the sample surface temperatures were calculated by a Monte Carlo method. Briefly, all quantities that are relevant for the calculation of the sample surface temperature are varied independently in intervals with their respective uncertainties and according to their respective distribution functions. The solution for one specific set of input quantities gives one value for the sample surface temperature. The calculation is performed for a large number of sets of input quantities resulting in a distribution of the sample surface temperature. From that distribution a mean value and a standard deviation can be calculated. The latter serves as the standard uncertainty for the sample surface temperature. More details can be found in Reference 22.

Table 11. The PTB uncertainty budget of the directional spectral emittance measurement of the Boron Nitride sample at 200 °C and 10 μm. (Absolute quantities are shown for the individual components.)

Uncertainty Components	**Sub components**	**Type**		**Value**
Temperature of reference blackbody		A		0.20 K
	Calibration of temperature sensor	A		
	Repeatability of resistance measurement	A		
	Uncertainty of resistance measurement	A		
Temperature of sample enclosure		A		0.20 K
	Calibration of temperature sensor	A		
	Repeatability of resistance measurement	A		
	Uncertainty of resistance measurement	A		
Temperature of detector		A		0.20 K
	Calibration of temperature sensor	A		
	Repeatability of resistance measurement	A		
	Uncertainty of resistance measurement	A		
Emissivity of enclosure		B		0.040
Emissivity of detector		B		0.040
Measured signal of spectrometer				0.00083
	Repeatability	A	0.00083	
	Nonlinearity	B	N.S.	
Temperature of sample surface				0.91 K
	Thermal conductivity of sample substrate	B	4.0 W m^{-1} K^{-1}	
	Thermal conductivity of contact layer	B	0.033 W m^{-1} K^{-1}	
	Thickness of heating plate	B	0.50 mm	
	Thickness of contact layer	B	0.10 mm	
	Thickness of sample substrate	B	0.20 mm	
	Temperature of heating plate	A	0.10 K	
	Temperature of enclosure	A	0.10 K	
	Hemispherical emittance of sample (iteratively determined)	A	0.030	
	Diameter of sample holder	B	5.0 mm*	
	Diameter of enclosure	B	5.0 mm*	
	Distance sample / enclosure	B	5.0 mm*	
Relative combined standard uncertainty (%)				0.70
Relative expanded uncertainty (k = 2) (%)				1.40

* Uncertainties of effective lengths in convection model

2.5 Processing of the Comparison Data

2.5.1 Description of Differences to be Compensated/Corrected

In this comparison, several factors need to be taken into account and compensated for, in order to properly compare results from all participants. These are: 1) the artefact-to-artefact variation, 2) the artefacts' stability, 3) the differences in spectral resolution, and 4) the differences in the spectral data interval.

2.5.1.1 Artefact-to-Artefact Variation

All artefacts were measured at room temperature (RT) at NIST using the IRIS system prior to their distribution to the other participants. The results are shown in Figure 12(a) to (c). Both the BN and OxIn exhibited considerable variation across the set of 4 artefacts. This is likely due, in part, to separate sources of the raw material used for the 2 mm thick artefacts, and the others artefacts. The SiC artefacts exhibit excellent uniformity. The method used to take into account the artefact variation is to normalize the results for each artefact to the mean value of the room temperature emittance measured by NIST, using a multiplicative correction factor, $f_i(\lambda)$, providing a RT-normalized emittance as shown in Equations 7 and 8:

$$\varepsilon_i'(\lambda,T) = \varepsilon_i(\lambda,T)\cdot f_i(\lambda) \quad , \qquad (7)$$

where

$$f_i(\lambda) = \frac{\sum_{i=1}^{n}\varepsilon_{i,3}(\lambda,RT)}{n\cdot\varepsilon_{i,3}(\lambda,RT)} \quad , \qquad (8)$$

and
i is the participant number,
n is the total number of participants (5),
the first element of a subscript pair refers to the participant artefact,
and the second element refers to the measurement lab (NIST).

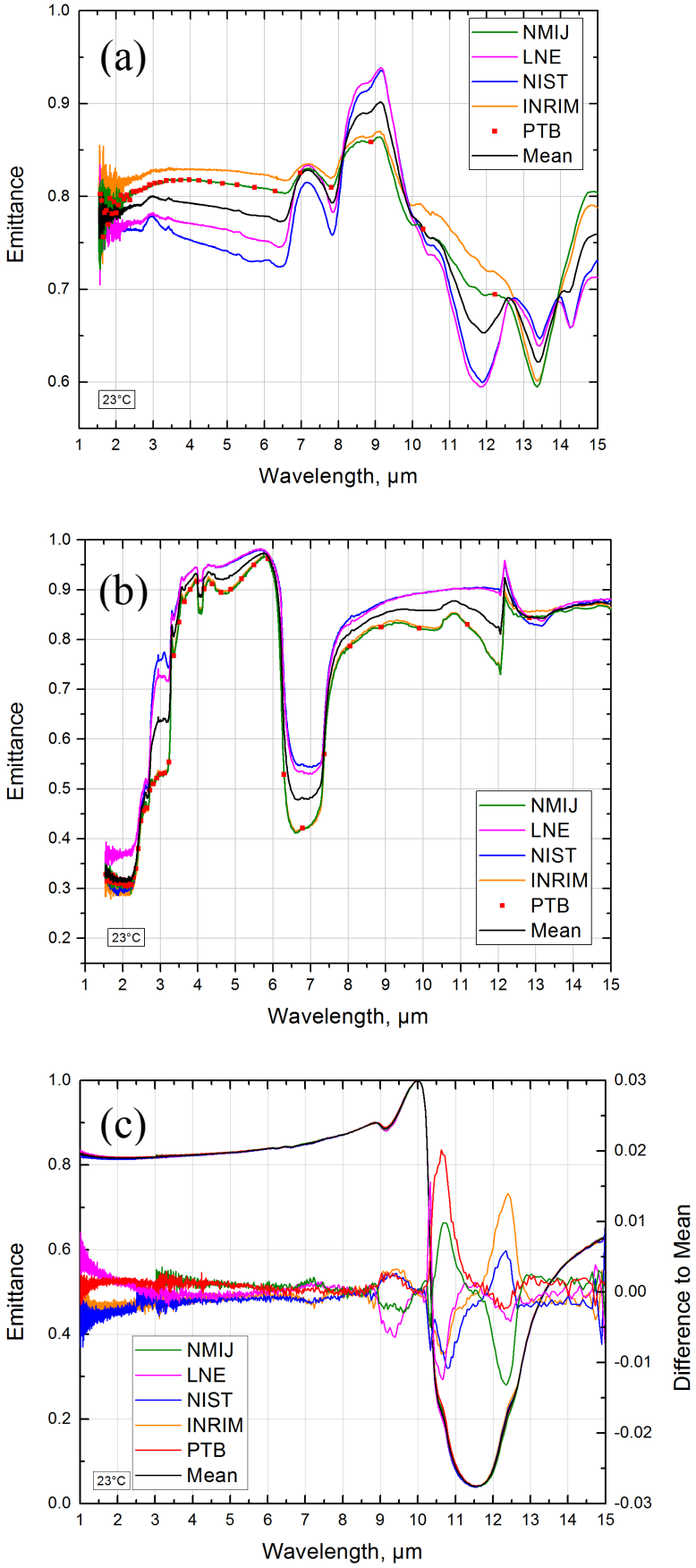

Figure 12. Plots of NIST-measured emittance of the a) OxIn, b) BN, and c) SiC sample sets. Curves representing the mean of each set of spectra are also shown in black. For silicon carbide the difference to the mean is also plotted against 2nd Y-axis.

2.5.1.2 Artefact Stability

All artefacts were returned to NIST after the participant's measurements were completed. They were re-measured at room temperature to determine whether any change had occurred. Both the BN and OxIn artefacts exhibited some significant changes. All of the BN changes occur in three spectral bands. Supplemental measurements indicated that the changes were variable upon exposure to air, purge, vacuum and heating. This indicated likely absorption and desorption of moisture from the air. Hence, all results for the affected filters at 2.2 µm, 3.0 µm, 3.6 µm, 6.4 µm, 7.0 µm, and 7.5 µm have been excluded from the comparison.

The only artefacts showing a significant non-reversible spectral change were the OxIn artefacts. The change in the infrared spectral emittance measured at RT for OxIn is shown in Figure 13 for all artefacts. Three participants heated artefacts up to and above 700 °C (LNE, NIST, and INRIM). The stability of the emittance in the NIST artefact was effectively

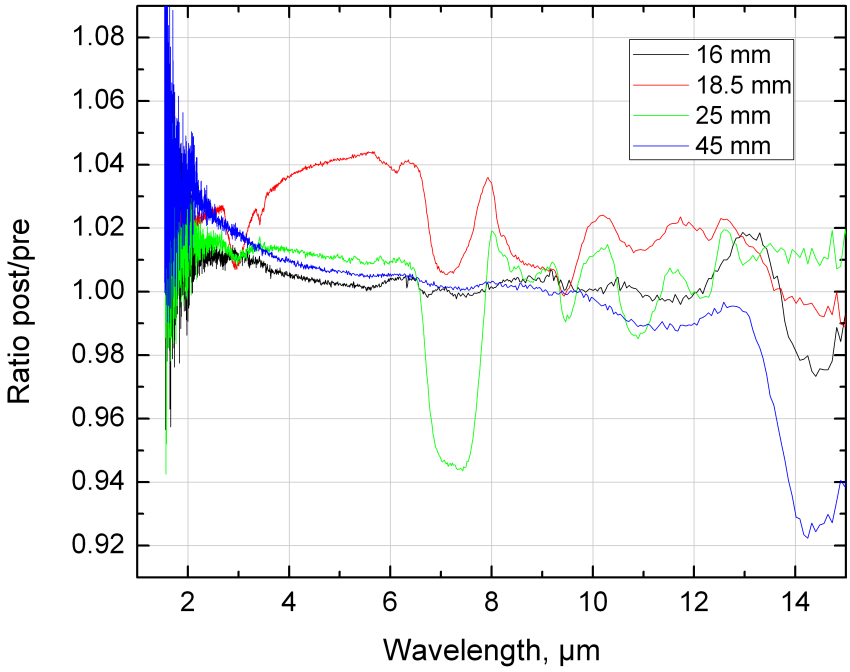

Figure 13. Change in the infrared spectral emittance measured at RT for OxIn after all elevated temperature measurements were completed.

monitored at 1550 nm by means of the artefact temperature measurement process, which includes an integrating sphere reflectance measurement.[6] An increasing deviation in emittance with temperature at 1550 nm from a linear trend was observed for temperatures above 500 °C, as shown in Figure 14. The time sequence of the measurements follows from the lowest temperature point in the lower left of the plot and continues up to 550 °C, followed by repeats at 350 °C and then 550 °C, with a very small change in emittance, followed by a gradual deviation from a linear increase in emittance with temperature up to the maximum measurement temperature of 800 °C. Finally, a room temperature measurement shows a permanent shift in emittance, upon repeated measurements. A linear fit is made to the lower temperature data (below 500 °C) and used to gauge how much change occurred at which temperature. The corrections, which sum to one, are expressed as percent of the total change

measured at RT, and applied as corrections to the data points at 550 °C, 600 °C, 700 °C, and 800 °C.

Similar behaviour was also directly observed by LNE, which performed RT measurements on their artefact between the elevated temperature runs. Therefore their result for the absolute emittance change was used for the LNE sample, NIST before and after measurements were used for NIST and INRIM samples. The split of how much change occurred at which temperature was derived from the time resolved NIST data for all three cases. Corrections to the emittance results were then made to the results at 550 °C and higher by subtraction of a corrective factor g_i, before normalizing for artefact-to-artefact variations using Equation 9.

$$g_i(T) = \begin{cases} h_i(T) \cdot \left(\varepsilon'_{i,pre}(\lambda, RT) - \varepsilon'_{i,post}(\lambda, RT)\right), i = 2,3,4 \\ 0, i = 1,5 \end{cases}, \qquad (9)$$

where

$$h_i(T) = \begin{cases} \begin{cases} 0.18, T = 550\ °C \\ 0.29, T = 600\ °C \\ 0.53, T = 700\ °C \end{cases}, i = 2 \\ \begin{cases} 0.07, T = 550\ °C \\ 0.11, T = 600\ °C \\ 0.20, T = 700\ °C \\ 0.62, T = 800\ °C \end{cases}, i = 3,4 \end{cases}$$

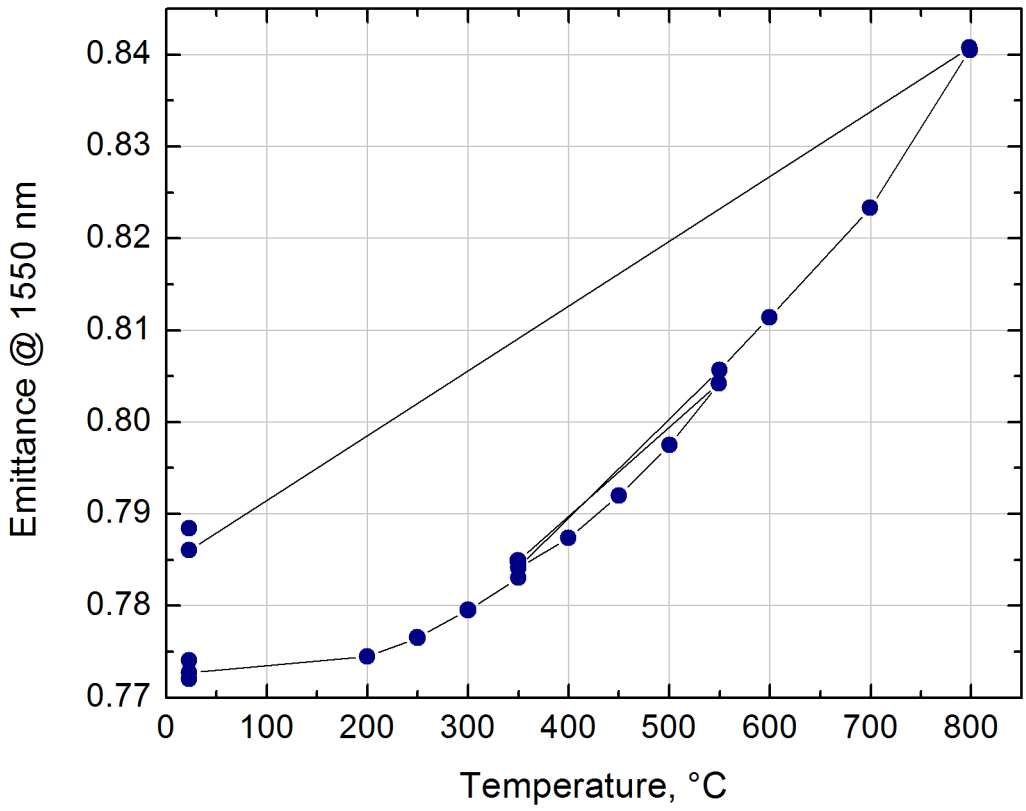

Figure 14. Emittance of the NIST OxIn artefact at 1550 nm, as measured with a filter radiometer and integrating sphere, used for caclulating corrections of sample change during heating.

The applied correction spectra are shown in Figure 15 for the INRIM, NIST and LNE results. The 45 mm artefact was initially measured by NMIJ up to 100 °C, shortly after receipt from NIST, and then after a long interval, shipped to and measured by PTB up to 250 °C. Subsequently, the 45 mm was returned to NIST and re-measured at RT. There is no evidence within the individual sets of results for NMIJ or PTB of a non-reversible change in emittance, and no change in the NIST RT measurement scale during the comparison. A plausible explanation for the change in the RT measurements for the 45 mm artefact, seen in Figure 13, considering the dates of the initial artefact production and when the NIST, NMIJ and PTB measurements took place, is that the changes are due to ageing of the material. Hence, for the comparison, we have used the NIST "pre" measurement for normalization of the NMIJ results and the NIST "post" measurement for the normalization of the PTB results described in Section 2.5.1.1.

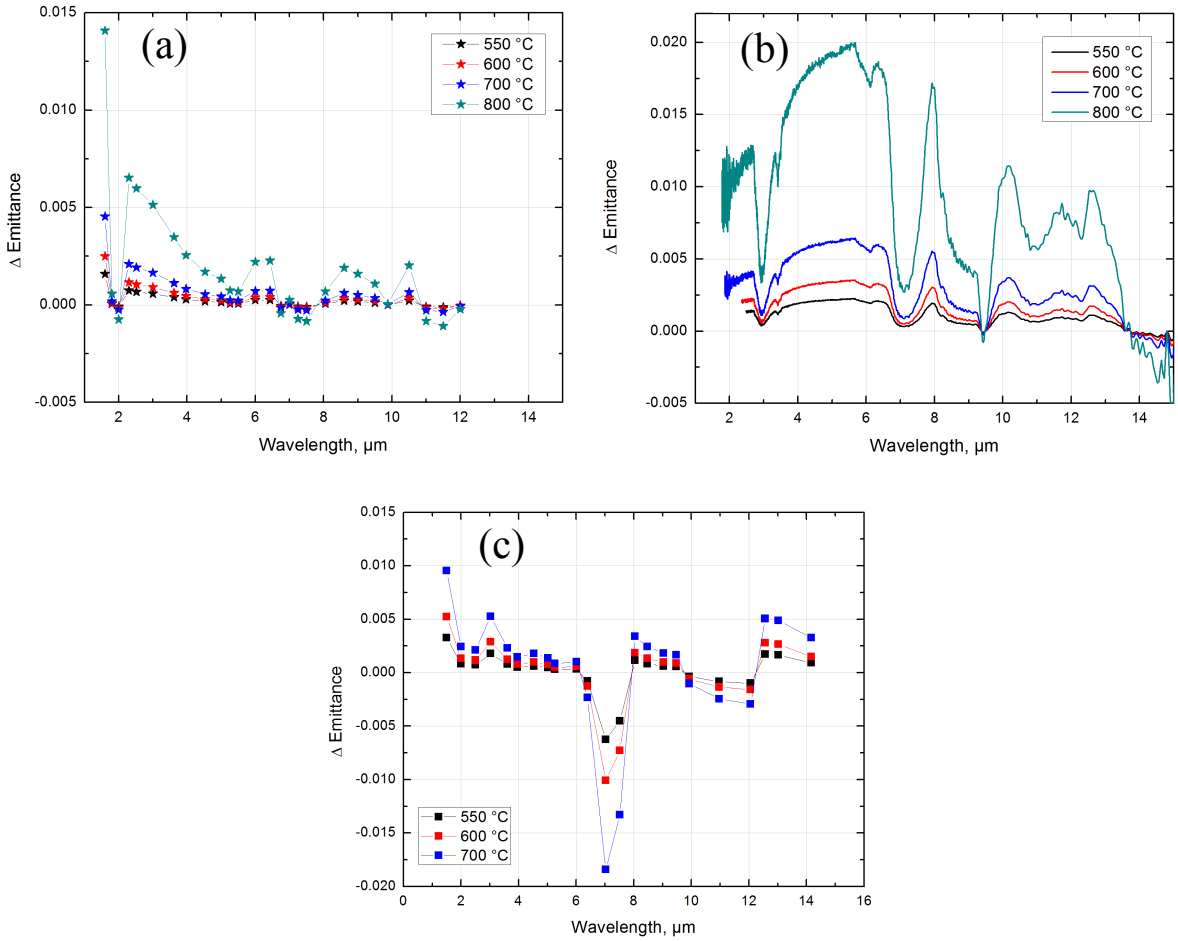

Figure 15. Corrections applied to OxIn spectral reflectance data to compensate for artefact change (drift) with exposure to heating: (a) INRIM, (b) NIST, and (c) LNE.

2.5.1.3 Spectral Resolution

Another important factor, resulting from the variety of instrumentation used by the participant NMIs, which needs to be evaluated is the difference in spectral resolution. A summary of the instrument types and spectral resolutions are shown in Table 12. The NMIJ, NIST and PTB spectral instruments are FT-IRs with constant and relatively high resolution. The INRIM spectral instrument is a monochromator for all wavelengths but 1.6 μm, where a filter is used, with comparable to slightly lower resolution at the shorter wavelengths. The LNE spectral

instrument employs a set of interference filters with the lowest resolution. Transmittance curves for all LNE filters used for the measurements are shown in Figure 16.

Table 12. Instruments and their spectral resolution.

Participant		Instrument Type	Spectral Resolution (cm^{-1})
1	NMIJ	FT-IR	4
2	LNE	Filter	600 to 100 (from 1.5 µm to 14 µm)
3	NIST	FT-IR	8
4	INRIM	Monochromator Filter	45 to 5 (from 2 µm to 12 µm) 300 nm at 1.6 µm
5	PTB	FT-IR	16

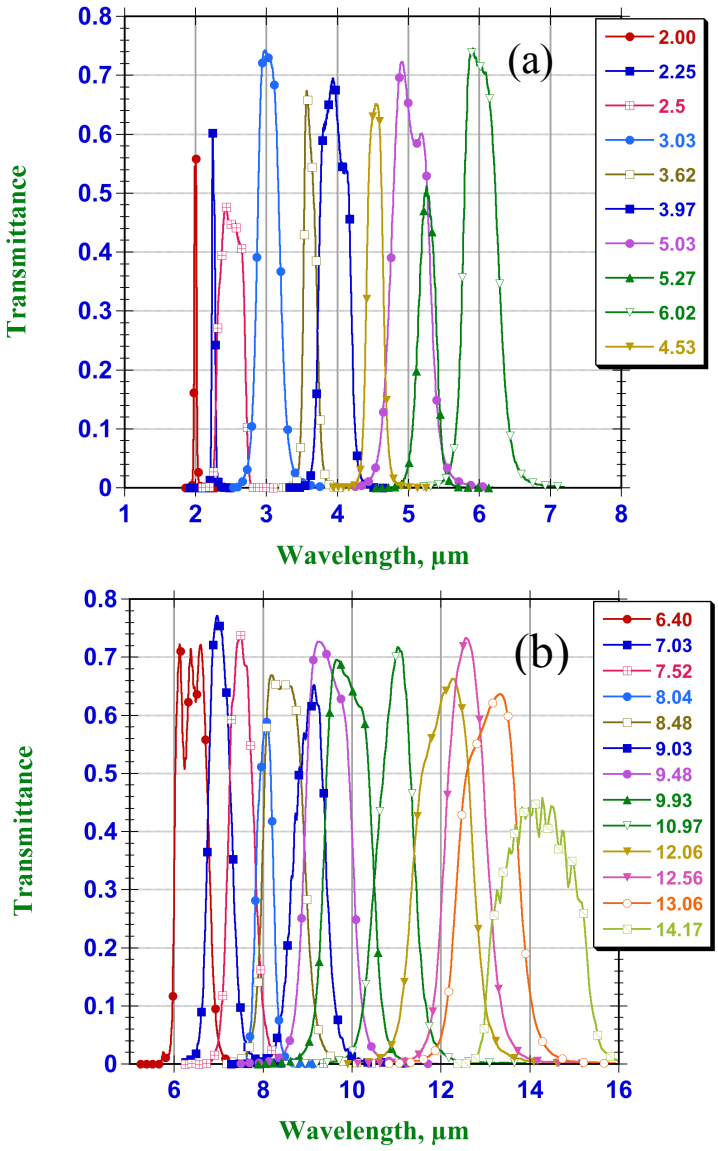

Figure 16. LNE filter transmittance spectra: a) below 6 µm, and b) above 6 µm.

Since all three materials exhibit spectral structure with features on a scale less than the spectral structure of the LNE filter widths, but greater than the resolution of the other systems, modifications of the directly measured emittance values have to be made. Our approach is to apply corrections based on the measured transmittance spectra of the LNE filters and the spectral responsivity of the LNE detector used to obtain the comparison values to obtain an equivalent emittance for comparison, $\varepsilon_i''(\lambda_k, T)$, as given by:

$$\varepsilon_{\mathrm{i}}''(\lambda_{\mathrm{k}}, T) = \frac{\sum_{\lambda_{\mathrm{k1}}}^{\lambda_{\mathrm{k2}}} (\varepsilon_{\mathrm{i}}'(\lambda, T) - g_{\mathrm{i}}(\lambda, T)) \cdot \tau_{\mathrm{k}}(\lambda) \cdot \Re(\lambda) \cdot B_{\lambda}(\lambda, T) \cdot \Delta\lambda}{\sum_{\lambda_{\mathrm{k1}}}^{\lambda_{\mathrm{k2}}} \tau_{\mathrm{k}}(\lambda) \cdot \Re(\lambda) \cdot B_{\lambda}(\lambda, T) \cdot \Delta\lambda} \quad , \qquad (10)$$

where
k is the filter number,
λ_{k1} and λ_{k2} are the wavelength limits of the region of transmittance of the filters,
$g_i(T)$ is the correction factor from Equation 9, only for OxIn; otherwise it is equal to 0,
$\tau_k(\lambda)$ is the spectral transmittance of filter k, and,
$\Re(\lambda)$ is the detector relative spectral responsivity.

Several of the filter spectra contain a minor amount of out-of-band transmittance. This has been included in the calculation. For a number of results at both the upper and lower limits of the spectral ranges, the participant's spectral coverage does not completely overlap the filter transmittance range. For the cases where the spectral overlap is at least 50 % of the filter transmittance range, Equation 10 is used, with either λ_{k1} or λ_{k2} replaced with the particpant's spectral limit for the measurement. For cases with less than 50 % overlap, the data is excluded from the comparison.

For the processing of the LNE data, the same averaging process is applied to the correction factor, $f_2(\lambda)$, from Section 2.5.1.1, to obtain a factor, $f'_2(\lambda)$, which can be used to appropriately correct the LNE data to compare it to mean values:

$$f'_2(\lambda_{\mathrm{k}}, T) = \frac{\sum_{\lambda_{\mathrm{k1}}}^{\lambda_{\mathrm{k2}}} f_2(\lambda, T) \cdot \tau_{\mathrm{k}}(\lambda) \cdot \Re(\lambda) \cdot B_{\lambda}(\lambda, T) \cdot \Delta\lambda}{\sum_{\lambda_{\mathrm{k1}}}^{\lambda_{\mathrm{k2}}} \tau_{\mathrm{k}}(\lambda) \cdot \Re(\lambda) \cdot B_{\lambda}(\lambda, T) \cdot \Delta\lambda} \quad . \qquad (11)$$

2.5.1.4 Spectral Data Interval

For the FT-IR based systems, the spectral data intervals are half the spectral resolution. For these systems, the data intervals are sufficient to carry out the averaging process described in Section 2.5.1.3. However, for the monochromator system of INRIM, this is not the case. The INRIM data interval is approximately 0.5 µm over most of the wavelength range, which is insufficient to perform the calculation of Equation 10. The wavelengths at which the INRIM data is provided correspond closely to the nominal values of the LNE filters. And since the INRIM spectral resolution is comparable to that of the NIST data, we can directly compare the INRIM and NIST data. In order to obtain appropriate filter averaged values for INRIM, we perform a two step process: 1) we obtain a ratio of the INRIM emittance value to the NIST

value at INRIM's wavelengths, and then 2) multiply the NIST filter averaged result by that ratio, as given by:

$$\varepsilon_4''(\lambda_k,T)=\varepsilon_3''(\lambda_k,T)\cdot\frac{\varepsilon_4'(\lambda_{4,j},T)-g_4(T)}{\varepsilon_3'(\lambda_{4,j},T)-g_3(T)} \quad , \qquad (12)$$

where
$\lambda_{4,j}$ are the wavelengths at which INRIM measured emittance, and
λ_k are the nominal LNE filter wavelengths.

2.5.2 Comparison Uncertainty Components

Each of the factors and the associated data processing steps described in the subsections of Section 2.5.1 result in contributions to the comparison uncertainty. The normalization process at room temperature, as well as the application of it to results at all temperatures, since we have to assume that the correction factor is independent of temperature, contribute uncertainty.

The normalization uncertainty component for the extrapolation increases with temperature. The only data available to quantify the uncertainty is the change in the spread of the participants' measured results with temperature. Data for OxIn is normalized by NIST room temperature data at the lowest temperature of each set (NMI) and shifted to the same starting point, e.g. at 100 °C. Data from each wavelength of all the participants start at the same point. The relative changes with temperature for all filter wavelengths, using this process, are shown in Figure 17. The uncertainty component associated with the extrapolation of the room

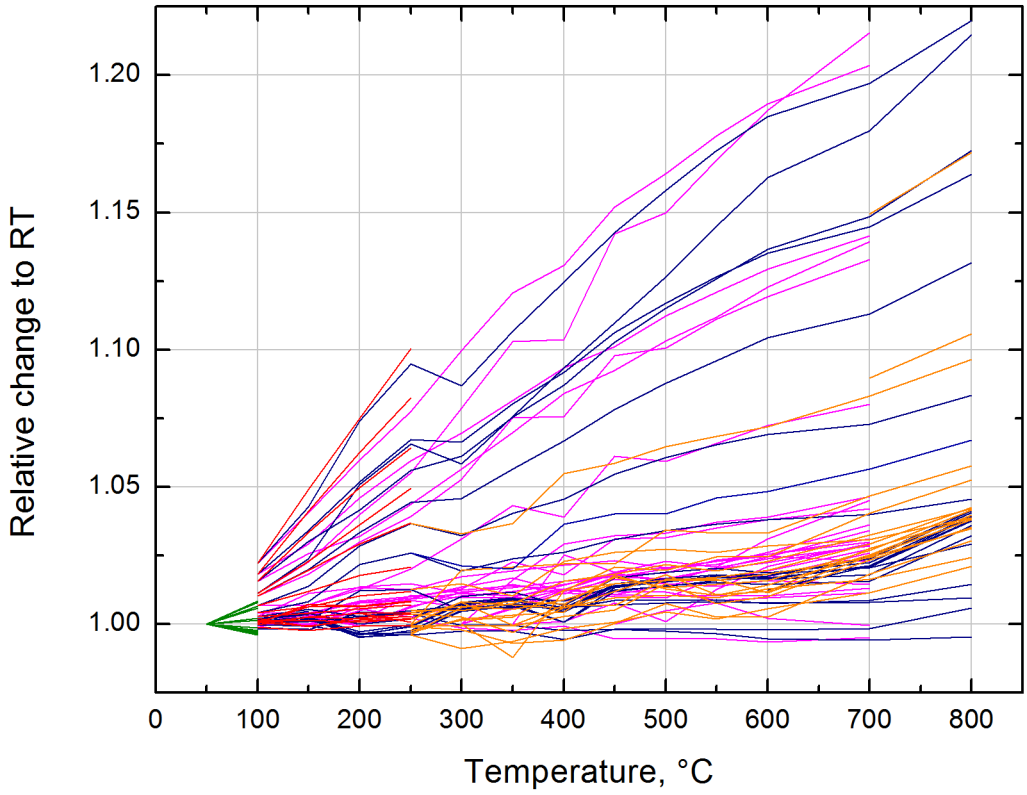

Figure 17. Data for OxIn is showing the relative change (to room temperature) in emittance vs. temperature for all filter wavelengths and participants (individual curves). The color labeling corresponds to that designated in Figure 12.

temperature normalization to the data at all temperatures, is taken to be 0.5 x the standard deviation of the spread for each individual wavelength as described.

An uncertainty contribution is added for the artifact stability corrections for OxIn. The uncertainties associated with the adjustment of the data for the LNE filter transmission and the detector response curve are included. And finally the effect of spectral resolution differences were evaluated but resulted in negligible contribution to the comparison uncertainty. The comparison uncertainty was calcualted using a minimum-maximum approach. All data is used with and without added uncertainties. Then the equivalent emittance for the comparison is calculated twice, with and without added uncertainties, and the difference of the two is used as to obtain the comparison uncertainty values.

2.5.3 Data Processing Procedure

A summary of the processing steps to obtain spectral emittance values for each participant that can be compared, as detailed in Section 2.5.1, is given as follows:

1. Calculate the mean of NIST-measured RT spectra,
2. Calculate ratios to the mean to generate correction spectra; calculate correction values for LNE using filter transmittance data, detector responsivity data and the Planck function.
3. Interpolate the lower resolution NMIJ and PTB data sets to match the wavelengths of NIST spectra.
4. Calculate correction for permanent sample emittance change at elevated temperatures for OxIn artefacts.
5. Apply individual correction spectra to data at all temperatures.
6. Calculate data points to compare to the LNE filter measurements: apply filter transmittance, detector response, and Planck function to NIST, NMIJ & PTB data.
7. Ratio the INRIM spectral data points (0.5 μm interval) to the NIST spectra; multiply NIST filter corrected values by the ratio.

These steps result in corrected emittance values and uncertainties for each participant. The overall process is illustrated graphically in Section 3.1.

2.5.4 Comparison Reference Value and Degrees of Equivalence

After preparation of the data for each participant, the results are compared. We employ the methodology recommended by the Consultative Committee on Photometry and Radiometry (CCT) Working Group on Key Comparisons (WG KG) [24,25] using weighted mean averaging with cut-off to obtain a nominal comparison reference value (CRV) $\varepsilon_{\mathrm{CRV}}(\lambda_{\mathrm{k}},T)$, for each filter wavelength, material and artefact temperature, is given by Equation 13. In the weighted mean calculation, each participant's values are weighted by their quoted standard uncertainties up to a cut-off point, which is given by the average of the standard uncertainties below the median of all the standard uncertainties, given by Equation 14.

$$\varepsilon_{\mathrm{CRV}} = \frac{\sum_i \varepsilon''_{\mathrm{i}} \cdot u^{-2}_{\mathrm{adj,\,i}}}{\sum_i u^{-2}_{\mathrm{adj,\,i}}} \quad , \qquad (13)$$

where

$$\begin{aligned} u_{adj,i}\left(\varepsilon''_i\right) &= u\left(\varepsilon''_i\right) \; for \; u\left(\varepsilon''_i\right) \geq u_{cut-off} \\ u_{adj,i}\left(\varepsilon''_i\right) &= u_{cut-off} \; for \; u\left(\varepsilon''_i\right) < u_{cut-off} \\ u_{cut-off} &= average\left\{u\left(\varepsilon''_i\right)\right\} \; for \; u\left(\varepsilon''_i\right) \leq median\left\{u\left(\varepsilon''_i\right)\right\} \end{aligned} \quad . \qquad (14)$$

The uncertainty for the CRV is given by:

$$u(\varepsilon_{\mathrm{CRV}}) = \frac{\sqrt{\sum_{\mathrm{i}} \frac{u^2(\varepsilon_{\mathrm{i}}^{''})}{u_{\mathrm{adj}}^4(\varepsilon_{\mathrm{i}}^{''})}}}{\sum_{\mathrm{i}} u^{-2}(\varepsilon_{\mathrm{i}}^{''})} \quad . \tag{15}$$

The individual participant's results are then compared to the $\varepsilon_{\mathrm{CRV}}$ values. The relative deviations from the $\varepsilon_{\mathrm{CRV}}$, $D_{\mathrm{i}}(\lambda_{\mathrm{k}},T)$, and their associated uncertainties, $U_{\mathrm{i}}(\lambda_{\mathrm{k}},T)$ are the unilateral Degrees of Equivalence (DoE), which are calculated according to Equations (16) and (17):

$$D_{\mathrm{i}} = \frac{\varepsilon_{\mathrm{i}}^{''} - \varepsilon_{\mathrm{CRV}}}{\varepsilon_{\mathrm{CRV}}} \quad , \tag{16}$$

$$U_{\mathrm{i}} = \varepsilon_{\mathrm{CRV}}^{-1} \cdot k(=2) \cdot \sqrt{u^2\left(\varepsilon_{\mathrm{i}}^{''}\right) + u^2(\varepsilon_{\mathrm{CRV}}) + u_{\mathrm{add}}^2 - 2 \cdot \frac{\frac{u^2\left(\varepsilon_{\mathrm{i}}^{''}\right)}{u_{\mathrm{adj}}^2\left(\varepsilon_{\mathrm{i}}^{''}\right)}}{\sum_j u_{\mathrm{adj}}^{-2}\left(\varepsilon_{\mathrm{j}}^{''}\right)}} \quad , \tag{17}$$

where the additional uncertainty component (u_{add}) is used to account for the normalization process, the correction applied for the temperature drift of the OxIn samples, the application of the LNE filter spectral transmittance and detector spectral response curves, and the differences in spectral resolution.

The error function, defined as

$$E_{\mathrm{i}}(\lambda,T) = \frac{U_{\mathrm{i}}(\lambda,T)}{|\mathrm{D_i}(\lambda,T)|} \quad , \tag{18}$$

is used to examine the results for outliers. If $E_{\mathrm{i}} \geq 3$, the result is deemed an outlier, and the corresponding data is excluded and the DoE are recalculated.

3 RESULTS

In the text and tables that follow, we identify the participants by number, and in the figures by the colors and symbols as shown in Table 13. The complete results are shown in Figures 20 to 65, for BN, OxIn, and SiC, and for all temperatures measured. The purple and blue symbols for NIST represent reflectometer and radiance measurement systems, respectively.

Table 13. Identification of data in results plots and tables.

NMI	Number	Symbol
NMIJ	1	▲
LNE	2	■
NIST	3	● ●
INRIM	4	★
PTB	5	▼

In Figure 18, the process previously summarized in Section 2.5.3 is illustrated with the example of the results for OxIn at 250 °C. Figure 18(a) shows the original spectral emittance data as submitted by the participant NMIs. The dispersion of the data is similar to the NIST room temperature results shown in Figure 13(a). After applying steps 1 through 5, the normalized corrected data in Figure 18(b) are obtained. The final steps 6 and 7 result in the emittance values shown in Figure 18(c), which are used for the comparison analysis.

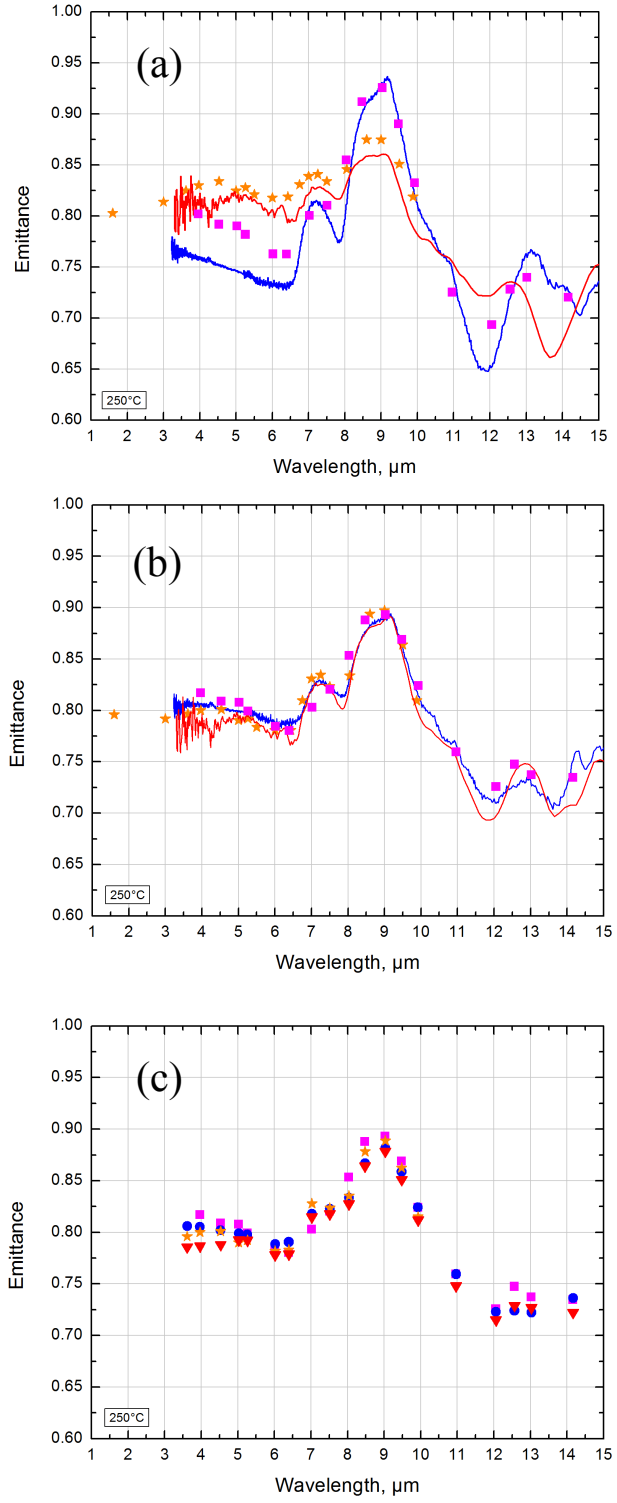

Figure 18. Spectral emittance results at 3 stages of the processing:
(a) initial data; (b) after step 5; and (c) at the end of the last step.

3.1 Boron Nitride

An overview of the temperature-dependent spectral emittance of the NIST BN artefact is shown in Figure 19. Curves of emittance for each temperature from 23 °C to 500 °C are shown in (a), and curves for the change in emittance from that at room temperature (RT) 23 °C are shown in (b). A comparison of RT spectra taken before and after heating shows changes in the regions of 1.5 µm to 2.5 µm, from 2.7 µm to 3.2 µm and from 6.5 µm to 7.5 µm. Subsequent examination of measurements after varying amounts of exposure to ambient air, as compared to "clean air" (air, with CO_2 and H_2O removed) revealed that the artefact was retaining varying amounts of OH causing considerable variability in the spectrum in the regions noted above. Hence, we decided to exclude data at 2.2 µm, 3 µm, 3.6 µm, 6.4 µm, 7 µm and 7.5 µm due to the instability.

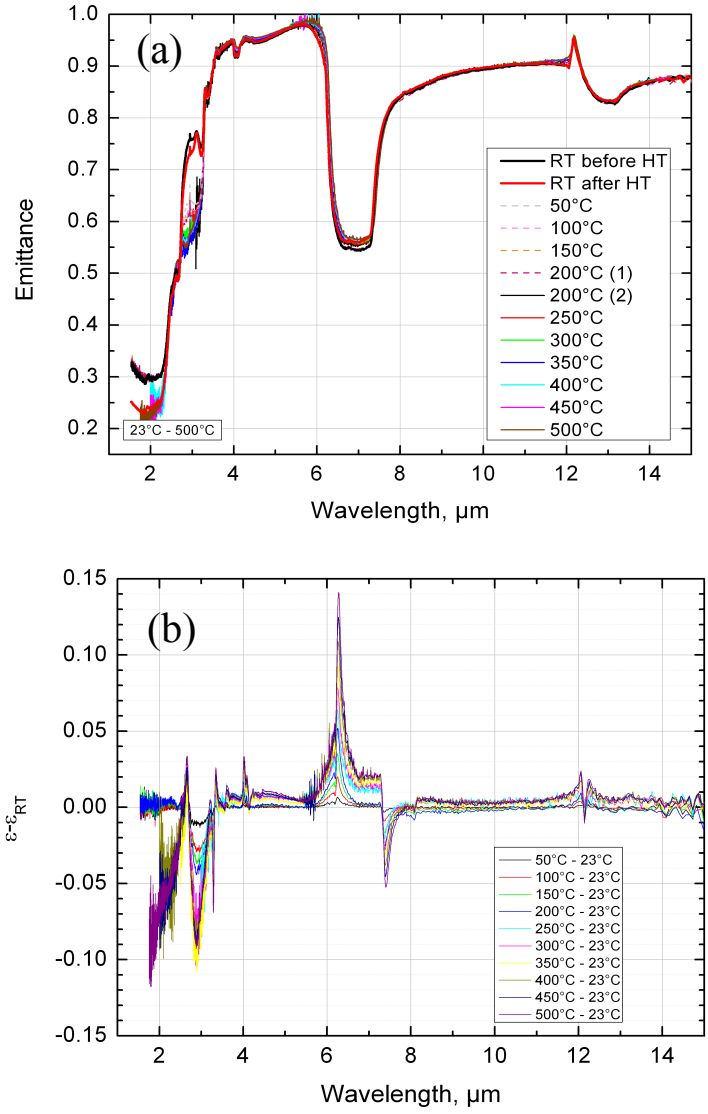

Figure 19. NIST spectral emittance results for BN: a) spectral emittance, and b) change in emittance from that at room temperature.

The unilateral relative DoE: the relative deviations and their expanded uncertainties (as error bars) for the BN measurements are shown in Figure 20 through Figure 30. The results are also tabulated in Appendix A.

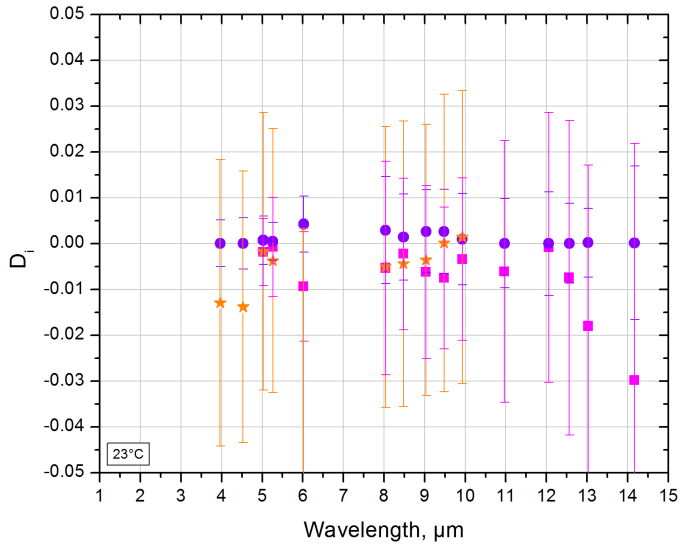

Figure 20. Unilateral DoE of BN results at 23 °C.

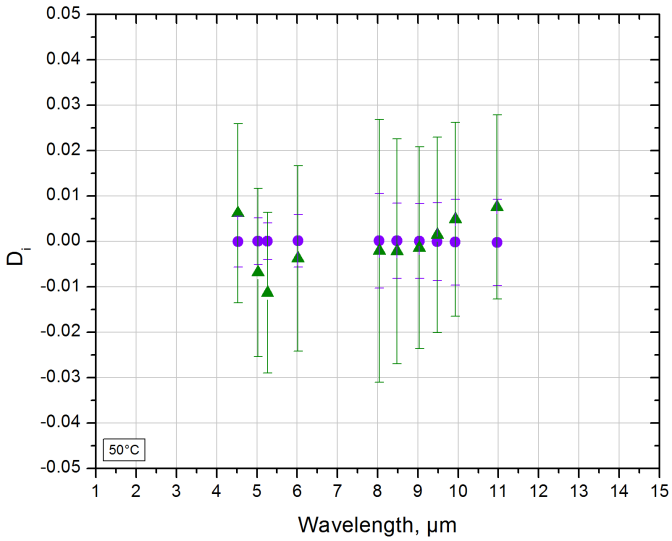

Figure 21. Unilateral DoE of BN results at 50 °C.

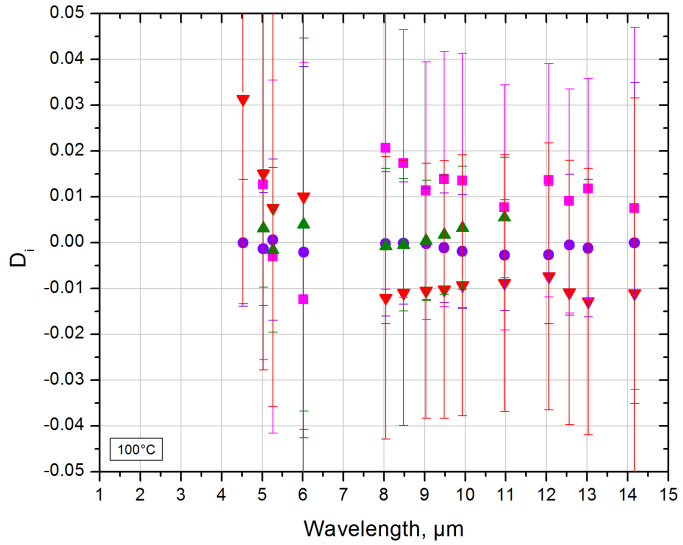

Figure 22. Unilateral DoE of BN results at 100 °C.

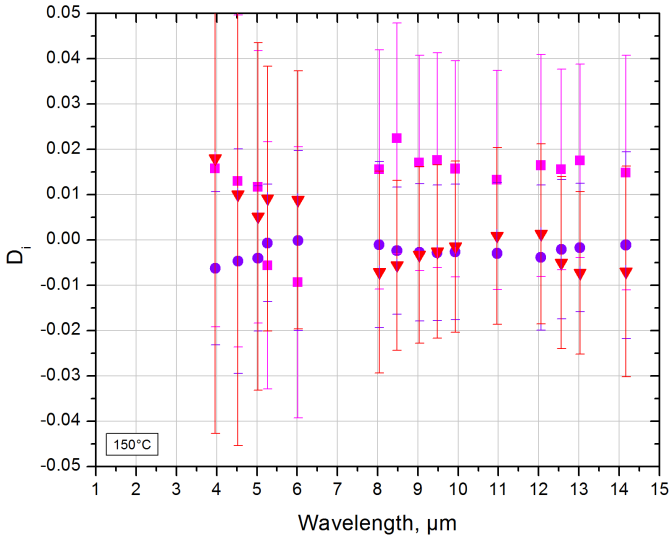

Figure 23. Unilateral DoE of BN results at 150 °C.

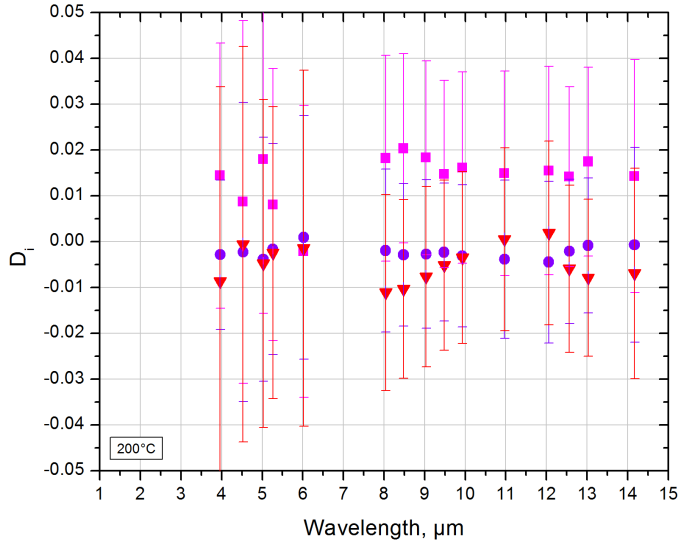

Figure 24. Unilateral DoE of BN results at 200 °C.

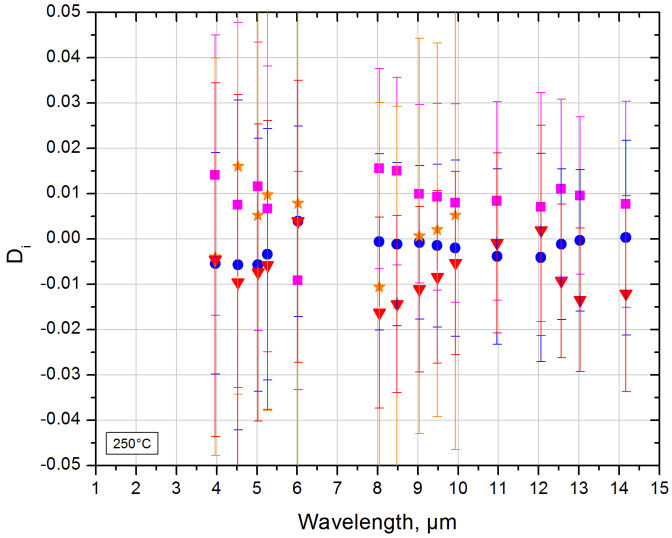

Figure 25. Unilateral DoE of BN results at 250 °C.

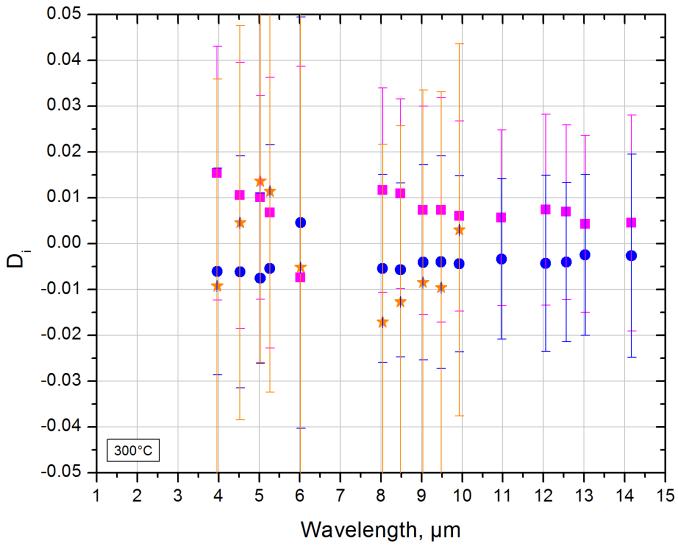

Figure 26. Unilateral DoE of BN results at 300 °C.

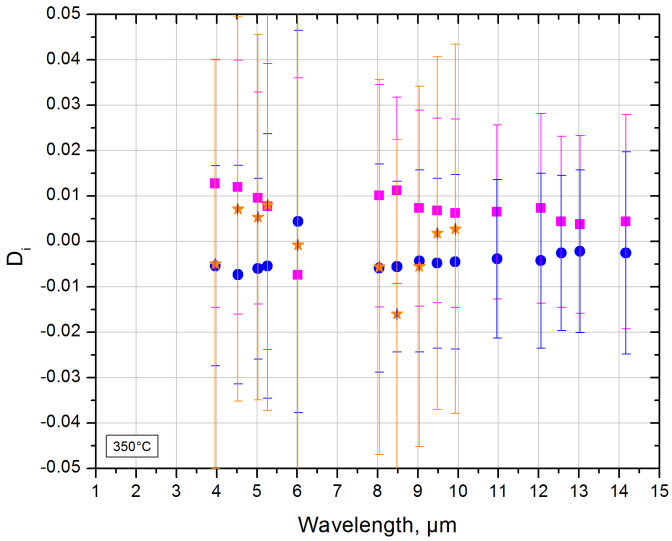

Figure 27. Unilateral DoE of BN results at 350 °C.

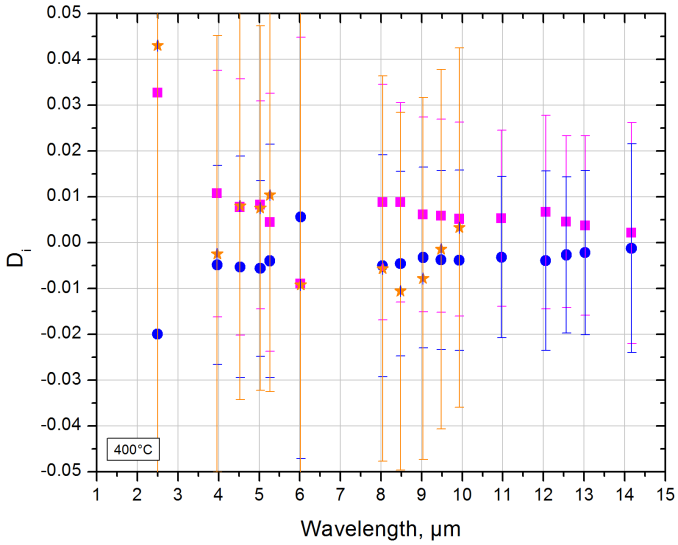

Figure 28. Unilateral DoE of BN results at 400 °C.

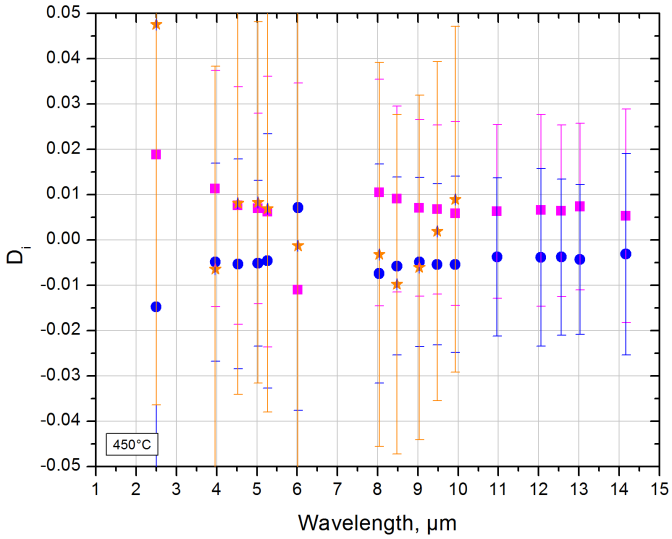

Figure 29. Unilateral DoE of BN results at 450 °C.

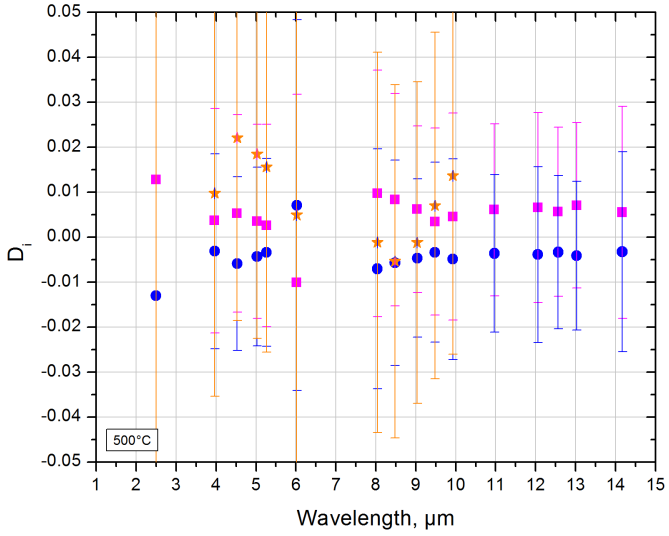

Figure 30. Unilateral DoE of BN results at 500 °C

3.2 Oxidized Inconel

An overview of the temperature dependent spectral emittance of the NIST OxIn artefact is shown in Figure 31. Curves of emittance for each temperature from 23 °C to 800 °C are shown in (a), and curves for the change in emittance from that at 23 °C (RT) are shown in (b).

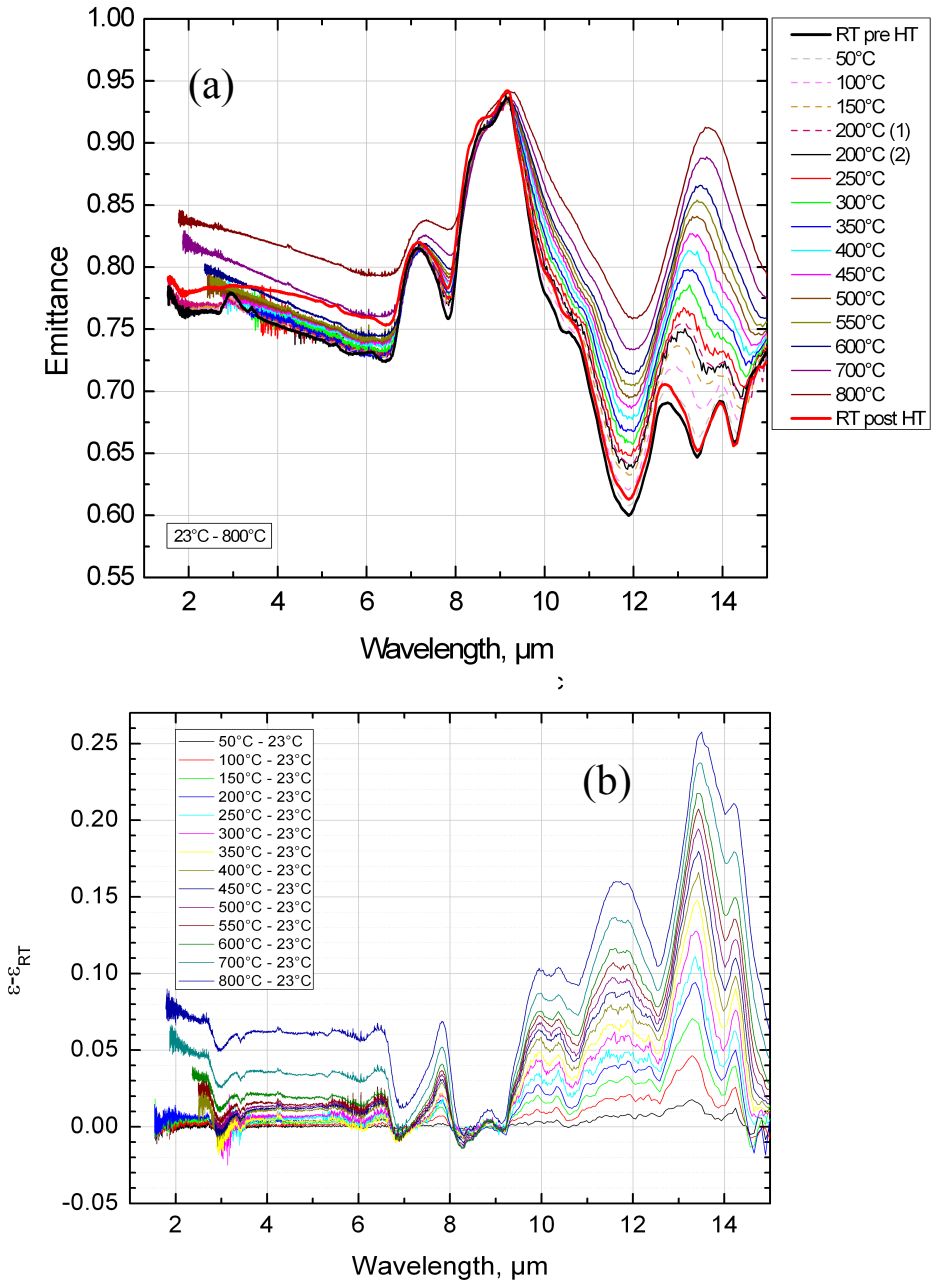

Figure 31. NIST spectral emittance results for oxidized Inconel: a) spectral emittance, and b) emittance difference from that at room temperature.

The unilateral relative DoE: the relative deviations and their expanded uncertainties (as error bars) for the OxIn measurements are shown in Figure 32 to Figure 46. The results are also tabulated in Appendix A.

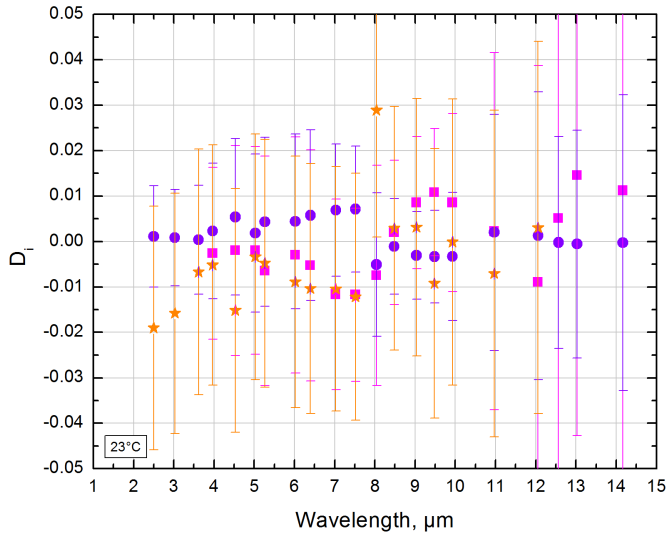

Figure 32. Unilateral DoE of OxIn results at 23 °C.

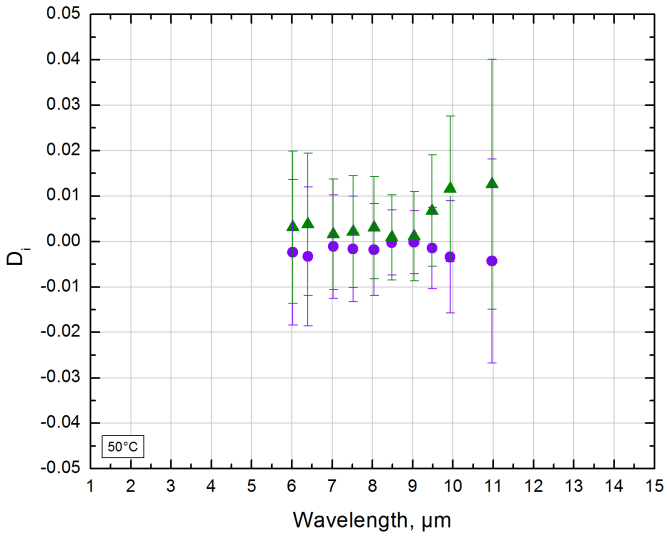

Figure 33. Unilateral DoE of OxIn results at 50 °C.

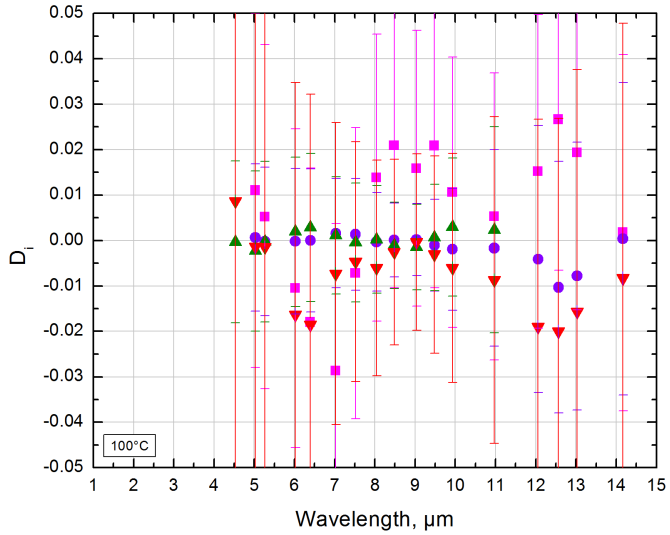

Figure 34. Unilateral DoE of OxIn results at 100 °C.

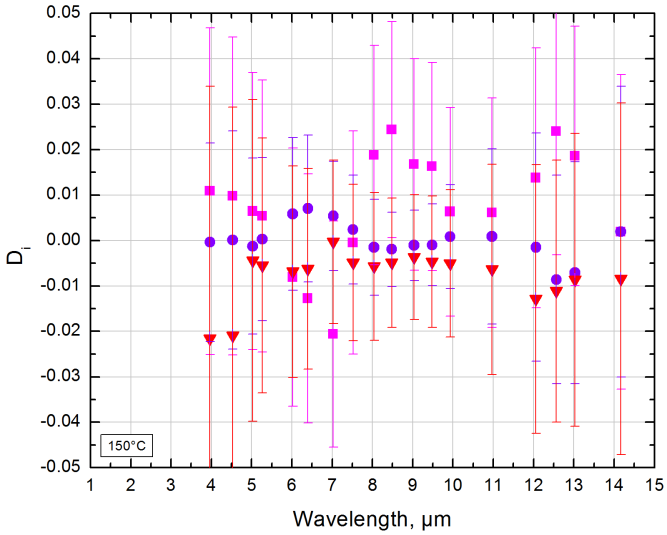

Figure 35. Unilateral DoE of OxIn results at 150 °C.

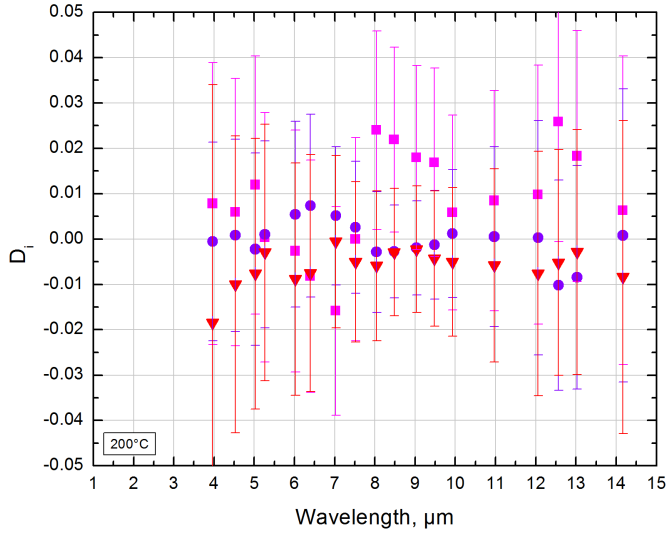

Figure 36. Unilateral DoE of OxIn results at 200 °C.

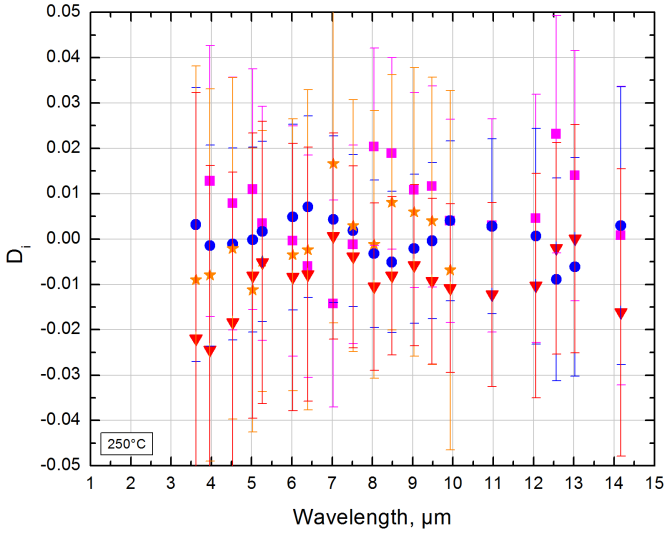

Figure 37. Unilateral DoE of OxIn results at 250 °C.

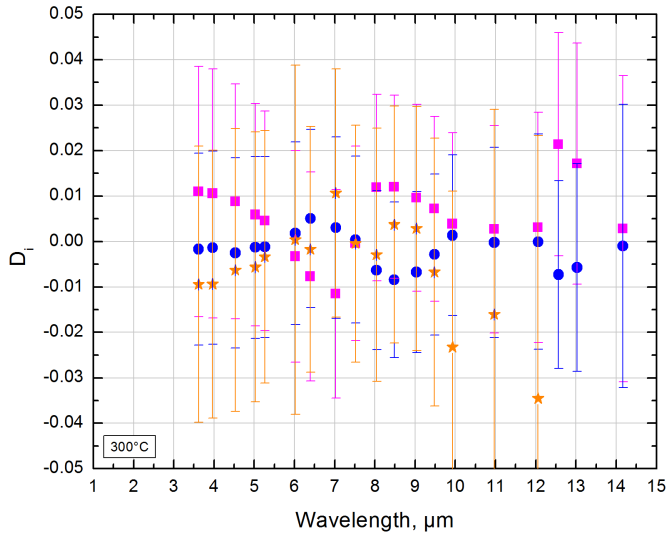

Figure 38. Unilateral DoE of OxIn results at 300 °C.

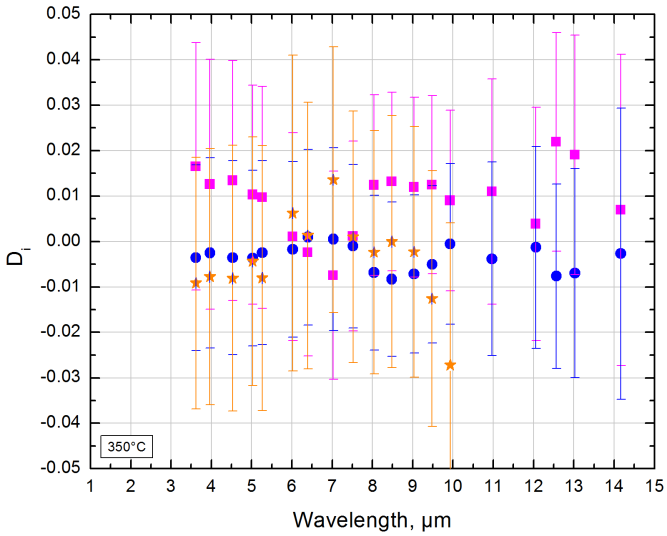

Figure 39. Unilateral DoE of OxIn results at 350 °C.

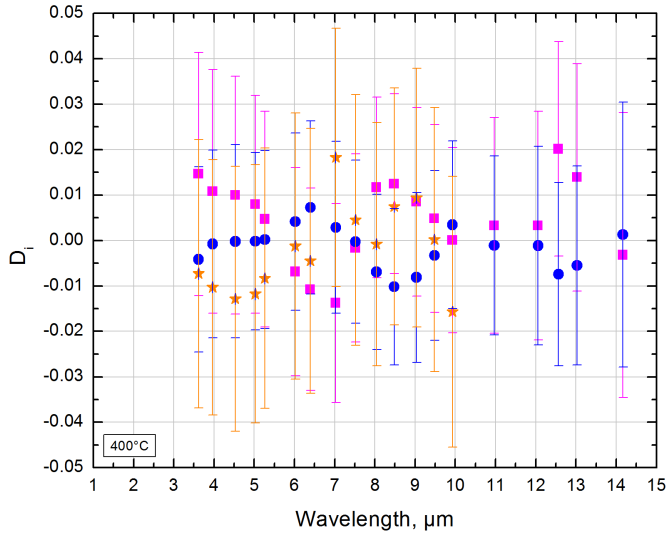

Figure 40. Unilateral DoE of OxIn results at 400 °C.

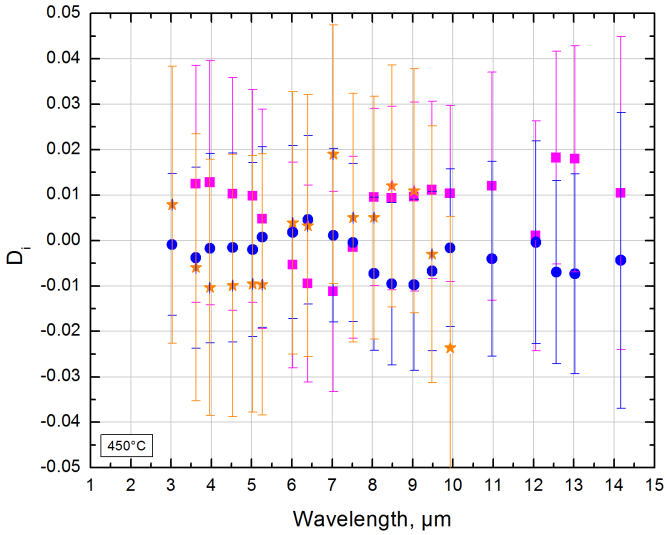

Figure 41. Unilateral DoE of OxIn results at 450 °C.

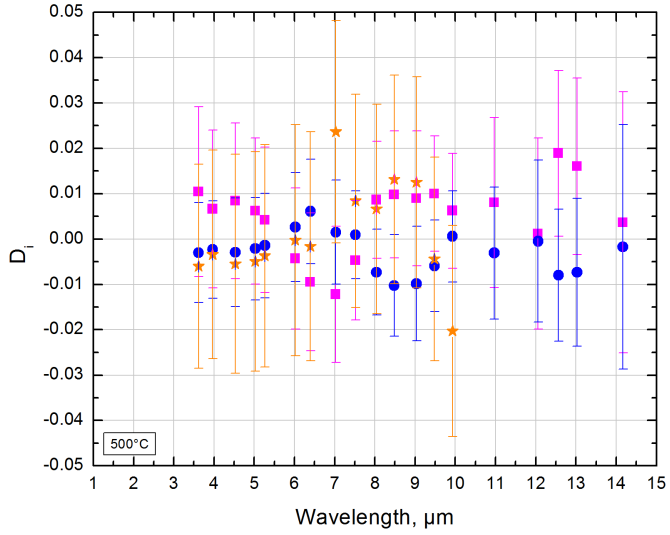

Figure 42. Unilateral DoE of OxIn results at 500 °C.

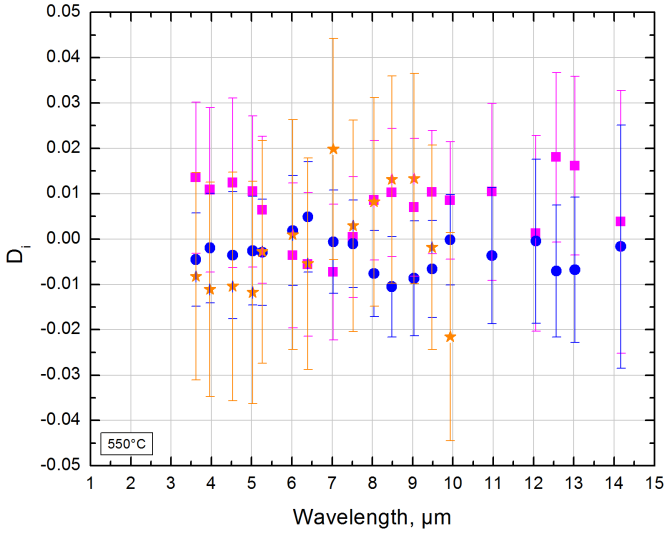

Figure 43. Unilateral DoE of OxIn results at 550 °C.

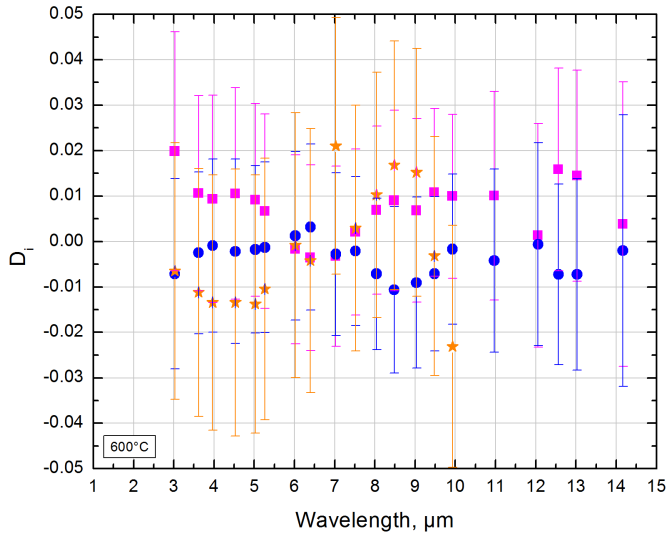

Figure 44. Unilateral DoE of OxIn results at 600 °C.

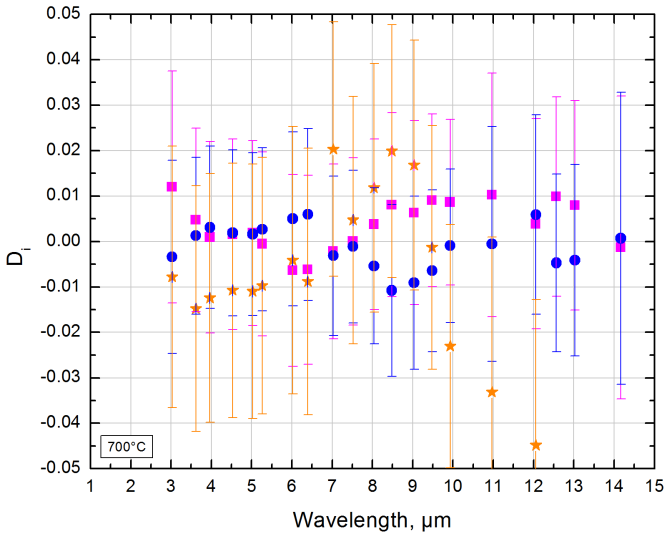

Figure 45. Unilateral DoE of OxIn results at 700 °C.

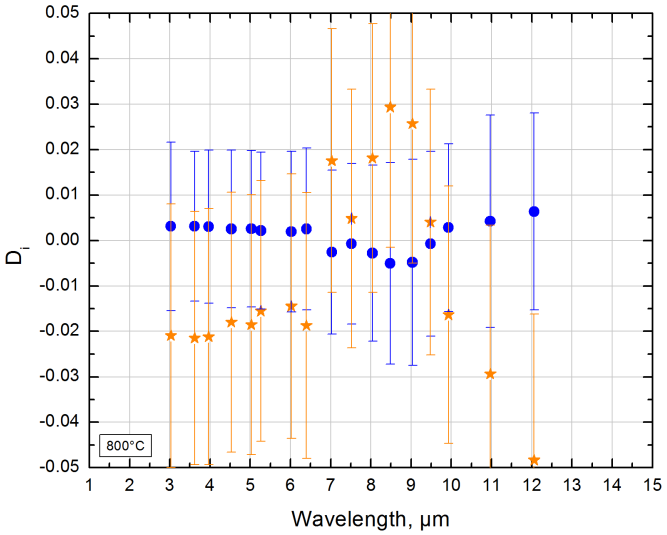

Figure 46. Unilateral DoE of OxIn results at 800 °C.

3.3 Silicon Carbide

An overview of the temperature dependent spectral emittance of the NIST SiC artefact is shown in Figure 47. Curves of emittance for each temperature from 23 °C to 800 °C are shown in (a), and curves for the change in emittance from that at 23 °C are shown in (b).

The unilateral relative DoE: the relative deviations and their expanded uncertainties (as error bars) for the SiC measurements are shown in Figure 48 to Figure 62. The results are also tabulated in Appendix A.

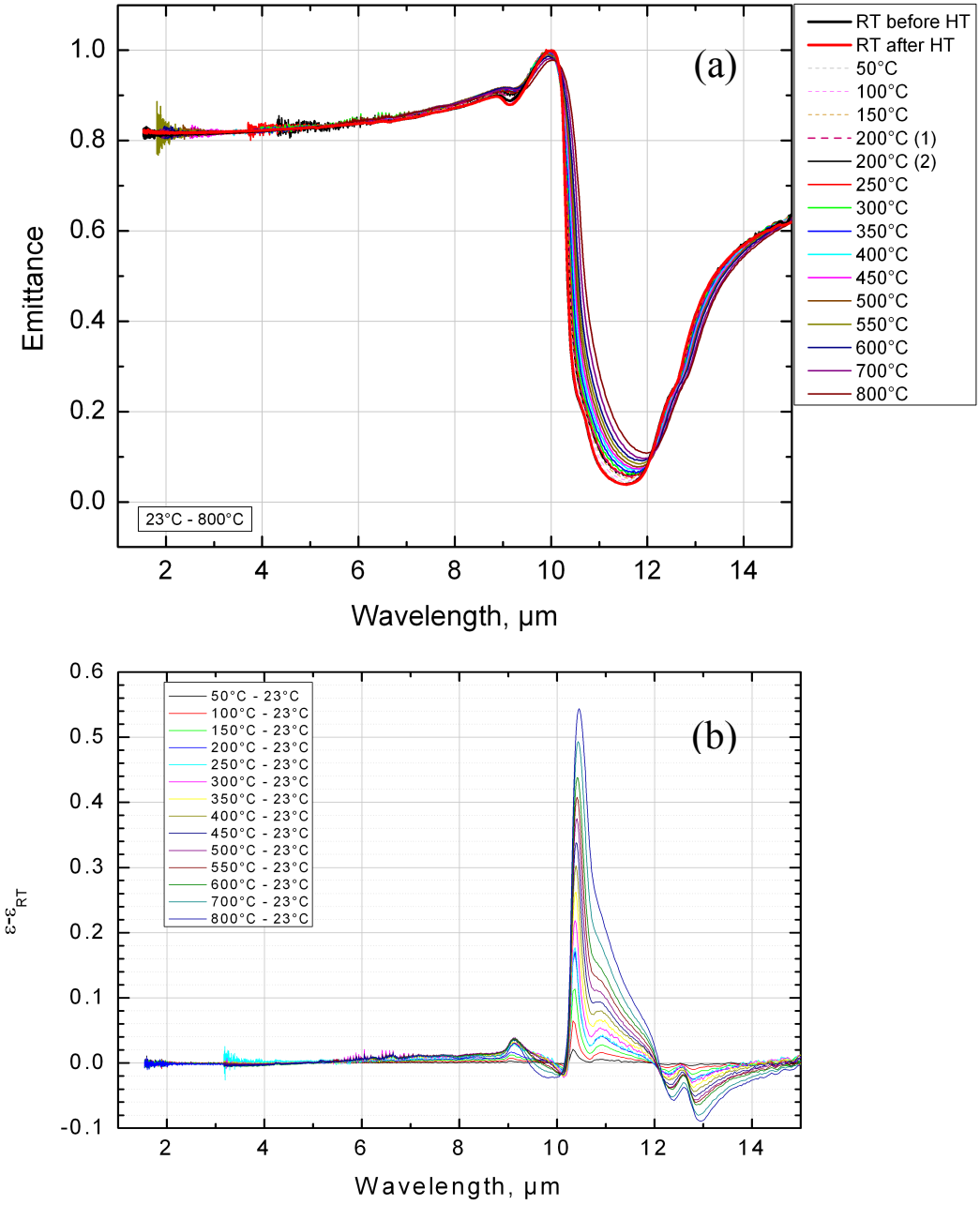

Figure 47. NIST spectral emittance results for SiC: a) spectral emittance, and b) emittance difference from that at room temperature.

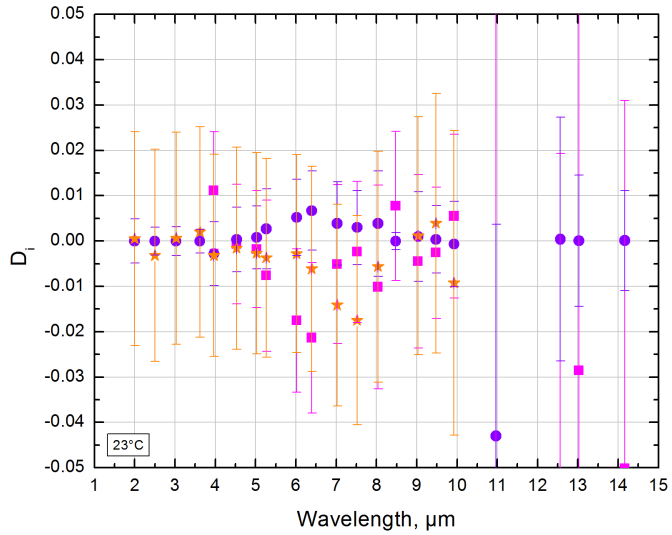

Figure 48. Unilateral DoE of SiC results at 23 °C.

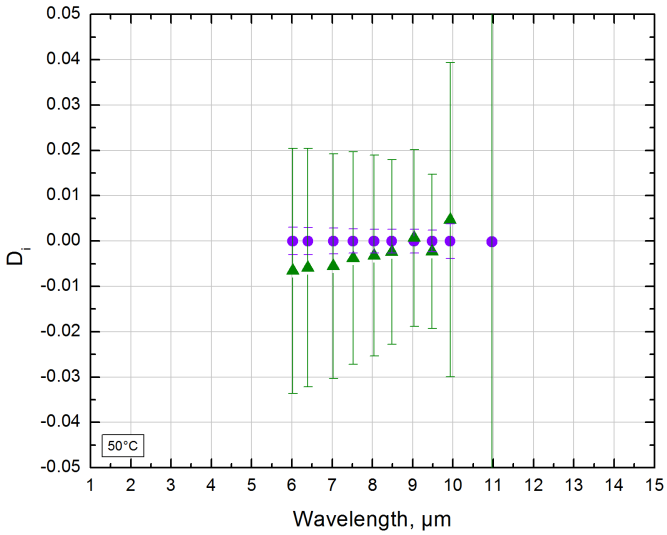

Figure 49. Unilateral DoE of SiC results at 50 °C.

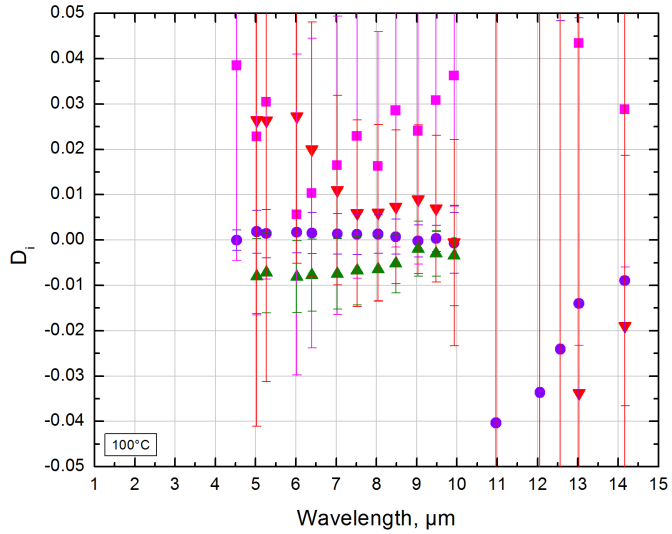

Figure 50. Unilateral DoE of SiC results at 100 °C.

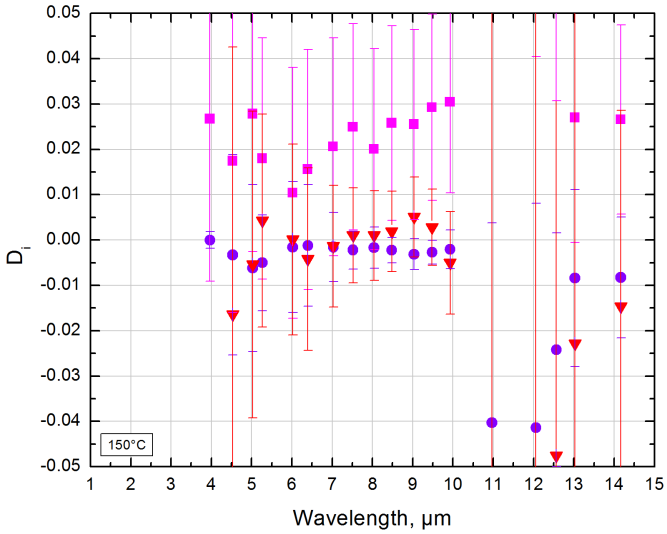

Figure 51. Unilateral DoE of SiC results at 150 °C.

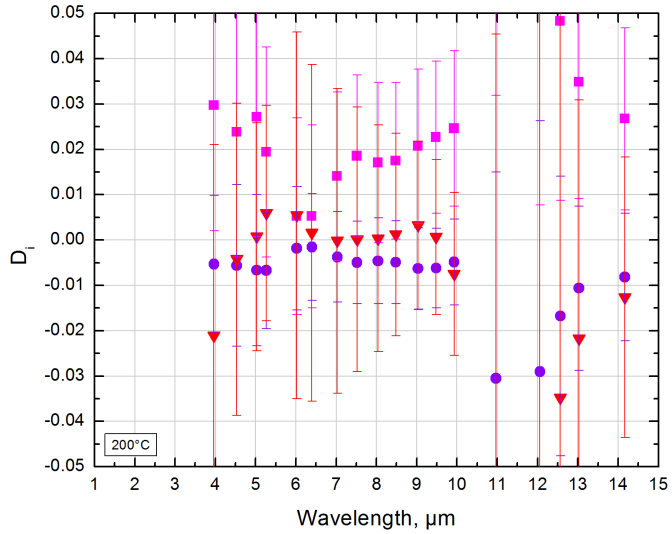

Figure 52. Unilateral DoE of SiC results at 200 °C.

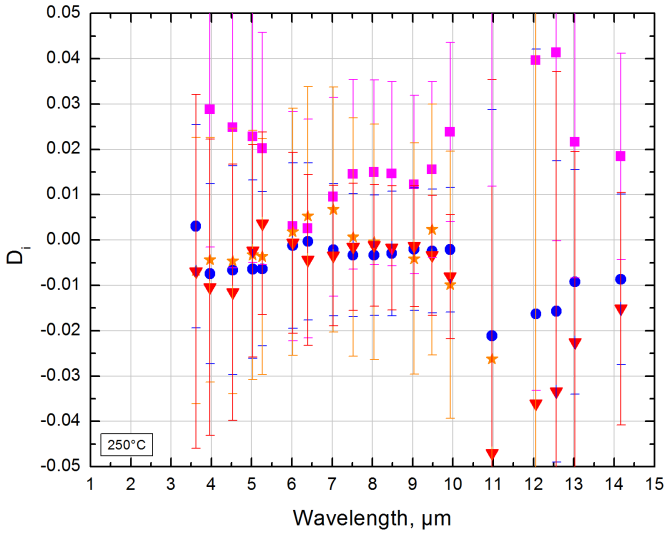

Figure 53. Unilateral DoE of SiC results at 250 °C.

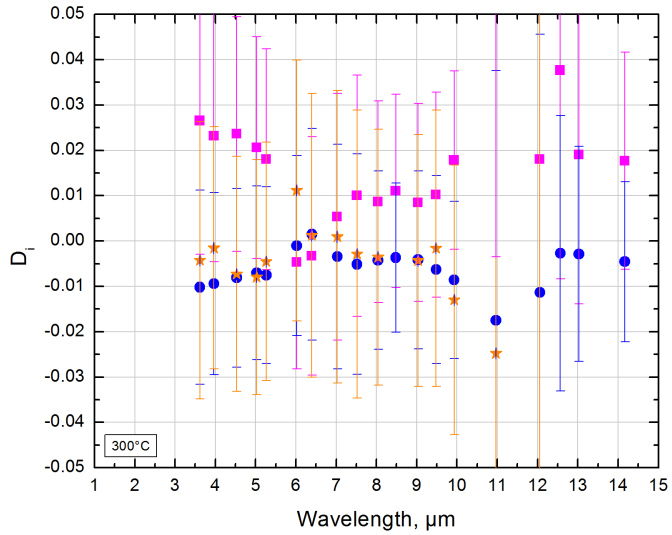

Figure 54. Unilateral DoE of SiC results at 300 °C.

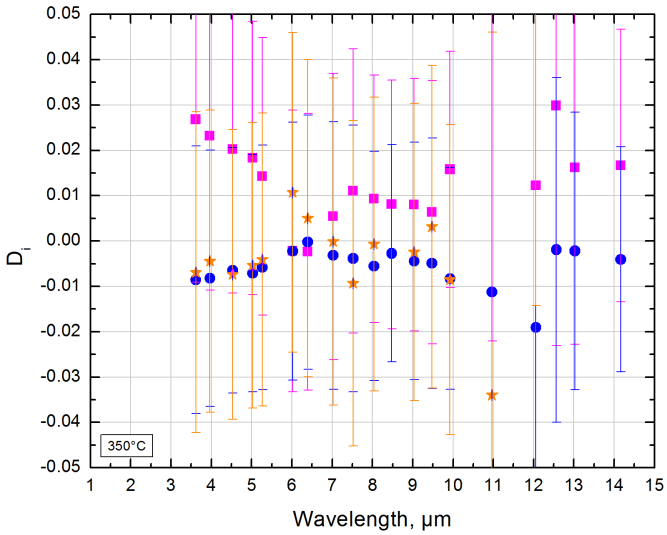

Figure 55. Unilateral DoE of SiC results at 350 °C.

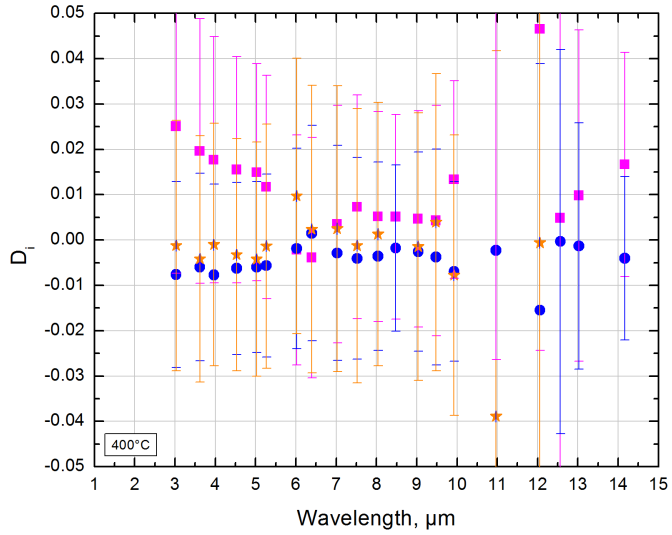

Figure 56. Unilateral DoE of SiC results at 400 °C.

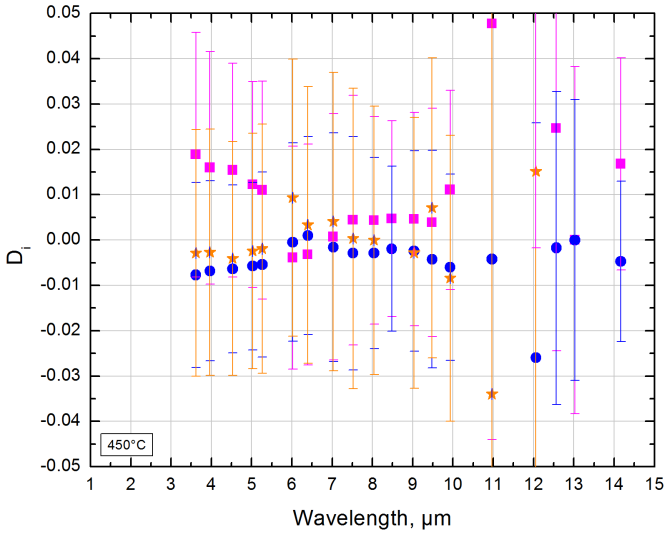

Figure 57. Unilateral DoE of SiC results at 450 °C.

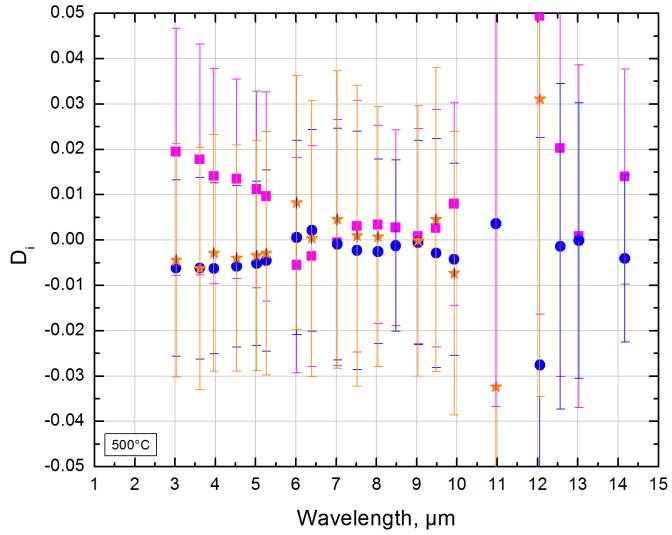

Figure 58. Unilateral DoE of SiC results at 500 °C.

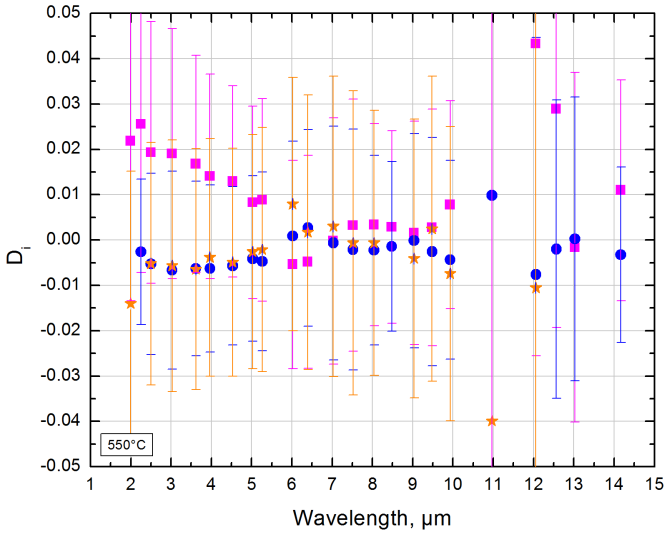

Figure 59. Unilateral DoE of SiC results at 550 °C.

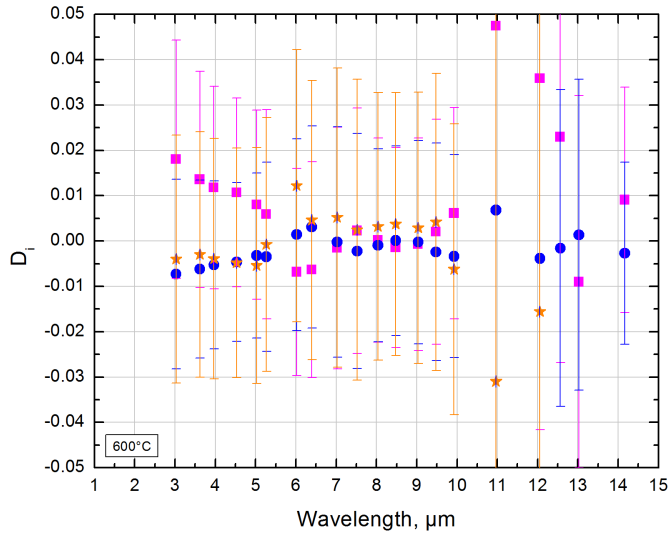

Figure 60. Unilateral DoE of SiC results at 600 °C.

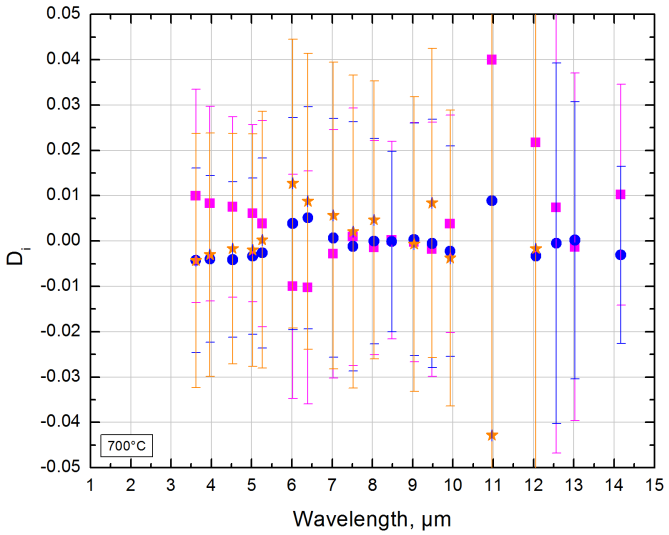

Figure 61. Unilateral DoE of SiC results at 700 °C.

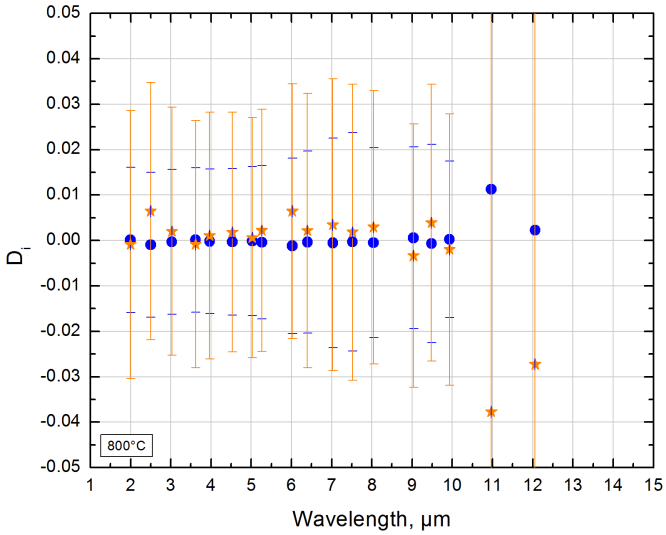

Figure 62. Unilateral DoE of SiC results at 800 °C.

3.4 Error Function Results

To analyse the DoE data shown in the plots and tables, we use the Error function given by Equation 18, which is a ratio of the expanded uncertainty of the relative deviations, $U(D\text{i})$ relative to the absolute value of the relative deviations Di. For the case in which the relative deviation is equal to the uncertainty, $E = 1$. All of the results have been combined into 3 summary plots shown in Figure 63 to Figure 65 for BN, OxIn, and SiC, respectively.

We see that the maximum $E_i(\lambda,T)$ is slightly less than 1.0 for BN, 1.5 for OxIn, and slightly less than 2.0 for SiC. Since we only consider a result to be outliers for $E_i \geq 3.0$, none of the results are in this category.

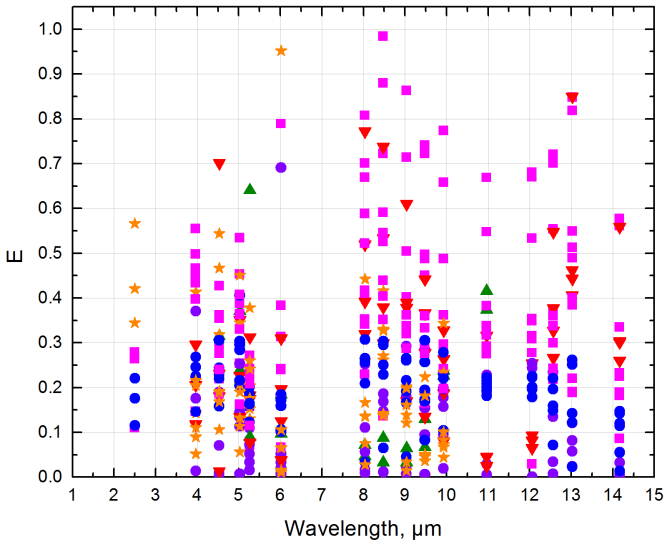

Figure 63. Summary plot of the Error function results for BN.

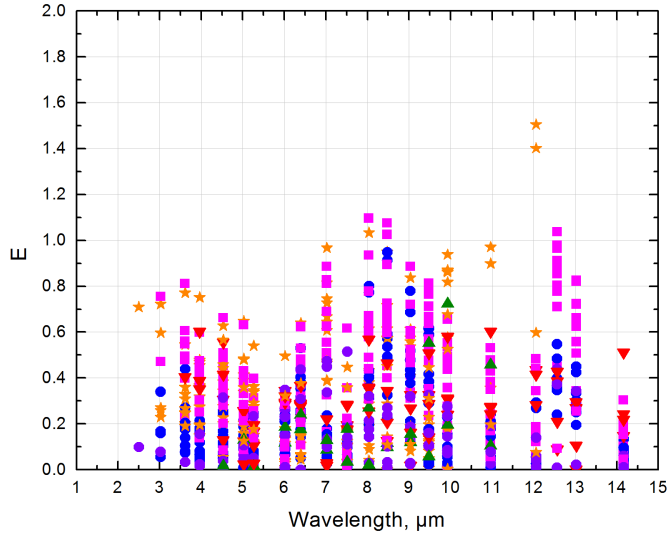

Figure 64. Summary plot of the Error function results for OxIn.

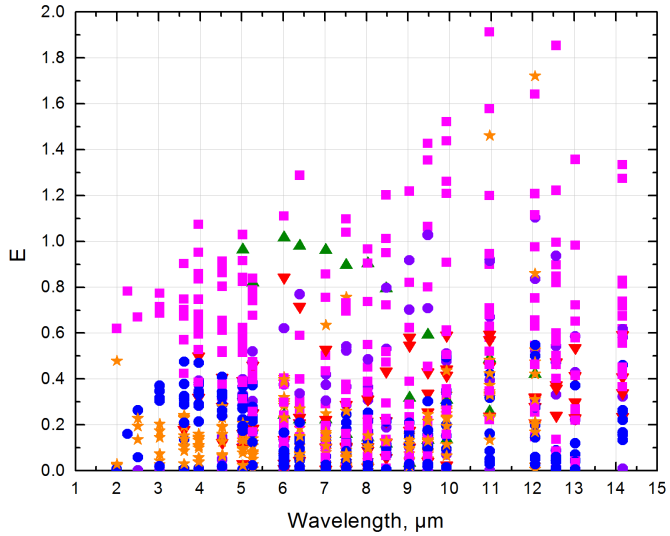

Figure 65. Summary plot of the Error function results for SiC.

The numbers of instances of the Error function, $E_i > 1$, for the entire set of results, are sorted by material and NMI in Table 14. The rate for the entire data set of 2041 points is 1.9 %. The overall rate for each NMI is less than 5 %, which indicates good overall agreement among the NMIs. Only for SiC does NMI #2 have a higher rate of 10.9 %. Several factors distinguish SiC from the other two materials and may account for the higher discrepancy rate. The SiC artefacts are polished and specular, which may interact differently to the background, as compared to the more diffuse artefacts of BN and OxIn. Secondly, the emittance nearly varies over the complete range of 0 to 1 in a short spectral range, from 10 µm to 14 µm. Hence errors in the spectral transmittance of the filters and detector responsivity will lead to offsets between NMI #2 and the rest.

Table 14. Number of instances of data points with the Error function greater than 1.

Material	**BN**			**OxIn**			**SiC**					**Totals**
NMI	**Total #**	**$E_i > 1$**	**Rate, %**	**Total #**	**$E_i > 1$**	**Rate, %**	**Total #**	**$E_i > 1$**	**Rate, %**	**$E_i > 1.5$**	**Rate, %**	**Rate %**
1	19	0	0	23	0	0	23	1	4.4	0	0	0
2	149	0	0	242	4	1.7	248	27	10.9	5	2.0	4.9
3	162	0	0	274	0	0	281	1	0.3	0	0	0.1
4	73	0	0	168	3	1.8	178	2	1.1	1	0.6	1.2
5	59	0	0	72	0	0	70	0	0.0	0	0	0
Totals	462	0	0	779	7	0.9	800	31	3.9	6	0.8	1.9

4 SUMMARY AND CONCLUSIONS

This CCT supplementary comparison investigated the agreement and the variability in infrared spectral emittance measurements performed by five NMIs. Artefacts of three different candidate standard materials, boron nitride, oxidized Inconel, and silicon carbide, were produced and measured by all laboratories. Due to the incompatible sample size requirements of their measurement instrumentation, sets of different sized specimens of the three materials were produced and measured. The pilot laboratory performed emittance measurements of all the artefacts, but only at room temperature (23 °C).

Spectral emittance measurements were performed over varying wavelength and temperature ranges by the NMIs, extending from 23 °C to 800 °C. Different portions of these ranges include results from two, three and four NMIs, repectively, and over which the comparisons were made. Several factors, including artefact-to-artefact variability, artefact stability, differing spectral resolutions, and differing data intervals were encountered and accommodated in the data processing. In planning any future comparisons, these factors warrant a high degree of consideration. It may be necessary to limit the comparison to smaller temperature and spectral ranges and/or to those participants with similar instrumental parameters such as spectral resolution and sample size accommodation. In any case, preliminary studies of the selected artefact materials are a crucial element, which can lessen the chance of unforseen problems during the intercomparison process.

Analysis of the results indicated good agreement between the NMIs considering the relative deviations and their uncertainties. Although some of the subsets of the results contained data with variation greater than expected for $k = 2$ expanded uncertainties (i.e. rate of 5 % outside), the deviations were not sufficient to be considered outliers.

The results of this comparison form a foundation for the establishment of CMCs (Calibration and Measurement Capabilities) at the participant NMIs, as well as a basis for future Key and Supplementary Comparisons of infrared emittance.

REFERENCES

[1] J. Hameury and W. Sabuga, "Bilateral intercomparison of total hemispherical emissivity and normal spectral emissivity measurements at BNM-LNE and PTB," (1999).

[2] M. Battuello, S. Clausen, J. Hameury, and P. Bloembergen, "The spectral emissivity of surface layers, currently applied in blackbody radiators, covering the spectral range from 0,9 to 20 μm: an international comparison," Proc. TEMPMEKO 1999, ed. TNO, 601-606 (1999).

[3] S. Redgrove, M. Battuello, "An intercomparison of normal spectral emissivity measurements between NPL (UK) and IMGC (Italy)", High Temp.-High Press. **27/28**, 135-146 (1995/1996).

[4] National Bureau of Standards Standard Reference Materials 1440 - 1447.

[5] B. Zhang, J. Redgrove, J. Clark, 2003/2007, "New apparatus for measurement of the spectral, angular, and total emissivity of solids" High Temp.-High Press. **35/36**(3), 289 – 302 (2004).

[6] C. P. Cagran, L. M. Hanssen, M. Noorma, A. V. Gura, S. N. Mekhontsev, "Temperature-resolved infrared spectral normal emissivity of SiC and Pt-10Rh for temperatures up to 900 °C," Intl. J. Thermophys. **28**, No. 2, 581-597 (2007).

[7] J. Ishii and A. Ono, "A Fourier transform spectrometer for accurate thermometric applications at low temperatures," AIP Conf. Proc., **684**, 705-710 (2003).

[8] A. Shimota, H. Kobayashi, and S. Kadokura, "Radiometric calibration for the airborne interferometric monitor for greenhouse gases simulator," Appl. Opt. **38**, 571–576 (1999).

[9] J. Ishii and A. Ono, "Uncertainty estimation for emissivity measurements near room temperature with a Fourier transform spectrometer," Meas. Sci. Technol. **12**, 2103-2112 (2001).

[10] J. Hameury, B. Hay and J.-R. Filtz, "Measurement of Infrared Spectral Directional Hemispherical Reflectance and Emissivity at BNM-LNE 1" Int. J. Thermophys. **26,** 1973-1983 (2005).

[11] J. Hameury, "Determination of uncertainties for emissivity measurements in the temperature range 200 - 800 °C", High Temp.-High Press. **30**, 223-228 (1998).

[12] L. M. Hanssen and K. A. Snail, "Integrating Spheres for Mid- and Near-Infrared Reflectometry" in *Handbook of Vibrational Spectroscopy*, Vol. 2, J. M. Chalmers and P. R. Griffiths, eds. (John Wiley & Sons, Ltd., Chichester, United Kingdom, 2002), 1175-1192.

[13] L. M. Hanssen and S. G. Kaplan, "Infrared diffuse reflectance instrumentation and standards at NIST," Anal. Chim. Acta **380,** 289-302 (1999).

[14] L. Hanssen, S. Kaplan, and S. Mekhontsev, "Fourier transform system for characterization of infrared spectral emittance of materials" in Proceedings TEMPMEKO 2001,VDE Verlag, Berlin, 265-270, (2002).

[15] L. M. Hanssen, S. N. Mekhontsev, and V. B. Khromchenko, "Infrared spectral emissivity characterization facility at NIST", Proc. SPIE **5405**, 1-12 (2004).

[16] L. M. Hanssen and S. N. Mekhontsev, "Low scatter optical system for emittance and temperature measurements," AIP Conf. Proc. **684**, 693-698 (2003).

[17] M. Battuello, T. Ricolfi, "A technique for deriving emissivity data for infrared pyrometry", High Temp.-High-Press. **21**, 303-309 (1989).

[18] L. M. Hanssen, C. P. Cagran, A. V. Prokhorov, S. N. Mekhontsev, and V. B. Khromchenko, "Use of a high-temperature integrating sphere reflectometer for surface-temperature measuremens," Int. J. Thermophys. **28**, No. 2, 566-580 (2007).
[19] T. Ricolfi, M. Battuello, F. Lanza, "Heat-pipe black-body reflectometer for room temperature emissivity measurements", J. Phys. E: Sci. Instrum. **19**, 697-700 (1986).
[20] M. Battuello, F. Lanza, T. Ricolfi, "A simple apparatus for measuring the normal spectral emissivity in the temperature range 600-1000 °C", in Proc. 2nd Symp. on Temperature Measurement in Industry and Science , IMEKO TC 12, Suhl, 125-130 (1984).
[21] C. Monte, B. Gutschwager, S. P. Morozova, and J. Hollandt, "Radiation thermometry and emissivity measurements under vacuum at the PTB," Int. J. Thermophys. **30**, 203-219 (2009).
[22] C. Monte and J. Hollandt, "The determination of the uncertainties of spectral emissivity measurements in air at the PTB," Metrologia **47**, 172-181 (2010).
[23] Joint Committee for Guides in Metrology (JCGM) "2008 Evaluation of Measurement Data—Supplement 1 to the 'Guide to the Expression of Uncertainty in Measurement'—Propagation of Distributions Using a Monte Carlo Method", JCGM 101:2008 (2008).
[24] R. Köhler, M. Stock and C. Garreau, "Final Report on the International Comparison of Luminous Responsivity CCPR-K3.b" (Appendix 4), Metrologia **41**, Tech. Suppl., 02001(2004).
[25] Appendix B of "Guidelines for CCPR Key Comparison Report Preparation", CCPR-G2.pdf, rev. 3, 2013, available on the kcdb.bipm.org website (http://www.bipm.org/en/committees/cc/ccpr/publications-cc.html).

Appendix A
Degrees of Equivalence Results Tables

The following Tables contain the final results of the infrared spectral emittance intercomparison CCT-S1. The tables are separated according to artefact material and temperature. The quantities shown are:

Em … measured emittance (corrected and normalized, = ε_i'')
U_{Em} … corresponding expanded uncertainty for *Em*
Degrees of Equivalence:
    D_i … Relative Deviation
    U_i … corresponding expanded uncertainty for D_i
E … Error function
ε_{CRV} … nominal comparison reference value
$U_{cut\text{-}off}$ … Cut-off limit for weighting

Table 15. Relative DoE for BN at 23 °C.

	LNE					NIST					INRIM						
CWL, µm	Em	U_{Em}	D_i	U_i	E	Em	U_{Em}	D_i	U_i	E	Em	U_{Em}	D_i	U_i	E	ε_{CRV}	$U_{cut\text{-}off}$
1.997																	
2.253																	
2.500																	
3.026																	
3.615																	
3.965						0.915	0.002	7E-05	0.005	0.014	0.903	0.028	-0.013	0.031	0.413	0.915	0.002
4.530						0.924	0.002	5E-05	0.006	0.009	0.911	0.027	-0.014	0.030	0.467	0.924	0.002
5.026	0.933	0.007	-0.002	0.007	0.254	0.935	0.001	0.001	0.005	0.134	0.933	0.028	-0.002	0.030	0.056	0.935	0.004
5.265	0.947	0.013	-0.001	0.011	0.070	0.949	0.001	5E-04	0.004	0.110	0.945	0.028	-0.004	0.029	0.130	0.948	0.007
6.019	0.876	0.013	-0.009	0.012	0.789	0.888	0.002	0.004	0.006	0.691	0.826	0.061	-0.066	0.069	0.952	0.884	0.007
6.395																	
7.026																	
7.518																	
8.040	0.804	0.022	-0.005	0.023	0.229	0.811	0.004	0.003	0.012	0.252	0.804	0.027	-0.005	0.031	0.166	0.808	0.013
8.479	0.827	0.016	-0.002	0.017	0.137	0.830	0.003	0.001	0.009	0.147	0.825	0.027	-0.004	0.031	0.142	0.829	0.009
9.034	0.843	0.019	-0.006	0.019	0.330	0.851	0.003	0.003	0.009	0.292	0.846	0.027	-0.004	0.030	0.121	0.849	0.011
9.479	0.848	0.015	-0.008	0.015	0.488	0.857	0.003	0.003	0.009	0.285	0.854	0.028	8E-05	0.032	0.002	0.854	0.009
9.927	0.856	0.017	-0.003	0.018	0.192	0.859	0.002	0.001	0.010	0.095	0.860	0.028	0.001	0.032	0.044	0.859	0.010
10.966	0.862	0.023	-0.006	0.029	0.214	0.867	0.002	6E-05	0.010	0.006						0.867	0.002
12.058	0.854	0.023	-0.001	0.029	0.029	0.855	0.002	8E-06	0.011	0.001						0.855	0.002
12.565	0.852	0.029	-0.007	0.034	0.218	0.858	0.003	7E-05	0.009	0.008						0.858	0.003
13.025	0.839	0.030	-0.018	0.035	0.513	0.855	0.003	2E-04	0.008	0.024						0.854	0.003
14.165	0.836	0.042	-0.030	0.052	0.577	0.862	0.003	1E-04	0.017	0.008						0.862	0.003

Table 16. Relative DoE for BN at 50 °C.

	NIST					NMIJ						
CWL, µm	Em	U_{Em}	D_i	U_i	E	Em	U_{Em}	D_i	U_i	E	ε_{CRV}	$U_{cut\text{-}off}$
1.997												
2.253												
2.500												
3.026												
3.615												
3.965												
4.530	0.924	0.002	-5E-05	0.006	0.009	0.929	0.018	0.006	0.020	0.315	0.924	0.002
5.026	0.937	0.001	4E-05	0.005	0.007	0.930	0.017	-0.007	0.019	0.370	0.937	0.001
5.265	0.942	0.001	6E-05	0.004	0.016	0.932	0.016	-0.011	0.018	0.640	0.942	0.001
6.019	0.866	0.003	1E-04	0.006	0.020	0.863	0.017	-0.004	0.020	0.184	0.866	0.003
6.395												
7.026												
7.518												
8.040	0.811	0.005	1E-04	0.010	0.009	0.810	0.022	-0.002	0.029	0.072	0.811	0.005
8.479	0.833	0.004	1E-04	0.008	0.012	0.831	0.020	-0.002	0.025	0.088	0.833	0.004
9.034	0.852	0.004	6E-05	0.008	0.007	0.851	0.018	-0.001	0.022	0.064	0.852	0.004
9.479	0.857	0.003	-6E-05	0.009	0.007	0.859	0.017	0.001	0.022	0.067	0.857	0.003
9.927	0.860	0.003	-2E-04	0.009	0.019	0.864	0.017	0.005	0.021	0.227	0.860	0.003
10.966	0.867	0.003	-3E-04	0.010	0.029	0.873	0.016	0.008	0.020	0.374	0.867	0.003
12.058												
12.565												
13.025												
14.165												

Table 17. Relative DoE for BN at 100 °C.

	LNE					NIST					NMIJ					PTB						
CWL, µm	Em	U_{Em}	D_i	U_i	E	Em	U_{Em}	D_i	U_i	E	Em	U_{Em}	D_i	U_i	E	Em	U_{Em}	D_i	U_i	E	ε_{CRV}	$U_{cut\text{-}off}$
1.997																						
2.253																						
2.500																						
3.026																						
3.615																						
3.965																						
4.530						0.924	0.002	-5E-05	0.014	0.004						0.953	0.039	0.031	0.045	0.701	0.924	0.002
5.026	0.950	0.034	0.013	0.038	0.331	0.937	0.001	-0.001	0.012	0.113	0.941	0.005	0.003	0.013	0.239	0.952	0.039	0.015	0.043	0.351	0.938	0.003
5.265	0.941	0.033	-0.003	0.039	0.080	0.945	0.001	0.001	0.018	0.033	0.943	0.005	-0.002	0.018	0.089	0.951	0.037	0.008	0.043	0.174	0.944	0.003
6.019	0.865	0.029	-0.012	0.052	0.240	0.874	0.003	-0.002	0.041	0.052	0.879	0.006	0.004	0.041	0.097	0.885	0.027	0.010	0.051	0.197	0.876	0.004
6.395																						
7.026																						
7.518																						
8.040	0.828	0.023	0.021	0.031	0.669	0.811	0.005	-3E-04	0.016	0.017	0.810	0.009	-0.001	0.017	0.046	0.801	0.023	-0.012	0.031	0.392	0.811	0.007
8.479	0.847	0.023	0.017	0.029	0.591	0.832	0.004	-1E-04	0.013	0.011	0.832	0.008	0.000	0.014	0.033	0.823	0.022	-0.011	0.029	0.379	0.832	0.006
9.034	0.862	0.022	0.011	0.028	0.402	0.852	0.004	-3E-04	0.012	0.023	0.852	0.007	0.000	0.013	0.033	0.843	0.022	-0.011	0.028	0.378	0.852	0.005
9.479	0.870	0.022	0.014	0.028	0.497	0.857	0.003	-0.001	0.012	0.095	0.859	0.007	0.002	0.013	0.129	0.849	0.022	-0.010	0.028	0.366	0.858	0.005
9.927	0.872	0.022	0.014	0.028	0.487	0.859	0.003	-0.002	0.012	0.157	0.864	0.007	0.003	0.013	0.237	0.853	0.023	-0.009	0.028	0.327	0.861	0.005
10.966	0.876	0.021	0.008	0.027	0.285	0.866	0.003	-0.003	0.012	0.228	0.874	0.007	0.005	0.013	0.415	0.861	0.023	-0.009	0.028	0.316	0.869	0.005
12.058	0.870	0.021	0.014	0.025	0.533	0.856	0.003	-0.003	0.015	0.179						0.852	0.024	-0.007	0.029	0.254	0.858	0.012
12.565	0.866	0.020	0.009	0.024	0.371	0.858	0.004	-0.001	0.015	0.034						0.849	0.024	-0.011	0.029	0.377	0.858	0.012
13.025	0.865	0.019	0.012	0.024	0.490	0.854	0.004	-0.001	0.015	0.082						0.844	0.024	-0.013	0.029	0.443	0.855	0.012
14.165	0.869	0.019	0.007	0.039	0.189	0.863	0.005	-9E-05	0.035	0.002						0.853	0.024	-0.011	0.043	0.260	0.863	0.012

Table 18. Relative DoE for BN at 150 °C.

	LNE					NIST					PTB						
CWL, µm	Em	U_{Em}	D_i	U_i	E	Em	U_{Em}	D_i	U_i	E	Em	U_{Em}	D_i	U_i	E	ε_{CRV}	$U_{cut\text{-}off}$
1.997																	
2.253																	
2.500																	
3.026																	
3.615																	
3.965	0.936	0.036	0.016	0.035	0.450	0.915	0.002	-0.006	0.017	0.371	0.938	0.058	0.018	0.061	0.296	0.921	0.019
4.530	0.941	0.032	0.013	0.037	0.354	0.925	0.002	-0.005	0.025	0.190	0.938	0.050	0.010	0.055	0.180	0.929	0.017
5.026	0.952	0.030	0.012	0.030	0.388	0.937	0.001	-0.004	0.016	0.254	0.946	0.038	0.005	0.038	0.135	0.941	0.016
5.265	0.941	0.028	-0.006	0.027	0.207	0.946	0.001	-0.001	0.013	0.052	0.955	0.030	0.009	0.029	0.312	0.947	0.015
6.019	0.872	0.024	-0.009	0.030	0.313	0.881	0.003	-2E-04	0.020	0.008	0.888	0.023	0.009	0.028	0.310	0.881	0.013
6.395																	
7.026																	
7.518																	
8.040	0.823	0.018	0.016	0.026	0.588	0.809	0.005	-0.001	0.018	0.057	0.804	0.014	-0.007	0.022	0.320	0.810	0.010
8.479	0.851	0.020	0.022	0.025	0.880	0.831	0.004	-0.002	0.014	0.168	0.828	0.014	-0.006	0.019	0.299	0.833	0.009
9.034	0.868	0.018	0.017	0.024	0.714	0.851	0.004	-0.003	0.015	0.180	0.850	0.014	-0.003	0.020	0.169	0.853	0.009
9.479	0.873	0.018	0.018	0.024	0.741	0.856	0.003	-0.003	0.015	0.192	0.856	0.014	-0.003	0.019	0.135	0.858	0.009
9.927	0.874	0.018	0.016	0.024	0.658	0.859	0.003	-0.003	0.015	0.178	0.860	0.014	-0.002	0.019	0.080	0.861	0.008
10.966	0.880	0.018	0.013	0.024	0.548	0.866	0.003	-0.003	0.016	0.191	0.870	0.014	0.001	0.020	0.045	0.869	0.008
12.058	0.874	0.018	0.016	0.024	0.670	0.856	0.003	-0.004	0.016	0.244	0.861	0.014	0.001	0.020	0.065	0.859	0.008
12.565	0.873	0.016	0.016	0.022	0.701	0.858	0.004	-0.002	0.015	0.135	0.855	0.013	-0.005	0.019	0.266	0.859	0.009
13.025	0.870	0.016	0.017	0.021	0.818	0.853	0.004	-0.002	0.014	0.121	0.849	0.013	-0.007	0.018	0.406	0.855	0.009
14.165	0.876	0.016	0.015	0.026	0.572	0.862	0.005	-0.001	0.021	0.056	0.857	0.013	-0.007	0.023	0.301	0.863	0.009

Table 19. Relative DoE for BN at 200 °C.

	LNE					NIST					PTB						
CWL, µm	Em	U_{Em}	D_i	U_i	E	Em	U_{Em}	D_i	U_i	E	Em	U_{Em}	D_i	U_i	E	ε_{CRV}	$U_{cut\text{-}off}$
1.997																	
2.253																	
2.500																	
3.026																	
3.615																	
3.965	0.932	0.028	0.014	0.029	0.498	0.916	0.002	-0.003	0.016	0.176	0.911	0.040	-0.009	0.043	0.206	0.919	0.015
4.530	0.935	0.026	0.009	0.040	0.219	0.925	0.002	-0.002	0.033	0.071	0.927	0.031	-0.001	0.043	0.014	0.927	0.014
5.026	0.958	0.024	0.018	0.034	0.534	0.937	0.001	-0.004	0.027	0.146	0.937	0.027	-0.005	0.036	0.134	0.941	0.013
5.265	0.956	0.022	0.008	0.030	0.271	0.947	0.001	-0.002	0.023	0.072	0.946	0.025	-0.002	0.032	0.078	0.949	0.012
6.019	0.884	0.020	-0.002	0.032	0.067	0.886	0.002	0.001	0.027	0.034	0.884	0.028	-0.001	0.039	0.038	0.886	0.011
6.395																	
7.026																	
7.518																	
8.040	0.824	0.015	0.018	0.022	0.807	0.807	0.005	-0.002	0.018	0.111	0.800	0.013	-0.011	0.021	0.520	0.809	0.009
8.479	0.848	0.015	0.020	0.021	0.984	0.829	0.004	-0.003	0.016	0.187	0.823	0.013	-0.010	0.019	0.533	0.832	0.009
9.034	0.868	0.015	0.018	0.021	0.863	0.850	0.004	-0.003	0.016	0.168	0.845	0.013	-0.008	0.020	0.389	0.852	0.008
9.479	0.870	0.015	0.015	0.020	0.722	0.855	0.003	-0.002	0.015	0.155	0.853	0.013	-0.005	0.019	0.277	0.857	0.008
9.927	0.875	0.015	0.016	0.021	0.773	0.858	0.003	-0.003	0.016	0.200	0.858	0.012	-0.004	0.019	0.188	0.861	0.008
10.966	0.882	0.015	0.015	0.022	0.669	0.866	0.003	-0.004	0.017	0.223	0.870	0.012	0.001	0.020	0.025	0.869	0.007
12.058	0.873	0.015	0.015	0.023	0.680	0.856	0.003	-0.004	0.018	0.254	0.862	0.011	0.002	0.020	0.093	0.860	0.007
12.565	0.872	0.013	0.014	0.020	0.721	0.858	0.004	-0.002	0.016	0.135	0.854	0.011	-0.006	0.018	0.327	0.859	0.007
13.025	0.869	0.015	0.017	0.021	0.848	0.853	0.004	-0.001	0.015	0.058	0.847	0.011	-0.008	0.017	0.462	0.854	0.008
14.165	0.874	0.015	0.014	0.025	0.561	0.861	0.005	-0.001	0.021	0.032	0.856	0.011	-0.007	0.023	0.303	0.862	0.008

Table 20. Relative DoE for BN at 250 °C.

	LNE					NIST					PTB					INRIM						
CWL, µm	Em	U_{Em}	D_i	U_i	E	Em	U_{Em}	D_i	U_i	E	Em	U_{Em}	D_i	U_i	E	Em	U_{Em}	D_i	U_i	E	ε_{CRV}	$U_{cut\text{-}off}$
1.997																						
2.253																						
2.500																						
3.026																						
3.615																						
3.965	0.940	0.024	0.014	0.031	0.455	0.922	0.009	-0.005	0.024	0.221	0.922	0.033	-0.005	0.039	0.118	0.923	0.038	-0.004	0.044	0.090	0.927	0.017
4.530	0.943	0.022	0.007	0.040	0.186	0.931	0.009	-0.006	0.036	0.158	0.927	0.024	-0.010	0.041	0.231	0.951	0.036	0.016	0.050	0.318	0.936	0.016
5.026	0.959	0.020	0.012	0.032	0.364	0.942	0.009	-0.006	0.028	0.205	0.941	0.022	-0.007	0.033	0.227	0.953	0.037	0.005	0.045	0.114	0.948	0.015
5.265	0.962	0.020	0.007	0.032	0.210	0.952	0.009	-0.003	0.028	0.123	0.950	0.021	-0.006	0.032	0.182	0.965	0.040	0.010	0.048	0.204	0.956	0.015
6.019	0.886	0.016	-0.009	0.024	0.383	0.898	0.009	0.004	0.021	0.185	0.898	0.024	0.004	0.031	0.125	0.901	0.065	0.008	0.074	0.107	0.894	0.013
6.395																						
7.026																						
7.518																						
8.040	0.827	0.013	0.015	0.022	0.701	0.813	0.008	-0.001	0.019	0.034	0.801	0.011	-0.016	0.021	0.772	0.805	0.031	-0.011	0.041	0.261	0.814	0.010
8.479	0.848	0.013	0.015	0.021	0.722	0.835	0.008	-0.001	0.018	0.066	0.824	0.011	-0.014	0.020	0.738	0.824	0.034	-0.014	0.044	0.327	0.836	0.010
9.034	0.865	0.013	0.010	0.020	0.504	0.856	0.008	-0.001	0.017	0.045	0.847	0.011	-0.011	0.018	0.610	0.857	0.036	0.001	0.044	0.014	0.856	0.010
9.479	0.870	0.013	0.009	0.021	0.451	0.861	0.008	-0.001	0.018	0.082	0.855	0.011	-0.008	0.019	0.442	0.864	0.033	0.002	0.041	0.049	0.862	0.009
9.927	0.872	0.013	0.008	0.022	0.361	0.863	0.008	-0.002	0.019	0.105	0.860	0.010	-0.005	0.020	0.264	0.869	0.042	0.005	0.052	0.101	0.865	0.009
10.966	0.881	0.013	0.008	0.022	0.382	0.871	0.008	-0.004	0.019	0.201	0.873	0.010	-0.001	0.020	0.046						0.874	0.009
12.058	0.870	0.013	0.007	0.025	0.277	0.861	0.008	-0.004	0.023	0.179	0.866	0.009	0.002	0.023	0.082						0.864	0.009
12.565	0.873	0.013	0.011	0.020	0.554	0.863	0.008	-0.001	0.017	0.071	0.856	0.009	-0.009	0.017	0.548						0.864	0.009
13.025	0.868	0.011	0.010	0.017	0.549	0.859	0.008	-4E-04	0.016	0.023	0.848	0.009	-0.013	0.016	0.849						0.860	0.009
14.165	0.874	0.011	0.008	0.023	0.335	0.868	0.008	3E-04	0.021	0.014	0.857	0.009	-0.012	0.022	0.559						0.867	0.009

Table 21. Relative DoE for BN at 300 °C.

	LNE					NIST					INRIM						
CWL, µm	Em	U_{Em}	D_i	U_i	E	Em	U_{Em}	D_i	U_i	E	Em	U_{Em}	D_i	U_i	E	ε_{CRV}	$U_{cut\text{-}off}$
1.997																	
2.253																	
2.500																	
3.026																	
3.615																	
3.965	0.942	0.022	0.015	0.028	0.555	0.922	0.009	-0.006	0.023	0.269	0.919	0.040	-0.009	0.045	0.205	0.928	0.016
4.530	0.946	0.020	0.010	0.029	0.362	0.931	0.009	-0.006	0.025	0.244	0.941	0.036	0.005	0.043	0.106	0.936	0.015
5.026	0.959	0.018	0.010	0.022	0.453	0.942	0.009	-0.008	0.019	0.406	0.962	0.036	0.014	0.039	0.344	0.949	0.014
5.265	0.964	0.018	0.007	0.030	0.229	0.952	0.009	-0.005	0.027	0.201	0.968	0.036	0.011	0.044	0.260	0.958	0.014
6.019	0.891	0.016	-0.007	0.046	0.161	0.902	0.009	0.005	0.045	0.101	0.893	0.061	-0.005	0.080	0.065	0.898	0.013
6.395																	
7.026																	
7.518																	
8.040	0.827	0.013	0.012	0.022	0.522	0.813	0.008	-0.005	0.021	0.265	0.803	0.029	-0.017	0.039	0.442	0.817	0.010
8.479	0.848	0.013	0.011	0.021	0.526	0.835	0.008	-0.006	0.019	0.303	0.829	0.030	-0.013	0.038	0.330	0.839	0.010
9.034	0.865	0.013	0.007	0.023	0.320	0.855	0.008	-0.004	0.021	0.192	0.851	0.033	-0.008	0.042	0.202	0.858	0.010
9.479	0.870	0.013	0.007	0.024	0.299	0.860	0.008	-0.004	0.023	0.173	0.855	0.033	-0.010	0.043	0.224	0.863	0.010
9.927	0.872	0.013	0.006	0.021	0.290	0.863	0.008	-0.004	0.019	0.230	0.869	0.033	0.003	0.041	0.073	0.866	0.010
10.966	0.879	0.011	0.006	0.019	0.292	0.871	0.008	-0.003	0.018	0.192						0.874	0.008
12.058	0.871	0.011	0.007	0.021	0.354	0.861	0.008	-0.004	0.019	0.226						0.865	0.008
12.565	0.872	0.011	0.007	0.019	0.360	0.863	0.008	-0.004	0.017	0.234						0.866	0.008
13.025	0.865	0.011	0.004	0.019	0.220	0.859	0.008	-0.002	0.018	0.142						0.861	0.008
14.165	0.873	0.011	0.004	0.024	0.190	0.867	0.008	-0.003	0.022	0.120						0.869	0.008

Table 22. Relative DoE for BN at 350 °C.

	LNE					NIST					INRIM						
CWL, µm	Em	U_{Em}	D_i	U_i	E	Em	U_{Em}	D_i	U_i	E	Em	U_{Em}	D_i	U_i	E	ε_{CRV}	$U_{cut\text{-}off}$
1.997																	
2.253																	
2.500																	
3.026																	
3.615																	
3.965	0.937	0.022	0.013	0.027	0.466	0.920	0.009	-0.005	0.022	0.246	0.921	0.040	-0.005	0.045	0.111	0.925	0.016
4.530	0.947	0.020	0.012	0.028	0.427	0.929	0.009	-0.007	0.024	0.305	0.943	0.036	0.007	0.042	0.168	0.936	0.015
5.026	0.955	0.018	0.010	0.023	0.407	0.940	0.009	-0.006	0.020	0.304	0.951	0.036	0.005	0.040	0.132	0.946	0.014
5.265	0.963	0.018	0.008	0.032	0.242	0.951	0.009	-0.005	0.029	0.186	0.963	0.036	0.008	0.045	0.176	0.956	0.014
6.019	0.893	0.016	-0.007	0.043	0.171	0.904	0.009	0.004	0.042	0.104	0.899	0.061	-0.001	0.078	0.011	0.900	0.013
6.395																	
7.026																	
7.518																	
8.040	0.825	0.013	0.010	0.024	0.410	0.812	0.008	-0.006	0.023	0.257	0.812	0.030	-0.006	0.041	0.137	0.816	0.010
8.479	0.848	0.013	0.011	0.021	0.546	0.833	0.008	-0.006	0.019	0.297	0.825	0.030	-0.016	0.038	0.416	0.838	0.010
9.034	0.864	0.013	0.007	0.022	0.337	0.854	0.008	-0.004	0.020	0.216	0.853	0.031	-0.006	0.040	0.139	0.857	0.010
9.479	0.869	0.013	0.007	0.020	0.333	0.859	0.008	-0.005	0.019	0.257	0.865	0.031	0.002	0.039	0.046	0.863	0.010
9.927	0.871	0.013	0.006	0.021	0.297	0.862	0.008	-0.004	0.019	0.234	0.868	0.033	0.003	0.041	0.067	0.865	0.010
10.966	0.879	0.011	0.006	0.019	0.338	0.870	0.008	-0.004	0.017	0.222						0.873	0.008
12.058	0.871	0.011	0.007	0.021	0.348	0.861	0.008	-0.004	0.019	0.222						0.865	0.008
12.565	0.869	0.011	0.004	0.019	0.228	0.863	0.008	-0.003	0.017	0.149						0.866	0.008
13.025	0.864	0.011	0.004	0.020	0.190	0.859	0.008	-0.002	0.018	0.122						0.860	0.008
14.165	0.872	0.011	0.004	0.024	0.182	0.866	0.008	-0.003	0.022	0.115						0.868	0.008

Table 23. Relative DoE for BN at 400 °C.

	LNE					NIST					INRIM						
CWL, µm	Em	U_{Em}	D_i	U_i	E	Em	U_{Em}	D_i	U_i	E	Em	U_{Em}	D_i	U_i	E	ε_{CRV}	$U_{cut\text{-}off}$
1.997																	
2.253																	
2.500	0.450	0.016	0.033	0.117	0.279	0.427	0.004	-0.020	0.114	0.176	0.455	0.025	0.043	0.125	0.345	0.436	0.010
3.026																	
3.615																	
3.965	0.938	0.022	0.011	0.027	0.397	0.923	0.009	-0.005	0.022	0.225	0.926	0.043	-0.002	0.048	0.052	0.928	0.016
4.530	0.944	0.020	0.008	0.028	0.276	0.932	0.009	-0.005	0.024	0.220	0.945	0.036	0.008	0.042	0.189	0.937	0.015
5.026	0.956	0.018	0.008	0.023	0.363	0.943	0.009	-0.006	0.019	0.296	0.955	0.036	0.008	0.040	0.190	0.948	0.014
5.265	0.961	0.018	0.004	0.028	0.158	0.953	0.009	-0.004	0.025	0.157	0.967	0.036	0.010	0.043	0.241	0.957	0.014
6.019	0.898	0.016	-0.009	0.054	0.167	0.911	0.009	0.006	0.053	0.106	0.897	0.065	-0.009	0.088	0.106	0.906	0.013
6.395																	
7.026																	
7.518																	
8.040	0.825	0.013	0.009	0.026	0.341	0.813	0.008	-0.005	0.024	0.210	0.813	0.030	-0.006	0.042	0.136	0.817	0.010
8.479	0.847	0.013	0.009	0.022	0.404	0.835	0.008	-0.005	0.020	0.229	0.830	0.030	-0.011	0.039	0.271	0.839	0.010
9.034	0.864	0.013	0.006	0.021	0.287	0.856	0.008	-0.003	0.020	0.166	0.852	0.031	-0.008	0.039	0.198	0.858	0.010
9.479	0.869	0.013	0.006	0.021	0.276	0.861	0.008	-0.004	0.020	0.195	0.863	0.031	-0.001	0.039	0.037	0.864	0.010
9.927	0.871	0.013	0.005	0.021	0.242	0.863	0.008	-0.004	0.020	0.197	0.869	0.031	0.003	0.039	0.083	0.866	0.010
10.966	0.879	0.011	0.005	0.019	0.275	0.871	0.008	-0.003	0.018	0.182						0.874	0.008
12.058	0.872	0.011	0.007	0.021	0.315	0.863	0.008	-0.004	0.020	0.201						0.866	0.008
12.565	0.871	0.011	0.005	0.019	0.243	0.865	0.008	-0.003	0.017	0.159						0.867	0.008
13.025	0.866	0.011	0.004	0.020	0.189	0.861	0.008	-0.002	0.018	0.122						0.862	0.008
14.165	0.871	0.011	0.002	0.024	0.086	0.868	0.008	-0.001	0.023	0.054						0.869	0.008

Table 24. Relative DoE for BN at 450 °C.

	LNE					NIST					INRIM						
CWL, µm	Em	U_{Em}	D_i	U_i	E	Em	U_{Em}	D_i	U_i	E	Em	U_{Em}	D_i	U_i	E	ε_{CRV}	$U_{cut\text{-}off}$
1.997																	
2.253																	
2.500	0.442	0.015	0.019	0.071	0.264	0.427	0.004	-0.015	0.067	0.220	0.454	0.024	0.048	0.084	0.566	0.434	0.009
3.026																	
3.615																	
3.965	0.939	0.020	0.011	0.026	0.434	0.924	0.009	-0.005	0.022	0.226	0.923	0.039	-0.006	0.045	0.143	0.929	0.015
4.530	0.944	0.018	0.008	0.026	0.288	0.932	0.009	-0.005	0.023	0.230	0.945	0.036	0.008	0.042	0.191	0.937	0.014
5.026	0.954	0.016	0.007	0.021	0.330	0.942	0.009	-0.005	0.018	0.284	0.955	0.036	0.008	0.040	0.207	0.947	0.013
5.265	0.963	0.016	0.006	0.030	0.208	0.953	0.009	-0.005	0.028	0.165	0.964	0.036	0.007	0.045	0.153	0.957	0.013
6.019	0.897	0.015	-0.011	0.046	0.241	0.913	0.009	0.007	0.045	0.159	0.906	0.063	-0.001	0.082	0.016	0.907	0.012
6.395																	
7.026																	
7.518																	
8.040	0.827	0.011	0.010	0.025	0.417	0.812	0.008	-0.007	0.024	0.308	0.815	0.030	-0.003	0.042	0.075	0.818	0.009
8.479	0.847	0.011	0.009	0.021	0.439	0.834	0.008	-0.006	0.020	0.295	0.831	0.028	-0.010	0.037	0.262	0.839	0.009
9.034	0.865	0.011	0.007	0.020	0.362	0.854	0.008	-0.005	0.019	0.261	0.853	0.030	-0.006	0.038	0.161	0.859	0.009
9.479	0.870	0.011	0.007	0.019	0.360	0.859	0.008	-0.005	0.018	0.305	0.866	0.030	0.002	0.037	0.051	0.864	0.010
9.927	0.872	0.011	0.006	0.020	0.286	0.862	0.008	-0.005	0.019	0.279	0.874	0.030	0.009	0.038	0.234	0.867	0.010
10.966	0.880	0.011	0.006	0.019	0.328	0.871	0.008	-0.004	0.017	0.216						0.874	0.008
12.058	0.872	0.011	0.007	0.021	0.308	0.863	0.008	-0.004	0.020	0.197						0.866	0.008
12.565	0.874	0.011	0.006	0.019	0.338	0.865	0.008	-0.004	0.017	0.221						0.869	0.008
13.025	0.871	0.011	0.007	0.018	0.400	0.860	0.008	-0.004	0.017	0.261						0.864	0.008
14.165	0.875	0.011	0.005	0.024	0.224	0.867	0.008	-0.003	0.022	0.142						0.870	0.008

Table 25. Relative DoE for BN at 500 °C.

	LNE					NIST					INRIM						
CWL, µm	Em	U_{Em}	D_i	U_i	E	Em	U_{Em}	D_i	U_i	E	Em	U_{Em}	D_i	U_i	E	ε_{CRV}	$U_{cut\text{-}off}$
1.997																	
2.253																	
2.500	0.441	0.015	0.013	0.116	0.110	0.430	0.004	-0.013	0.113	0.115	0.459	0.024	0.052	0.124	0.421	0.436	0.009
3.026																	
3.615																	
3.965	0.932	0.018	0.004	0.025	0.146	0.926	0.009	-0.003	0.022	0.146	0.938	0.039	0.010	0.045	0.216	0.929	0.014
4.530	0.944	0.016	0.005	0.022	0.240	0.934	0.009	-0.006	0.019	0.305	0.960	0.036	0.022	0.041	0.544	0.939	0.013
5.026	0.951	0.015	0.004	0.022	0.163	0.943	0.009	-0.004	0.020	0.216	0.965	0.036	0.018	0.041	0.451	0.947	0.012
5.265	0.959	0.015	0.003	0.023	0.115	0.953	0.009	-0.003	0.021	0.163	0.972	0.036	0.016	0.041	0.378	0.957	0.012
6.019	0.901	0.013	-0.010	0.042	0.241	0.917	0.009	0.007	0.041	0.172	0.915	0.058	0.005	0.075	0.066	0.910	0.011
6.395																	
7.026																	
7.518																	
8.040	0.826	0.011	0.010	0.027	0.352	0.812	0.008	-0.007	0.027	0.265	0.817	0.028	-0.001	0.042	0.028	0.818	0.009
8.479	0.847	0.011	0.008	0.024	0.352	0.835	0.008	-0.006	0.023	0.251	0.835	0.028	-0.005	0.039	0.138	0.840	0.009
9.034	0.865	0.011	0.006	0.019	0.335	0.855	0.008	-0.005	0.018	0.266	0.858	0.028	-0.001	0.036	0.034	0.859	0.009
9.479	0.866	0.011	0.003	0.021	0.166	0.860	0.008	-0.003	0.020	0.170	0.869	0.030	0.007	0.039	0.181	0.863	0.010
9.927	0.871	0.011	0.005	0.023	0.197	0.863	0.008	-0.005	0.022	0.220	0.879	0.030	0.014	0.040	0.344	0.867	0.010
10.966	0.880	0.011	0.006	0.019	0.317	0.871	0.008	-0.004	0.017	0.209						0.874	0.008
12.058	0.873	0.011	0.007	0.021	0.311	0.864	0.008	-0.004	0.020	0.199						0.867	0.008
12.565	0.874	0.011	0.006	0.019	0.300	0.866	0.008	-0.003	0.017	0.197						0.869	0.008
13.025	0.871	0.011	0.007	0.018	0.384	0.861	0.008	-0.004	0.017	0.251						0.864	0.008
14.165	0.875	0.011	0.005	0.024	0.232	0.867	0.008	-0.003	0.022	0.147						0.870	0.008

Table 26. Relative DoE for OxIn at 23 °C.

	LNE					NIST					INRIM						
CWL, µm	Em	U_{Em}	D_i	U_i	E	Em	U_{Em}	D_i	U_i	E	Em	U_{Em}	D_i	U_i	E	ε_{CRV}	$U_{cut\text{-}off}$
1.997																	
2.253																	
2.500						0.796	0.005	0.001	0.011	0.099	0.780	0.020	-0.019	0.027	0.710	0.795	0.005
3.026						0.804	0.005	0.001	0.011	0.078	0.791	0.020	-0.016	0.026	0.597	0.803	0.005
3.615						0.801	0.005	4E-04	0.012	0.033	0.795	0.020	-0.007	0.027	0.248	0.801	0.005
3.965	0.795	0.014	-0.003	0.019	0.138	0.799	0.005	0.002	0.015	0.155	0.793	0.020	-0.005	0.026	0.196	0.798	0.009
4.530	0.790	0.017	-0.002	0.023	0.085	0.796	0.005	0.005	0.017	0.315	0.780	0.020	-0.015	0.027	0.566	0.792	0.011
5.026	0.790	0.016	-0.002	0.023	0.087	0.793	0.005	0.002	0.017	0.107	0.789	0.020	-0.003	0.027	0.125	0.791	0.011
5.265	0.782	0.018	-0.006	0.025	0.256	0.791	0.005	0.004	0.019	0.234	0.784	0.020	-0.005	0.027	0.176	0.788	0.012
6.019	0.779	0.019	-0.003	0.026	0.114	0.785	0.005	0.004	0.019	0.231	0.775	0.020	-0.009	0.028	0.322	0.781	0.012
6.395	0.777	0.018	-0.005	0.025	0.206	0.786	0.005	0.006	0.019	0.308	0.773	0.020	-0.010	0.027	0.377	0.781	0.012
7.026	0.804	0.017	-0.012	0.021	0.555	0.819	0.004	0.007	0.015	0.473	0.805	0.022	-0.010	0.027	0.387	0.813	0.010
7.518	0.802	0.015	-0.012	0.019	0.617	0.817	0.004	0.007	0.014	0.514	0.802	0.022	-0.012	0.027	0.447	0.812	0.009
8.040	0.825	0.020	-0.007	0.024	0.308	0.827	0.004	-0.005	0.016	0.321	0.855	0.023	0.029	0.028	1.033	0.831	0.012
8.479	0.867	0.014	0.002	0.016	0.127	0.864	0.003	-0.001	0.011	0.102	0.867	0.023	0.003	0.027	0.108	0.865	0.008
9.034	0.889	0.013	0.009	0.015	0.589	0.879	0.002	-0.003	0.010	0.320	0.884	0.025	0.003	0.028	0.110	0.882	0.007
9.479	0.860	0.012	0.011	0.014	0.773	0.848	0.003	-0.003	0.010	0.326	0.843	0.025	-0.009	0.030	0.311	0.851	0.007
9.927	0.812	0.015	0.009	0.020	0.437	0.802	0.004	-0.003	0.014	0.234	0.805	0.025	-1E-04	0.031	0.004	0.805	0.010
10.966	0.727	0.027	0.002	0.039	0.057	0.727	0.006	0.002	0.026	0.078	0.721	0.024	-0.007	0.036	0.196	0.726	0.015
12.058	0.668	0.029	-0.009	0.048	0.187	0.675	0.007	0.001	0.032	0.040	0.677	0.024	0.003	0.041	0.075	0.674	0.016
12.565	0.675	0.035	0.005	0.055	0.092	0.672	0.007	-2E-04	0.023	0.009						0.672	0.007
13.025	0.667	0.035	0.015	0.057	0.255	0.657	0.007	-0.001	0.025	0.022						0.658	0.007
14.165	0.701	0.046	0.011	0.073	0.153	0.693	0.007	-3E-04	0.033	0.008						0.693	0.007

Table 27. Relative DoE for OxIn at 50 °C.

	NIST					NMIJ						
CWL, µm	Em	U_{Em}	D_i	U_i	E	Em	U_{Em}	D_i	U_i	E	ε_{CRV}	$U_{cut\text{-}off}$
1.997												
2.253												
2.500												
3.026												
3.615												
3.965												
4.530												
5.026												
5.265												
6.019	0.785	0.007	-0.002	0.016	0.149	0.789	0.008	0.003	0.017	0.186	0.786	0.007
6.395	0.787	0.007	-0.003	0.015	0.214	0.792	0.007	0.004	0.016	0.240	0.790	0.007
7.026	0.820	0.006	-0.001	0.011	0.099	0.822	0.007	0.002	0.012	0.128	0.821	0.006
7.518	0.817	0.006	-0.002	0.012	0.141	0.820	0.007	0.002	0.012	0.177	0.819	0.006
8.040	0.829	0.005	-0.002	0.010	0.176	0.833	0.006	0.003	0.011	0.271	0.830	0.005
8.479	0.867	0.003	0.000	0.007	0.034	0.868	0.006	0.001	0.009	0.098	0.867	0.003
9.034	0.877	0.002	0.000	0.007	0.024	0.878	0.007	0.001	0.010	0.120	0.877	0.002
9.479	0.843	0.004	-0.001	0.009	0.161	0.849	0.008	0.007	0.012	0.553	0.844	0.004
9.927	0.798	0.005	-0.003	0.012	0.276	0.810	0.010	0.012	0.016	0.724	0.801	0.005
10.966	0.726	0.008	-0.004	0.022	0.191	0.739	0.014	0.013	0.028	0.458	0.729	0.008
12.058												
12.565												
13.025												
14.165												

Table 28. Relative DoE for OxIn at 100 °C.

	LNE					NIST					NMIJ					PTB						
CWL, µm	Em	U_{Em}	D_i	U_i	E	Em	U_{Em}	D_i	U_i	E	Em	U_{Em}	D_i	U_i	E	Em	U_{Em}	D_i	U_i	E	ε_{CRV}	$U_{cut\text{-}off}$
1.997																						
2.253																						
2.500																						
3.026																						
3.615																						
3.965																						
4.530											0.790	0.010	-3E-04	0.018	0.018	0.797	0.052	0.009	0.067	0.129	0.790	0.010
5.026	0.802	0.029	0.011	0.039	0.283	0.794	0.007	0.001	0.016	0.043	0.791	0.010	-0.002	0.018	0.131	0.792	0.046	-0.001	0.059	0.024	0.793	0.009
5.265	0.796	0.028	0.005	0.038	0.138	0.792	0.007	-2E-04	0.016	0.012	0.791	0.010	-3E-04	0.018	0.016	0.791	0.042	-0.002	0.054	0.028	0.792	0.008
6.019	0.777	0.026	-0.010	0.035	0.298	0.785	0.007	-2E-04	0.016	0.011	0.787	0.008	0.002	0.016	0.118	0.772	0.039	-0.016	0.051	0.320	0.785	0.008
6.395	0.773	0.025	-0.018	0.034	0.529	0.787	0.007	-6E-06	0.016	0.000	0.789	0.008	0.003	0.016	0.175	0.773	0.039	-0.019	0.051	0.365	0.787	0.008
7.026	0.795	0.026	-0.029	0.032	0.886	0.820	0.006	0.002	0.012	0.133	0.819	0.008	0.001	0.013	0.087	0.812	0.026	-0.007	0.033	0.220	0.818	0.007
7.518	0.812	0.025	-0.007	0.032	0.224	0.819	0.006	0.001	0.012	0.109	0.818	0.008	-4E-04	0.013	0.034	0.815	0.020	-0.005	0.026	0.177	0.818	0.007
8.040	0.841	0.025	0.014	0.032	0.439	0.829	0.005	-3E-04	0.011	0.030	0.830	0.007	3E-04	0.012	0.022	0.825	0.019	-0.006	0.024	0.254	0.830	0.006
8.479	0.884	0.027	0.021	0.031	0.668	0.866	0.003	8E-05	0.008	0.010	0.865	0.007	-0.001	0.010	0.115	0.864	0.017	-0.003	0.020	0.125	0.866	0.005
9.034	0.892	0.026	0.016	0.030	0.523	0.878	0.002	2E-04	0.008	0.030	0.876	0.007	-0.001	0.009	0.156	0.877	0.016	0.000	0.019	0.019	0.878	0.005
9.479	0.865	0.026	0.021	0.031	0.668	0.846	0.003	-0.001	0.010	0.103	0.848	0.008	0.001	0.012	0.058	0.844	0.017	-0.003	0.022	0.141	0.847	0.006
9.927	0.814	0.023	0.011	0.030	0.357	0.804	0.005	-0.002	0.013	0.145	0.808	0.009	0.003	0.015	0.196	0.801	0.019	-0.006	0.025	0.240	0.805	0.007
10.966	0.739	0.019	0.005	0.032	0.168	0.734	0.008	-0.002	0.022	0.077	0.737	0.010	0.002	0.023	0.104	0.728	0.023	-0.009	0.036	0.242	0.735	0.009
12.058	0.706	0.018	0.015	0.035	0.440	0.692	0.010	-0.004	0.029	0.140						0.682	0.028	-0.019	0.046	0.416	0.695	0.014
12.565	0.717	0.018	0.027	0.033	0.803	0.691	0.009	-0.010	0.028	0.372						0.685	0.030	-0.020	0.047	0.427	0.699	0.014
13.025	0.698	0.018	0.019	0.035	0.559	0.680	0.009	-0.008	0.029	0.265						0.674	0.033	-0.016	0.053	0.294	0.685	0.013
14.165	0.705	0.018	0.002	0.039	0.045	0.704	0.009	4E-04	0.034	0.011						0.697	0.034	-0.008	0.056	0.148	0.703	0.013

Table 29. Relative DoE for OxIn at 150 °C.

	LNE					NIST					PTB						
CWL, µm	Em	U_{Em}	D_i	U_i	E	Em	U_{Em}	D_i	U_i	E	Em	U_{Em}	D_i	U_i	E	ε_{CRV}	$U_{cut\text{-}off}$
1.997																	
2.253																	
2.500																	
3.026																	
3.615																	
3.965	0.811	0.031	0.011	0.036	0.303	0.802	0.006	-4E-04	0.022	0.017	0.785	0.046	-0.022	0.056	0.388	0.802	0.019
4.530	0.806	0.028	0.010	0.035	0.281	0.798	0.006	1E-04	0.024	0.005	0.781	0.040	-0.021	0.050	0.416	0.798	0.017
5.026	0.801	0.025	0.006	0.031	0.212	0.795	0.007	-0.001	0.019	0.064	0.792	0.029	-0.004	0.035	0.124	0.796	0.016
5.265	0.797	0.025	0.005	0.030	0.180	0.793	0.007	3E-04	0.018	0.017	0.788	0.023	-0.005	0.028	0.196	0.793	0.015
6.019	0.776	0.022	-0.008	0.028	0.283	0.787	0.007	0.006	0.017	0.348	0.777	0.018	-0.007	0.023	0.294	0.782	0.013
6.395	0.773	0.021	-0.013	0.027	0.465	0.788	0.007	0.007	0.016	0.438	0.778	0.017	-0.006	0.022	0.282	0.783	0.012
7.026	0.798	0.021	-0.021	0.025	0.827	0.819	0.006	0.005	0.012	0.449	0.815	0.016	0.000	0.018	0.018	0.815	0.011
7.518	0.819	0.021	-4E-04	0.025	0.018	0.822	0.006	0.002	0.012	0.199	0.816	0.015	-0.005	0.017	0.281	0.820	0.010
8.040	0.847	0.021	0.019	0.024	0.777	0.830	0.005	-0.002	0.011	0.143	0.826	0.015	-0.006	0.016	0.353	0.831	0.010
8.479	0.888	0.022	0.024	0.024	1.025	0.865	0.003	-0.002	0.008	0.238	0.863	0.014	-0.005	0.014	0.344	0.867	0.008
9.034	0.894	0.021	0.017	0.023	0.720	0.878	0.002	-0.001	0.008	0.135	0.876	0.014	-0.004	0.014	0.267	0.879	0.008
9.479	0.864	0.020	0.016	0.023	0.712	0.850	0.003	-0.001	0.009	0.107	0.846	0.013	-0.005	0.014	0.325	0.850	0.008
9.927	0.814	0.019	0.006	0.023	0.276	0.809	0.005	0.001	0.011	0.073	0.805	0.013	-0.005	0.016	0.311	0.809	0.009
10.966	0.745	0.016	0.006	0.025	0.242	0.741	0.008	0.001	0.019	0.046	0.735	0.014	-0.006	0.023	0.275	0.740	0.011
12.058	0.713	0.015	0.014	0.029	0.483	0.702	0.009	-0.001	0.025	0.059	0.694	0.016	-0.013	0.030	0.434	0.703	0.012
12.565	0.725	0.016	0.024	0.027	0.885	0.702	0.008	-0.009	0.023	0.374	0.700	0.017	-0.011	0.029	0.385	0.708	0.012
13.025	0.711	0.016	0.019	0.029	0.653	0.693	0.008	-0.007	0.024	0.291	0.692	0.019	-0.009	0.032	0.269	0.698	0.012
14.165	0.712	0.015	0.002	0.035	0.055	0.712	0.008	0.002	0.032	0.061	0.705	0.019	-0.008	0.039	0.218	0.711	0.012

Table 30. Relative DoE for OxIn at 200 °C.

	LNE					NIST					PTB						
CWL, µm	Em	U_{Em}	D_i	U_i	E	Em	U_{Em}	D_i	U_i	E	Em	U_{Em}	D_i	U_i	E	ε_{CRV}	$U_{cut\text{-}off}$
1.997																	
2.253																	
2.500																	
3.026																	
3.615																	
3.965	0.809	0.025	0.008	0.031	0.251	0.803	0.006	-0.001	0.022	0.025	0.788	0.042	-0.018	0.053	0.351	0.803	0.016
4.530	0.803	0.022	0.006	0.029	0.202	0.799	0.006	0.001	0.021	0.038	0.791	0.025	-0.010	0.033	0.305	0.799	0.014
5.026	0.807	0.021	0.012	0.028	0.419	0.796	0.007	-0.002	0.021	0.104	0.792	0.022	-0.008	0.030	0.256	0.798	0.014
5.265	0.794	0.020	0.000	0.028	0.015	0.794	0.007	0.001	0.021	0.051	0.791	0.021	-0.003	0.028	0.105	0.793	0.013
6.019	0.782	0.018	-0.003	0.027	0.099	0.788	0.007	0.005	0.020	0.267	0.777	0.017	-0.009	0.026	0.344	0.784	0.012
6.395	0.777	0.017	-0.008	0.026	0.320	0.789	0.007	0.007	0.020	0.365	0.778	0.018	-0.008	0.026	0.287	0.783	0.012
7.026	0.802	0.017	-0.016	0.023	0.689	0.819	0.005	0.005	0.015	0.338	0.814	0.014	-0.001	0.019	0.030	0.815	0.009
7.518	0.821	0.017	0.000	0.022	0.001	0.823	0.005	0.003	0.015	0.177	0.817	0.012	-0.005	0.018	0.283	0.821	0.009
8.040	0.852	0.017	0.024	0.022	1.096	0.830	0.005	-0.003	0.013	0.214	0.827	0.012	-0.006	0.016	0.359	0.832	0.008
8.479	0.886	0.017	0.022	0.020	1.075	0.864	0.003	-0.003	0.010	0.270	0.864	0.012	-0.003	0.014	0.207	0.867	0.007
9.034	0.896	0.017	0.018	0.020	0.886	0.878	0.002	-0.002	0.010	0.188	0.878	0.011	-0.002	0.014	0.163	0.880	0.007
9.479	0.868	0.016	0.017	0.021	0.812	0.852	0.003	-0.001	0.012	0.104	0.850	0.011	-0.004	0.015	0.287	0.853	0.007
9.927	0.818	0.015	0.006	0.021	0.273	0.814	0.004	0.001	0.014	0.085	0.809	0.010	-0.005	0.016	0.307	0.813	0.007
10.966	0.753	0.014	0.008	0.024	0.350	0.747	0.007	0.001	0.020	0.026	0.742	0.010	-0.006	0.021	0.272	0.747	0.009
12.058	0.718	0.013	0.010	0.029	0.343	0.711	0.009	3E-04	0.026	0.012	0.705	0.011	-0.008	0.027	0.282	0.711	0.010
12.565	0.738	0.013	0.026	0.026	0.978	0.712	0.008	-0.010	0.023	0.438	0.715	0.011	-0.005	0.025	0.209	0.719	0.010
13.025	0.725	0.013	0.018	0.028	0.662	0.706	0.007	-0.008	0.025	0.343	0.710	0.012	-0.003	0.027	0.106	0.712	0.010
14.165	0.724	0.013	0.006	0.034	0.186	0.720	0.008	0.001	0.032	0.025	0.714	0.013	-0.008	0.035	0.243	0.720	0.010

Table 31. Relative DoE for OxIn at 250 °C.

	LNE					NIST					PTB					INRIM						
CWL, µm	Em	U_{Em}	D_i	U_i	E	Em	U_{Em}	D_i	U_i	E	Em	U_{Em}	D_i	U_i	E	Em	U_{Em}	D_i	U_i	E	ε_{CRV}	$U_{cut-off}$
1.997																						
2.253																						
2.500																						
3.026																						
3.615						0.806	0.007	0.003	0.030	0.105	0.786	0.044	-0.022	0.054	0.404	0.796	0.038	-0.009	0.047	0.190	0.803	0.023
3.965	0.817	0.022	0.013	0.030	0.427	0.805	0.007	-0.001	0.022	0.065	0.787	0.031	-0.024	0.041	0.602	0.800	0.032	-0.008	0.041	0.193	0.807	0.015
4.530	0.809	0.020	0.008	0.028	0.282	0.802	0.007	-0.001	0.021	0.051	0.788	0.025	-0.018	0.033	0.555	0.801	0.028	-0.002	0.038	0.055	0.803	0.014
5.026	0.808	0.019	0.011	0.027	0.413	0.799	0.007	0.000	0.020	0.007	0.793	0.023	-0.008	0.031	0.257	0.790	0.023	-0.011	0.031	0.358	0.799	0.013
5.265	0.799	0.018	0.003	0.026	0.132	0.798	0.007	0.002	0.020	0.083	0.792	0.023	-0.005	0.031	0.166	0.793	0.021	-0.005	0.029	0.169	0.796	0.013
6.019	0.784	0.016	0.000	0.025	0.017	0.789	0.007	0.005	0.020	0.237	0.778	0.020	-0.008	0.029	0.285	0.782	0.021	-0.003	0.030	0.116	0.785	0.012
6.395	0.780	0.016	-0.006	0.025	0.244	0.791	0.007	0.007	0.020	0.355	0.779	0.019	-0.008	0.028	0.277	0.783	0.025	-0.002	0.035	0.067	0.785	0.011
7.026	0.803	0.016	-0.014	0.023	0.625	0.818	0.008	0.004	0.018	0.237	0.815	0.016	0.001	0.023	0.029	0.828	0.027	0.017	0.035	0.474	0.814	0.012
7.518	0.820	0.015	-0.001	0.022	0.055	0.823	0.008	0.002	0.017	0.110	0.818	0.014	-0.004	0.020	0.195	0.824	0.021	0.003	0.028	0.106	0.821	0.011
8.040	0.853	0.016	0.020	0.022	0.935	0.834	0.008	-0.003	0.016	0.198	0.828	0.012	-0.011	0.018	0.568	0.835	0.023	-0.001	0.030	0.041	0.836	0.010
8.479	0.888	0.016	0.019	0.021	0.894	0.867	0.008	-0.005	0.016	0.325	0.864	0.012	-0.008	0.017	0.465	0.878	0.023	0.008	0.028	0.288	0.871	0.010
9.034	0.893	0.016	0.011	0.022	0.501	0.882	0.009	-0.002	0.016	0.128	0.878	0.012	-0.006	0.018	0.325	0.889	0.026	0.006	0.032	0.189	0.884	0.010
9.479	0.869	0.015	0.012	0.022	0.523	0.859	0.009	-4E-04	0.017	0.023	0.851	0.011	-0.009	0.018	0.508	0.863	0.025	0.004	0.032	0.126	0.859	0.010
9.927	0.824	0.014	0.004	0.022	0.178	0.824	0.008	0.004	0.018	0.229	0.812	0.010	-0.011	0.019	0.581	0.815	0.030	-0.007	0.040	0.172	0.821	0.009
10.966	0.760	0.013	0.003	0.024	0.127	0.760	0.007	0.003	0.019	0.145	0.748	0.010	-0.012	0.020	0.603						0.757	0.008
12.058	0.726	0.013	0.005	0.027	0.167	0.723	0.007	0.001	0.024	0.027	0.715	0.009	-0.010	0.025	0.415						0.723	0.008
12.565	0.747	0.013	0.023	0.026	0.885	0.724	0.007	-0.009	0.022	0.398	0.729	0.009	-0.002	0.023	0.088						0.731	0.008
13.025	0.737	0.013	0.014	0.028	0.507	0.722	0.007	-0.006	0.024	0.254	0.727	0.010	7E-05	0.025	0.003						0.727	0.008
14.165	0.735	0.012	0.001	0.033	0.023	0.736	0.007	0.003	0.031	0.096	0.722	0.011	-0.016	0.032	0.511						0.734	0.009

Table 32. Relative DoE for OxIn at 300 °C.

	LNE					NIST					INRIM						
CWL, µm	Em	U_{Em}	D_i	U_i	E	Em	U_{Em}	D_i	U_i	E	Em	U_{Em}	D_i	U_i	E	ε_{CRV}	$U_{cut\text{-}off}$
1.997																	
2.253																	
2.500																	
3.026																	
3.615	0.817	0.020	0.011	0.028	0.399	0.807	0.008	-0.002	0.021	0.079	0.800	0.023	-0.009	0.030	0.310	0.808	0.014
3.965	0.816	0.020	0.011	0.027	0.386	0.806	0.008	-0.001	0.021	0.062	0.800	0.022	-0.009	0.029	0.318	0.808	0.014
4.530	0.812	0.018	0.009	0.026	0.341	0.803	0.008	-0.003	0.021	0.120	0.800	0.023	-0.006	0.031	0.202	0.805	0.013
5.026	0.806	0.017	0.006	0.024	0.240	0.800	0.008	-0.001	0.020	0.065	0.797	0.022	-0.006	0.030	0.189	0.801	0.012
5.265	0.804	0.016	0.005	0.024	0.190	0.799	0.008	-0.001	0.020	0.061	0.797	0.020	-0.003	0.028	0.122	0.800	0.012
6.019	0.786	0.015	-0.003	0.023	0.141	0.790	0.008	0.002	0.020	0.089	0.789	0.028	4E-04	0.038	0.011	0.789	0.011
6.395	0.782	0.015	-0.008	0.023	0.335	0.792	0.008	0.005	0.020	0.259	0.787	0.018	-0.002	0.027	0.064	0.788	0.011
7.026	0.806	0.015	-0.012	0.023	0.501	0.818	0.008	0.003	0.020	0.154	0.824	0.019	0.011	0.027	0.390	0.815	0.011
7.518	0.824	0.014	0.000	0.021	0.019	0.825	0.008	4E-04	0.018	0.022	0.824	0.019	-5E-04	0.026	0.018	0.825	0.011
8.040	0.850	0.015	0.012	0.021	0.579	0.835	0.008	-0.006	0.018	0.361	0.838	0.022	-0.003	0.028	0.105	0.840	0.011
8.479	0.885	0.015	0.012	0.020	0.597	0.867	0.008	-0.008	0.017	0.493	0.878	0.021	0.004	0.026	0.143	0.874	0.012
9.034	0.897	0.015	0.010	0.021	0.466	0.883	0.008	-0.007	0.018	0.378	0.891	0.022	0.003	0.027	0.106	0.889	0.012
9.479	0.871	0.014	0.007	0.020	0.353	0.863	0.008	-0.003	0.018	0.161	0.859	0.023	-0.007	0.029	0.229	0.865	0.011
9.927	0.833	0.014	0.004	0.020	0.192	0.831	0.008	0.001	0.018	0.077	0.810	0.027	-0.023	0.034	0.677	0.830	0.011
10.966	0.770	0.012	0.003	0.023	0.118	0.767	0.007	-2E-04	0.021	0.011	0.755	0.032	-0.016	0.045	0.356	0.768	0.010
12.058	0.735	0.012	0.003	0.025	0.122	0.733	0.007	-5E-05	0.024	0.002	0.708	0.040	-0.035	0.058	0.597	0.733	0.009
12.565	0.755	0.012	0.021	0.025	0.873	0.734	0.007	-0.007	0.021	0.354						0.739	0.007
13.025	0.752	0.012	0.017	0.027	0.646	0.736	0.007	-0.006	0.023	0.250						0.740	0.007
14.165	0.751	0.012	0.003	0.034	0.084	0.748	0.007	-0.001	0.031	0.032						0.749	0.007

Table 33. Relative DoE for OxIn at 350 °C.

	LNE					NIST					INRIM						
CWL, µm	Em	U_{Em}	D_i	U_i	E	Em	U_{Em}	D_i	U_i	E	Em	U_{Em}	D_i	U_i	E	ε_{CRV}	$U_{cut\text{-}off}$
1.997																	
2.253																	
2.500																	
3.026																	
3.615	0.822	0.020	0.017	0.027	0.606	0.805	0.007	-0.004	0.020	0.176	0.801	0.021	-0.009	0.028	0.329	0.808	0.014
3.965	0.816	0.020	0.013	0.027	0.458	0.804	0.007	-0.002	0.021	0.119	0.800	0.021	-0.008	0.028	0.274	0.806	0.014
4.530	0.813	0.018	0.013	0.026	0.509	0.800	0.007	-0.004	0.021	0.167	0.796	0.021	-0.008	0.029	0.277	0.803	0.013
5.026	0.808	0.017	0.010	0.024	0.428	0.796	0.007	-0.004	0.019	0.189	0.796	0.020	-0.004	0.027	0.159	0.799	0.012
5.265	0.805	0.016	0.010	0.024	0.397	0.795	0.007	-0.002	0.020	0.121	0.791	0.021	-0.008	0.029	0.275	0.797	0.012
6.019	0.787	0.015	0.001	0.023	0.047	0.785	0.007	-0.002	0.019	0.090	0.791	0.025	0.006	0.035	0.179	0.787	0.011
6.395	0.785	0.015	-0.002	0.023	0.107	0.787	0.007	0.001	0.019	0.051	0.788	0.021	0.001	0.029	0.046	0.787	0.011
7.026	0.809	0.014	-0.007	0.023	0.326	0.815	0.008	0.001	0.020	0.026	0.826	0.021	0.014	0.029	0.466	0.815	0.011
7.518	0.826	0.014	0.001	0.021	0.057	0.824	0.008	-0.001	0.018	0.056	0.826	0.021	0.001	0.028	0.037	0.825	0.011
8.040	0.850	0.014	0.012	0.020	0.623	0.834	0.008	-0.007	0.017	0.402	0.837	0.021	-0.002	0.027	0.089	0.839	0.011
8.479	0.884	0.014	0.013	0.020	0.673	0.865	0.008	-0.008	0.017	0.488	0.872	0.022	0.000	0.028	0.001	0.872	0.011
9.034	0.899	0.014	0.012	0.020	0.605	0.882	0.009	-0.007	0.017	0.412	0.887	0.022	-0.002	0.028	0.081	0.889	0.012
9.479	0.880	0.014	0.012	0.020	0.637	0.865	0.009	-0.005	0.017	0.289	0.858	0.022	-0.013	0.028	0.446	0.869	0.011
9.927	0.843	0.013	0.009	0.020	0.453	0.835	0.008	-0.001	0.018	0.030	0.812	0.024	-0.027	0.031	0.869	0.835	0.011
10.966	0.786	0.012	0.011	0.025	0.443	0.775	0.007	-0.004	0.021	0.179						0.778	0.007
12.058	0.745	0.012	0.004	0.026	0.150	0.741	0.007	-0.001	0.022	0.058						0.742	0.007
12.565	0.763	0.012	0.022	0.024	0.912	0.741	0.007	-0.008	0.020	0.375						0.747	0.007
13.025	0.767	0.012	0.019	0.026	0.724	0.748	0.007	-0.007	0.023	0.302						0.753	0.007
14.165	0.768	0.012	0.007	0.034	0.203	0.761	0.007	-0.003	0.032	0.083						0.763	0.007

Table 34. Relative DoE for OxIn at 400 °C.

	LNE					NIST					INRIM						
CWL, µm	Em	U_{Em}	D_i	U_i	E	Em	U_{Em}	D_i	U_i	E	Em	U_{Em}	D_i	U_i	E	ε_{CRV}	$U_{cut\text{-}off}$
1.997																	
2.253																	
2.500																	
3.026																	
3.615	0.826	0.020	0.015	0.027	0.547	0.811	0.007	-0.004	0.020	0.204	0.808	0.022	-0.007	0.030	0.247	0.814	0.014
3.965	0.820	0.019	0.011	0.027	0.403	0.811	0.007	-0.001	0.021	0.037	0.803	0.021	-0.010	0.028	0.366	0.811	0.013
4.530	0.815	0.018	0.010	0.026	0.382	0.807	0.007	-2E-04	0.021	0.009	0.797	0.021	-0.013	0.029	0.441	0.807	0.013
5.026	0.811	0.017	0.008	0.024	0.331	0.804	0.007	-2E-04	0.020	0.009	0.795	0.021	-0.012	0.028	0.415	0.805	0.012
5.265	0.807	0.016	0.005	0.024	0.198	0.803	0.007	2E-04	0.020	0.010	0.796	0.021	-0.008	0.029	0.290	0.803	0.012
6.019	0.786	0.015	-0.007	0.023	0.299	0.795	0.007	0.004	0.020	0.211	0.791	0.021	-0.001	0.029	0.042	0.792	0.011
6.395	0.782	0.014	-0.011	0.022	0.482	0.796	0.007	0.007	0.019	0.381	0.787	0.021	-0.004	0.029	0.153	0.791	0.011
7.026	0.805	0.014	-0.014	0.022	0.629	0.819	0.008	0.003	0.019	0.152	0.831	0.021	0.018	0.028	0.644	0.816	0.011
7.518	0.827	0.014	-0.002	0.021	0.080	0.829	0.008	0.000	0.018	0.014	0.832	0.021	0.005	0.028	0.164	0.829	0.011
8.040	0.852	0.014	0.012	0.020	0.589	0.836	0.008	-0.007	0.017	0.404	0.841	0.021	-0.001	0.027	0.031	0.842	0.011
8.479	0.885	0.014	0.012	0.020	0.631	0.866	0.008	-0.010	0.017	0.592	0.881	0.021	0.007	0.026	0.287	0.875	0.011
9.034	0.898	0.014	0.009	0.021	0.412	0.883	0.009	-0.008	0.019	0.435	0.899	0.022	0.009	0.028	0.330	0.891	0.011
9.479	0.876	0.014	0.005	0.021	0.235	0.869	0.009	-0.003	0.019	0.176	0.872	0.022	2E-04	0.029	0.007	0.871	0.011
9.927	0.839	0.013	5E-05	0.020	0.002	0.842	0.008	0.003	0.018	0.189	0.826	0.022	-0.016	0.030	0.526	0.839	0.011
10.966	0.786	0.013	0.003	0.024	0.139	0.783	0.007	-0.001	0.020	0.055						0.784	0.007
12.058	0.755	0.012	0.003	0.025	0.130	0.751	0.007	-0.001	0.022	0.052						0.752	0.007
12.565	0.772	0.012	0.020	0.024	0.853	0.751	0.007	-0.007	0.020	0.368						0.757	0.007
13.025	0.774	0.012	0.014	0.025	0.557	0.760	0.007	-0.006	0.022	0.251						0.764	0.007
14.165	0.769	0.012	-0.003	0.031	0.102	0.772	0.007	0.001	0.029	0.045						0.771	0.007

Table 35. Relative DoE for OxIn at 450 °C.

	LNE					NIST					INRIM						
CWL, µm	Em	U_{Em}	D_i	U_i	E	Em	U_{Em}	D_i	U_i	E	Em	U_{Em}	D_i	U_i	E	ε_{CRV}	$U_{cut\text{-}off}$
1.997																	
2.253																	
2.500																	
3.026						0.805	0.007	-0.001	0.016	0.056	0.812	0.022	0.008	0.030	0.258	0.805	0.007
3.615	0.825	0.019	0.012	0.026	0.478	0.812	0.007	-0.004	0.020	0.190	0.810	0.022	-0.006	0.029	0.202	0.815	0.013
3.965	0.824	0.019	0.013	0.027	0.475	0.812	0.007	-0.002	0.021	0.081	0.805	0.021	-0.010	0.028	0.366	0.813	0.013
4.530	0.818	0.018	0.010	0.026	0.400	0.808	0.007	-0.002	0.021	0.073	0.802	0.021	-0.010	0.029	0.344	0.810	0.012
5.026	0.815	0.016	0.010	0.023	0.418	0.806	0.007	-0.002	0.019	0.106	0.800	0.021	-0.010	0.028	0.339	0.808	0.012
5.265	0.808	0.016	0.005	0.024	0.196	0.805	0.007	0.001	0.020	0.037	0.796	0.021	-0.010	0.029	0.337	0.804	0.012
6.019	0.791	0.015	-0.005	0.023	0.237	0.797	0.007	0.002	0.019	0.095	0.799	0.021	0.004	0.029	0.135	0.796	0.011
6.395	0.787	0.014	-0.009	0.022	0.439	0.798	0.007	0.005	0.019	0.247	0.797	0.021	0.003	0.029	0.113	0.794	0.011
7.026	0.808	0.014	-0.011	0.022	0.509	0.819	0.008	0.001	0.019	0.060	0.833	0.021	0.019	0.028	0.667	0.818	0.011
7.518	0.829	0.014	-0.001	0.020	0.074	0.830	0.008	0.000	0.017	0.026	0.834	0.021	0.005	0.027	0.184	0.830	0.011
8.040	0.850	0.014	0.010	0.019	0.489	0.836	0.008	-0.007	0.017	0.433	0.847	0.021	0.005	0.027	0.189	0.842	0.011
8.479	0.881	0.014	0.009	0.020	0.462	0.865	0.008	-0.010	0.018	0.535	0.884	0.021	0.012	0.027	0.452	0.873	0.011
9.034	0.901	0.014	0.010	0.021	0.463	0.884	0.009	-0.010	0.019	0.519	0.903	0.021	0.011	0.027	0.407	0.893	0.011
9.479	0.887	0.014	0.011	0.020	0.569	0.871	0.009	-0.007	0.018	0.385	0.875	0.022	-0.003	0.028	0.107	0.877	0.011
9.927	0.857	0.013	0.010	0.019	0.535	0.847	0.008	-0.002	0.017	0.093	0.828	0.022	-0.024	0.029	0.818	0.848	0.011
10.966	0.803	0.013	0.012	0.025	0.477	0.790	0.007	-0.004	0.021	0.187						0.793	0.007
12.058	0.761	0.011	0.001	0.025	0.042	0.760	0.007	-4E-04	0.022	0.018						0.760	0.007
12.565	0.778	0.012	0.018	0.023	0.777	0.759	0.007	-0.007	0.020	0.346						0.764	0.007
13.025	0.789	0.012	0.018	0.025	0.721	0.770	0.008	-0.007	0.022	0.334						0.775	0.008
14.165	0.796	0.012	0.010	0.034	0.303	0.784	0.007	-0.004	0.033	0.134						0.787	0.007

Table 36. Relative DoE for OxIn at 500 °C.

	LNE					NIST					INRIM						
CWL, µm	Em	U_{Em}	D_i	U_i	E	Em	U_{Em}	D_i	U_i	E	Em	U_{Em}	D_i	U_i	E	ε_{CRV}	$U_{cut\text{-}off}$
1.997																	
2.253																	
2.500																	
3.026																	
3.615	0.825	0.018	0.010	0.019	0.560	0.814	0.007	-0.003	0.011	0.271	0.811	0.021	-0.006	0.023	0.267	0.816	0.013
3.965	0.821	0.017	0.007	0.017	0.381	0.813	0.007	-0.002	0.011	0.214	0.813	0.021	-0.003	0.023	0.148	0.815	0.012
4.530	0.819	0.015	0.008	0.017	0.489	0.810	0.007	-0.003	0.012	0.245	0.808	0.021	-0.005	0.024	0.227	0.812	0.011
5.026	0.814	0.015	0.006	0.016	0.386	0.807	0.007	-0.002	0.011	0.188	0.805	0.021	-0.005	0.024	0.204	0.809	0.011
5.265	0.810	0.014	0.004	0.016	0.264	0.806	0.007	-0.001	0.012	0.123	0.804	0.021	-0.004	0.025	0.150	0.807	0.011
6.019	0.793	0.013	-0.004	0.016	0.276	0.798	0.007	0.003	0.012	0.220	0.796	0.021	-3E-04	0.026	0.010	0.796	0.010
6.395	0.787	0.013	-0.009	0.015	0.623	0.799	0.007	0.006	0.012	0.530	0.793	0.021	-0.002	0.025	0.064	0.794	0.010
7.026	0.807	0.013	-0.012	0.015	0.811	0.818	0.008	0.002	0.012	0.132	0.837	0.021	0.024	0.024	0.967	0.817	0.010
7.518	0.827	0.013	-0.005	0.013	0.356	0.831	0.008	0.001	0.010	0.098	0.838	0.021	0.008	0.024	0.358	0.831	0.010
8.040	0.850	0.013	0.009	0.013	0.670	0.836	0.008	-0.007	0.009	0.773	0.848	0.021	0.007	0.023	0.288	0.843	0.010
8.479	0.882	0.013	0.010	0.014	0.702	0.864	0.008	-0.010	0.011	0.913	0.885	0.021	0.013	0.023	0.572	0.873	0.011
9.034	0.901	0.013	0.009	0.015	0.605	0.884	0.009	-0.010	0.013	0.779	0.904	0.021	0.012	0.023	0.536	0.893	0.011
9.479	0.887	0.013	0.010	0.013	0.788	0.873	0.009	-0.006	0.010	0.588	0.875	0.021	-0.004	0.022	0.196	0.878	0.011
9.927	0.855	0.012	0.006	0.013	0.493	0.851	0.008	0.001	0.010	0.060	0.833	0.021	-0.020	0.023	0.871	0.850	0.010
10.966	0.805	0.012	0.008	0.019	0.429	0.796	0.007	-0.003	0.015	0.211						0.798	0.007
12.058	0.768	0.011	0.001	0.021	0.057	0.767	0.007	-5E-04	0.018	0.027						0.768	0.007
12.565	0.786	0.011	0.019	0.018	1.036	0.765	0.007	-0.008	0.015	0.547						0.771	0.007
13.025	0.798	0.011	0.016	0.019	0.825	0.779	0.008	-0.007	0.016	0.450						0.785	0.008
14.165	0.801	0.011	0.004	0.029	0.127	0.797	0.008	-0.002	0.027	0.064						0.798	0.008

Table 37. Relative DoE for OxIn at 550 °C.

	LNE					NIST					INRIM						
CWL, µm	Em	U_{Em}	D_i	U_i	E	Em	U_{Em}	D_i	U_i	E	Em	U_{Em}	D_i	U_i	E	ε_{CRV}	$U_{cut\text{-}off}$
1.997																	
2.253																	
2.500																	
3.026																	
3.615	0.830	0.016	0.014	0.017	0.811	0.815	0.007	-0.005	0.010	0.439	0.812	0.021	-0.008	0.023	0.360	0.819	0.012
3.965	0.824	0.016	0.011	0.018	0.598	0.814	0.007	-0.002	0.012	0.164	0.807	0.021	-0.011	0.024	0.469	0.816	0.012
4.530	0.822	0.015	0.012	0.019	0.662	0.809	0.007	-0.004	0.014	0.256	0.803	0.021	-0.010	0.025	0.413	0.812	0.011
5.026	0.817	0.015	0.011	0.017	0.631	0.806	0.007	-0.003	0.012	0.216	0.799	0.021	-0.012	0.025	0.480	0.808	0.011
5.265	0.812	0.014	0.006	0.016	0.396	0.805	0.007	-0.003	0.012	0.247	0.805	0.021	-0.003	0.025	0.114	0.807	0.011
6.019	0.793	0.013	-0.004	0.016	0.226	0.797	0.007	0.002	0.012	0.156	0.797	0.021	0.001	0.025	0.038	0.796	0.010
6.395	0.790	0.013	-0.006	0.016	0.351	0.798	0.007	0.005	0.012	0.404	0.790	0.019	-0.005	0.023	0.232	0.795	0.010
7.026	0.813	0.013	-0.007	0.015	0.484	0.818	0.008	-0.001	0.011	0.054	0.835	0.021	0.020	0.024	0.815	0.819	0.010
7.518	0.833	0.013	0.000	0.013	0.031	0.832	0.008	-0.001	0.010	0.105	0.835	0.021	0.003	0.023	0.126	0.833	0.010
8.040	0.849	0.013	0.009	0.013	0.650	0.835	0.008	-0.008	0.009	0.801	0.849	0.021	0.008	0.023	0.357	0.842	0.010
8.479	0.881	0.013	0.010	0.014	0.726	0.863	0.008	-0.011	0.011	0.948	0.883	0.021	0.013	0.023	0.575	0.872	0.011
9.034	0.898	0.013	0.007	0.015	0.460	0.884	0.009	-0.009	0.013	0.686	0.904	0.021	0.013	0.023	0.575	0.892	0.011
9.479	0.890	0.013	0.010	0.014	0.764	0.875	0.009	-0.007	0.011	0.616	0.879	0.021	-0.002	0.023	0.082	0.880	0.011
9.927	0.861	0.013	0.009	0.013	0.655	0.854	0.008	-2E-04	0.010	0.016	0.835	0.021	-0.022	0.023	0.938	0.854	0.011
10.966	0.813	0.013	0.010	0.020	0.532	0.802	0.007	-0.004	0.015	0.244						0.805	0.007
12.058	0.776	0.012	0.001	0.022	0.057	0.774	0.007	-5E-04	0.018	0.025						0.775	0.007
12.565	0.790	0.012	0.018	0.019	0.964	0.771	0.007	-0.007	0.015	0.484						0.776	0.007
13.025	0.806	0.012	0.016	0.020	0.820	0.788	0.008	-0.007	0.016	0.424						0.793	0.008
14.165	0.813	0.012	0.004	0.029	0.132	0.809	0.008	-0.002	0.027	0.062						0.810	0.008

Table 38. Relative DoE for OxIn at 600 °C.

	LNE					NIST					INRIM						
CWL, µm	Em	U_{Em}	D_i	U_i	E	Em	U_{Em}	D_i	U_i	E	Em	U_{Em}	D_i	U_i	E	ε_{CRV}	$U_{cut\text{-}off}$
1.997																	
2.253																	
2.500																	
3.026	0.841	0.019	0.020	0.026	0.755	0.818	0.008	-0.007	0.021	0.340	0.819	0.021	-0.006	0.028	0.229	0.824	0.013
3.615	0.831	0.015	0.011	0.021	0.494	0.821	0.007	-0.002	0.018	0.140	0.814	0.021	-0.011	0.027	0.410	0.823	0.011
3.965	0.827	0.016	0.009	0.023	0.410	0.819	0.007	-0.001	0.019	0.046	0.808	0.021	-0.013	0.028	0.479	0.819	0.012
4.530	0.823	0.015	0.011	0.023	0.453	0.813	0.007	-0.002	0.020	0.106	0.804	0.021	-0.013	0.029	0.458	0.815	0.011
5.026	0.818	0.014	0.009	0.021	0.431	0.809	0.007	-0.002	0.018	0.096	0.800	0.021	-0.014	0.028	0.484	0.811	0.011
5.265	0.814	0.013	0.007	0.021	0.312	0.808	0.007	-0.001	0.019	0.070	0.800	0.021	-0.010	0.029	0.363	0.809	0.010
6.019	0.796	0.013	-0.002	0.021	0.082	0.799	0.007	0.001	0.019	0.067	0.797	0.021	-0.001	0.029	0.029	0.798	0.010
6.395	0.794	0.012	-0.004	0.020	0.174	0.799	0.007	0.003	0.018	0.174	0.793	0.021	-0.004	0.029	0.145	0.797	0.010
7.026	0.818	0.012	-0.003	0.020	0.165	0.819	0.008	-0.003	0.018	0.155	0.838	0.021	0.021	0.028	0.745	0.821	0.010
7.518	0.837	0.012	0.002	0.018	0.113	0.834	0.008	-0.002	0.016	0.127	0.838	0.021	0.003	0.027	0.108	0.836	0.010
8.040	0.848	0.012	0.007	0.019	0.373	0.836	0.008	-0.007	0.017	0.428	0.851	0.021	0.010	0.027	0.380	0.842	0.010
8.479	0.879	0.012	0.009	0.020	0.454	0.862	0.008	-0.011	0.018	0.582	0.886	0.021	0.017	0.027	0.614	0.871	0.010
9.034	0.898	0.012	0.007	0.020	0.338	0.884	0.009	-0.009	0.019	0.480	0.906	0.021	0.015	0.027	0.558	0.892	0.011
9.479	0.892	0.012	0.011	0.018	0.586	0.876	0.009	-0.007	0.017	0.417	0.880	0.021	-0.003	0.026	0.120	0.882	0.010
9.927	0.867	0.012	0.010	0.018	0.552	0.857	0.008	-0.002	0.017	0.101	0.838	0.021	-0.023	0.027	0.867	0.858	0.010
10.966	0.820	0.012	0.010	0.023	0.439	0.808	0.008	-0.004	0.020	0.208						0.812	0.008
12.058	0.784	0.011	0.001	0.025	0.055	0.783	0.007	-0.001	0.022	0.026						0.783	0.007
12.565	0.795	0.011	0.016	0.022	0.710	0.777	0.007	-0.007	0.020	0.366						0.783	0.007
13.025	0.813	0.011	0.014	0.023	0.624	0.796	0.008	-0.007	0.021	0.343						0.801	0.008
14.165	0.826	0.011	0.004	0.031	0.123	0.821	0.008	-0.002	0.030	0.066						0.822	0.008

Table 39. Relative DoE for OxIn at 700 °C.

	LNE					NIST					INRIM						
CWL, µm	Em	U_{Em}	D_i	U_i	E	Em	U_{Em}	D_i	U_i	E	Em	U_{Em}	D_i	U_i	E	ε_{CRV}	$U_{cut\text{-}off}$
1.997																	
2.253																	
2.500																	
3.026	0.846	0.017	0.012	0.026	0.471	0.833	0.008	-0.003	0.021	0.159	0.829	0.021	-0.008	0.029	0.271	0.835	0.013
3.615	0.837	0.014	0.005	0.020	0.235	0.834	0.008	0.001	0.017	0.075	0.821	0.021	-0.015	0.027	0.545	0.833	0.011
3.965	0.830	0.015	0.001	0.021	0.044	0.832	0.008	0.003	0.018	0.173	0.819	0.021	-0.012	0.027	0.454	0.829	0.011
4.530	0.826	0.014	0.002	0.021	0.076	0.826	0.008	0.002	0.018	0.105	0.816	0.021	-0.011	0.028	0.383	0.825	0.011
5.026	0.823	0.013	0.002	0.020	0.091	0.822	0.007	0.002	0.018	0.090	0.812	0.021	-0.011	0.028	0.391	0.821	0.010
5.265	0.818	0.013	-0.001	0.020	0.027	0.821	0.007	0.003	0.018	0.150	0.811	0.021	-0.010	0.028	0.345	0.819	0.010
6.019	0.804	0.012	-0.006	0.021	0.302	0.813	0.007	0.005	0.019	0.261	0.806	0.021	-0.004	0.029	0.140	0.809	0.010
6.395	0.802	0.012	-0.006	0.021	0.299	0.812	0.007	0.006	0.019	0.315	0.800	0.021	-0.009	0.029	0.299	0.807	0.010
7.026	0.826	0.012	-0.002	0.019	0.113	0.825	0.008	-0.003	0.018	0.179	0.844	0.021	0.020	0.028	0.727	0.827	0.010
7.518	0.842	0.012	0.000	0.018	0.001	0.841	0.008	-0.001	0.017	0.065	0.846	0.021	0.005	0.027	0.174	0.842	0.010
8.040	0.849	0.012	0.004	0.019	0.202	0.841	0.008	-0.005	0.017	0.314	0.856	0.021	0.012	0.027	0.433	0.846	0.010
8.479	0.880	0.012	0.008	0.020	0.400	0.863	0.008	-0.011	0.019	0.571	0.890	0.021	0.020	0.028	0.716	0.873	0.010
9.034	0.899	0.012	0.006	0.020	0.312	0.886	0.009	-0.009	0.019	0.477	0.909	0.021	0.017	0.027	0.612	0.894	0.011
9.479	0.895	0.012	0.009	0.019	0.475	0.881	0.009	-0.006	0.018	0.362	0.885	0.021	-0.001	0.027	0.048	0.887	0.010
9.927	0.873	0.012	0.009	0.018	0.474	0.865	0.008	-0.001	0.017	0.055	0.846	0.021	-0.023	0.027	0.861	0.866	0.010
10.966	0.831	0.011	0.010	0.027	0.383	0.822	0.008	-0.001	0.026	0.020	0.795	0.021	-0.033	0.034	0.970	0.822	0.009
12.058	0.797	0.011	0.004	0.023	0.168	0.799	0.007	0.006	0.022	0.269	0.759	0.021	-0.045	0.032	1.401	0.794	0.009
12.565	0.802	0.011	0.010	0.022	0.450	0.790	0.007	-0.005	0.020	0.240						0.794	0.007
13.025	0.821	0.011	0.008	0.023	0.344	0.811	0.008	-0.004	0.021	0.195						0.814	0.008
14.165	0.844	0.011	-0.001	0.033	0.040	0.845	0.008	0.001	0.032	0.022						0.845	0.008

Table 40. Relative DoE for OxIn at 800 °C.

	NIST					INRIM						
CWL, µm	Em	U_{Em}	D_i	U_i	E	Em	U_{Em}	D_i	U_i	E	ε_{CRV}	$U_{cut\text{-}off}$
1.997												
2.253												
2.500												
3.026	0.853	0.008	0.003	0.019	0.168	0.833	0.021	-0.021	0.029	0.722	0.851	0.008
3.615	0.850	0.008	0.003	0.016	0.191	0.830	0.021	-0.021	0.028	0.771	0.848	0.008
3.965	0.848	0.008	0.003	0.017	0.181	0.827	0.021	-0.021	0.028	0.751	0.845	0.008
4.530	0.841	0.008	0.003	0.017	0.146	0.824	0.021	-0.018	0.029	0.627	0.839	0.008
5.026	0.837	0.008	0.003	0.017	0.150	0.820	0.021	-0.019	0.029	0.647	0.835	0.008
5.265	0.835	0.008	0.002	0.017	0.124	0.821	0.021	-0.016	0.029	0.541	0.834	0.008
6.019	0.829	0.008	0.002	0.018	0.110	0.815	0.021	-0.014	0.029	0.496	0.827	0.008
6.395	0.828	0.008	0.003	0.018	0.143	0.810	0.021	-0.019	0.029	0.640	0.825	0.008
7.026	0.836	0.008	-0.003	0.018	0.143	0.853	0.021	0.018	0.029	0.607	0.838	0.008
7.518	0.849	0.008	-0.001	0.018	0.041	0.854	0.021	0.005	0.028	0.170	0.850	0.008
8.040	0.846	0.008	-0.003	0.019	0.144	0.864	0.021	0.018	0.030	0.614	0.849	0.008
8.479	0.866	0.009	-0.005	0.022	0.227	0.896	0.021	0.029	0.031	0.950	0.871	0.009
9.034	0.889	0.009	-0.005	0.023	0.212	0.916	0.021	0.026	0.031	0.837	0.893	0.009
9.479	0.887	0.009	-0.001	0.020	0.037	0.891	0.021	0.004	0.029	0.139	0.887	0.009
9.927	0.874	0.009	0.003	0.018	0.154	0.857	0.021	-0.016	0.028	0.577	0.871	0.009
10.966	0.836	0.008	0.004	0.023	0.182	0.808	0.021	-0.029	0.033	0.898	0.833	0.008
12.058	0.816	0.007	0.006	0.022	0.294	0.771	0.021	-0.048	0.032	1.505	0.810	0.007
12.565												
13.025												
14.165												

Table 41. Relative DoE for SiC at 23 °C.

	LNE					NIST					INRIM						
CWL, µm	Em	U_{Em}	D_i	U_i	E	Em	U_{Em}	D_i	U_i	E	Em	U_{Em}	D_i	U_i	E	ε_{CRV}	$U_{cut\text{-}off}$
1.997						0.820	0.001	0.000	0.005	0.001	0.820	0.019	0.001	0.024	0.023	0.820	0.001
2.253																	
2.500						0.818	0.001	6E-06	0.003	0.002	0.816	0.019	-0.003	0.023	0.136	0.818	0.001
3.026						0.819	0.001	-1E-06	0.003	0.000	0.820	0.019	0.001	0.023	0.027	0.819	0.001
3.615						0.823	0.001	-3E-06	0.003	0.001	0.824	0.019	0.002	0.023	0.087	0.823	0.001
3.965	0.836	0.012	0.011	0.013	0.858	0.824	0.001	-0.003	0.007	0.394	0.824	0.019	-0.003	0.022	0.143	0.827	0.006
4.530	0.826	0.012	-0.001	0.013	0.049	0.827	0.001	4E-04	0.007	0.050	0.825	0.019	-0.002	0.022	0.071	0.827	0.006
5.026	0.828	0.012	-0.002	0.013	0.140	0.830	0.001	0.001	0.007	0.113	0.827	0.019	-0.003	0.022	0.121	0.829	0.006
5.265	0.823	0.015	-0.008	0.017	0.457	0.831	0.001	0.003	0.009	0.303	0.826	0.019	-0.004	0.022	0.168	0.829	0.008
6.019	0.820	0.014	-0.018	0.016	1.109	0.839	0.001	0.005	0.008	0.621	0.832	0.019	-0.003	0.022	0.129	0.834	0.007
6.395	0.818	0.015	-0.021	0.017	1.286	0.842	0.001	0.007	0.009	0.769	0.831	0.020	-0.006	0.023	0.270	0.836	0.008
7.026	0.843	0.016	-0.005	0.018	0.290	0.850	0.001	0.004	0.009	0.419	0.835	0.020	-0.014	0.022	0.635	0.847	0.008
7.518	0.856	0.015	-0.002	0.016	0.153	0.861	0.001	0.003	0.008	0.366	0.843	0.021	-0.017	0.023	0.757	0.858	0.008
8.040	0.861	0.021	-0.010	0.022	0.450	0.873	0.001	0.004	0.012	0.332	0.865	0.023	-0.006	0.025	0.222	0.870	0.011
8.479	0.890	0.014	0.008	0.016	0.472	0.883	0.001	-1E-05	0.002	0.006						0.883	0.001
9.034	0.886	0.018	-0.004	0.019	0.234	0.891	0.001	0.001	0.010	0.102	0.891	0.024	0.001	0.026	0.046	0.890	0.009
9.479	0.911	0.015	-0.003	0.014	0.178	0.914	0.001	4E-04	0.007	0.051	0.917	0.027	0.004	0.029	0.138	0.914	0.008
9.927	0.864	0.017	0.006	0.018	0.304	0.859	0.001	-0.001	0.009	0.071	0.851	0.030	-0.009	0.034	0.274	0.859	0.009
10.966	0.158	0.046	-0.147	0.253	0.581	0.177	0.003	-0.043	0.047	0.920	0.198	0.004	0.071	0.049	1.461	0.185	0.004
12.058	0.089	0.046	-0.387	0.321	1.207	0.136	0.003	-0.061	0.056	1.103	0.160	0.004	0.100	0.058	1.720	0.145	0.004
12.565	0.213	0.047	-0.167	0.186	0.896	0.256	0.002	4E-04	0.027	0.015						0.256	0.002
13.025	0.377	0.041	-0.029	0.107	0.266	0.389	0.002	6E-05	0.014	0.004						0.389	0.002
14.165	0.551	0.047	-0.050	0.081	0.618	0.580	0.002	1E-04	0.011	0.009						0.580	0.002

Table 42. Relative DoE for SiC at 50 °C.

	NIST					NMIJ						
CWL, µm	Em	U_{Em}	D_i	U_i	E	Em	U_{Em}	D_i	U_i	E	ε_{CRV}	$U_{cut\text{-}off}$
1.997												
2.253												
2.500												
3.026												
3.615												
3.965												
4.530												
5.026												
5.265												
6.019	0.839	0.001	5E-06	0.003	0.002	0.834	0.023	-0.007	0.027	0.243	0.839	0.001
6.395	0.843	0.001	5E-06	0.003	0.002	0.838	0.022	-0.006	0.026	0.224	0.843	0.001
7.026	0.852	0.001	5E-06	0.003	0.002	0.847	0.021	-0.006	0.025	0.223	0.852	0.001
7.518	0.862	0.001	3E-06	0.003	0.001	0.859	0.020	-0.004	0.023	0.160	0.862	0.001
8.040	0.874	0.001	3E-06	0.003	0.001	0.872	0.019	-0.003	0.022	0.145	0.874	0.001
8.479	0.886	0.001	2E-06	0.003	0.001	0.884	0.018	-0.002	0.020	0.117	0.886	0.001
9.034	0.892	0.001	-7E-07	0.003	3E-04	0.893	0.017	0.001	0.019	0.035	0.892	0.001
9.479	0.917	0.001	3E-06	0.002	0.001	0.915	0.015	-0.002	0.017	0.134	0.917	0.001
9.927	0.837	0.001	-3E-06	0.004	0.001	0.841	0.029	0.005	0.035	0.136	0.837	0.001
10.966	0.160	0.003	-2E-04	0.071	0.002	0.222	0.126	0.387	0.791	0.489	0.160	0.003
12.058												
12.565												
13.025												
14.165												

Table 43. Relative DoE for SiC at 100 °C.

	LNE					NIST					NMIJ					PTB						
CWL, µm	Em	U_{Em}	D_i	U_i	E	Em	U_{Em}	D_i	U_i	E	Em	U_{Em}	D_i	U_i	E	Em	U_{Em}	D_i	U_i	E	ε_{CRV}	$U_{cut\text{-}off}$
1.997																						
2.253																						
2.500																						
3.026																						
3.615																						
3.965																						
4.530	0.858	0.035	0.038	0.043	0.896	0.827	0.001	-1E-05	0.002	0.006											0.827	0.001
5.026	0.848	0.033	0.023	0.039	0.580	0.830	0.001	0.002	0.005	0.392	0.822	0.008	-0.008	0.008	0.964	0.851	0.056	0.026	0.067	0.392	0.829	0.004
5.265	0.851	0.032	0.030	0.039	0.780	0.827	0.001	0.001	0.005	0.262	0.820	0.008	-0.007	0.009	0.819	0.847	0.048	0.026	0.058	0.458	0.825	0.004
6.019	0.843	0.030	0.006	0.035	0.159	0.840	0.001	0.002	0.005	0.376	0.832	0.007	-0.008	0.008	1.017	0.861	0.027	0.027	0.032	0.842	0.838	0.004
6.395	0.851	0.029	0.010	0.034	0.303	0.844	0.001	0.002	0.005	0.337	0.836	0.007	-0.008	0.008	0.980	0.859	0.024	0.020	0.028	0.715	0.842	0.004
7.026	0.866	0.028	0.017	0.033	0.502	0.853	0.001	0.001	0.004	0.306	0.845	0.007	-0.007	0.008	0.961	0.861	0.018	0.011	0.021	0.528	0.852	0.004
7.518	0.882	0.027	0.023	0.031	0.730	0.864	0.001	0.001	0.004	0.287	0.857	0.007	-0.007	0.008	0.895	0.868	0.018	0.006	0.021	0.288	0.862	0.004
8.040	0.889	0.026	0.016	0.030	0.549	0.876	0.001	0.001	0.004	0.308	0.869	0.007	-0.006	0.007	0.904	0.880	0.017	0.006	0.019	0.311	0.875	0.004
8.479	0.912	0.027	0.029	0.030	0.949	0.887	0.001	0.001	0.004	0.189	0.882	0.006	-0.005	0.006	0.794	0.893	0.015	0.007	0.017	0.433	0.886	0.003
9.034	0.916	0.026	0.024	0.029	0.820	0.894	0.001	-2E-04	0.004	0.054	0.893	0.006	-0.002	0.006	0.318	0.903	0.015	0.009	0.016	0.546	0.895	0.003
9.479	0.946	0.027	0.031	0.029	1.063	0.918	0.001	3E-04	0.003	0.115	0.915	0.005	-0.003	0.005	0.593	0.925	0.015	0.007	0.016	0.430	0.918	0.003
9.927	0.876	0.024	0.036	0.029	1.260	0.845	0.001	-0.001	0.007	0.093	0.842	0.010	-0.003	0.011	0.308	0.845	0.019	-0.001	0.023	0.024	0.845	0.005
10.966	0.194	0.009	0.097	0.108	0.899	0.170	0.003	-0.040	0.102	0.395	0.189	0.044	0.068	0.265	0.259	0.162	0.062	-0.085	0.362	0.236	0.177	0.006
12.058	0.168	0.009	0.086	0.115	0.752	0.150	0.003	-0.034	0.108	0.311	0.134	0.048	-0.138	0.328	0.421	0.140	0.071	-0.097	0.468	0.208	0.155	0.006
12.565	0.290	0.010	0.065	0.077	0.847	0.266	0.002	-0.024	0.072	0.332						0.256	0.065	-0.059	0.246	0.240	0.272	0.006
13.025	0.426	0.012	0.043	0.067	0.651	0.403	0.002	-0.014	0.063	0.222						0.395	0.055	-0.034	0.148	0.229	0.409	0.007
14.165	0.587	0.016	0.029	0.035	0.829	0.565	0.003	-0.009	0.028	0.324						0.559	0.044	-0.019	0.081	0.235	0.570	0.009

Table 44. Relative DoE for SiC at 150 °C.

	LNE					NIST					PTB						
CWL, µm	Em	U_{Em}	D_i	U_i	E	Em	U_{Em}	D_i	U_i	E	Em	U_{Em}	D_i	U_i	E	ε_{CRV}	$U_{cut\text{-}off}$
1.997																	
2.253																	
2.500																	
3.026																	
3.615																	
3.965	0.846	0.029	0.027	0.036	0.746	0.824	0.001	-1E-05	0.002	0.008						0.824	0.001
4.530	0.844	0.027	0.017	0.033	0.522	0.826	0.001	-0.003	0.022	0.148	0.816	0.048	-0.016	0.059	0.278	0.829	0.014
5.026	0.858	0.025	0.028	0.030	0.915	0.830	0.001	-0.006	0.018	0.334	0.831	0.028	-0.005	0.034	0.160	0.835	0.013
5.265	0.848	0.024	0.018	0.027	0.676	0.829	0.001	-0.005	0.011	0.474	0.836	0.022	0.004	0.023	0.184	0.833	0.011
6.019	0.850	0.022	0.010	0.028	0.377	0.840	0.001	-0.002	0.014	0.108	0.842	0.016	0.000	0.021	0.007	0.842	0.009
6.395	0.859	0.022	0.016	0.026	0.589	0.844	0.001	-0.001	0.013	0.088	0.842	0.016	-0.004	0.020	0.208	0.845	0.008
7.026	0.873	0.021	0.021	0.024	0.857	0.854	0.001	-0.002	0.008	0.203	0.854	0.012	-0.001	0.013	0.102	0.855	0.006
7.518	0.888	0.021	0.025	0.023	1.096	0.865	0.001	-0.002	0.004	0.524	0.868	0.011	0.001	0.010	0.101	0.867	0.006
8.040	0.896	0.020	0.020	0.022	0.904	0.877	0.001	-0.002	0.005	0.365	0.880	0.010	0.001	0.010	0.103	0.879	0.005
8.479	0.914	0.020	0.026	0.021	1.201	0.889	0.001	-0.002	0.003	0.797	0.893	0.010	0.002	0.009	0.216	0.891	0.005
9.034	0.923	0.020	0.026	0.021	1.217	0.897	0.001	-0.003	0.003	0.918	0.904	0.010	0.005	0.009	0.580	0.900	0.005
9.479	0.950	0.020	0.029	0.021	1.427	0.920	0.001	-0.003	0.003	1.028	0.926	0.010	0.003	0.008	0.337	0.923	0.005
9.927	0.880	0.018	0.030	0.020	1.520	0.852	0.001	-0.002	0.004	0.477	0.850	0.012	-0.005	0.011	0.442	0.854	0.006
10.966	0.208	0.009	0.106	0.055	1.912	0.181	0.003	-0.040	0.044	0.914	0.173	0.033	-0.080	0.176	0.456	0.188	0.006
12.058	0.171	0.009	0.104	0.063	1.640	0.148	0.003	-0.041	0.049	0.836	0.142	0.039	-0.079	0.250	0.317	0.155	0.006
12.565	0.286	0.010	0.067	0.036	1.853	0.262	0.002	-0.024	0.026	0.937	0.255	0.036	-0.048	0.132	0.359	0.268	0.006
13.025	0.413	0.011	0.027	0.028	0.982	0.398	0.002	-0.008	0.020	0.430	0.393	0.031	-0.023	0.076	0.298	0.402	0.006
14.165	0.583	0.013	0.027	0.021	1.274	0.563	0.003	-0.008	0.013	0.618	0.560	0.025	-0.015	0.043	0.339	0.568	0.008

Table 45. Relative DoE for SiC at 200 °C.

	LNE					NIST					PTB						
CWL, µm	Em	U_{Em}	D_i	U_i	E	Em	U_{Em}	D_i	U_i	E	Em	U_{Em}	D_i	U_i	E	ε_{CRV}	$U_{cut\text{-}off}$
1.997																	
2.253																	
2.500																	
3.026																	
3.615																	
3.965	0.852	0.024	0.030	0.028	1.073	0.823	0.001	-0.005	0.015	0.349	0.810	0.036	-0.021	0.042	0.499	0.828	0.013
4.530	0.851	0.022	0.024	0.028	0.863	0.826	0.001	-0.006	0.018	0.315	0.827	0.028	-0.004	0.034	0.122	0.831	0.011
5.026	0.858	0.021	0.027	0.026	1.028	0.830	0.001	-0.007	0.017	0.399	0.836	0.020	0.001	0.025	0.030	0.836	0.010
5.265	0.851	0.020	0.019	0.023	0.838	0.830	0.001	-0.007	0.013	0.520	0.840	0.020	0.006	0.024	0.250	0.835	0.010
6.019	0.847	0.018	0.005	0.022	0.242	0.841	0.001	-0.002	0.014	0.134	0.847	0.034	0.005	0.040	0.134	0.842	0.010
6.395	0.851	0.018	0.005	0.020	0.259	0.845	0.001	-0.002	0.012	0.130	0.848	0.032	0.002	0.037	0.043	0.846	0.009
7.026	0.870	0.017	0.014	0.019	0.754	0.855	0.001	-0.004	0.010	0.374	0.858	0.030	-2E-04	0.034	0.005	0.858	0.009
7.518	0.887	0.017	0.019	0.018	1.039	0.866	0.001	-0.005	0.009	0.543	0.871	0.026	2E-04	0.029	0.005	0.871	0.009
8.040	0.898	0.017	0.017	0.018	0.965	0.879	0.001	-0.005	0.009	0.485	0.883	0.023	4E-04	0.025	0.014	0.883	0.009
8.479	0.911	0.017	0.017	0.017	1.011	0.891	0.001	-0.005	0.009	0.531	0.896	0.021	0.001	0.022	0.056	0.895	0.009
9.034	0.924	0.016	0.021	0.017	1.219	0.900	0.001	-0.006	0.009	0.702	0.908	0.018	0.003	0.019	0.175	0.905	0.008
9.479	0.949	0.016	0.023	0.017	1.353	0.922	0.001	-0.006	0.009	0.708	0.929	0.017	0.001	0.017	0.039	0.928	0.008
9.927	0.885	0.015	0.025	0.017	1.437	0.860	0.001	-0.005	0.009	0.512	0.858	0.016	-0.007	0.018	0.415	0.864	0.008
10.966	0.216	0.009	0.087	0.055	1.577	0.193	0.002	-0.030	0.046	0.670	0.186	0.021	-0.066	0.112	0.593	0.199	0.006
12.058	0.163	0.009	0.076	0.068	1.114	0.147	0.003	-0.029	0.055	0.524	0.143	0.025	-0.055	0.171	0.321	0.152	0.006
12.565	0.274	0.009	0.048	0.039	1.222	0.257	0.002	-0.017	0.031	0.543	0.252	0.024	-0.035	0.093	0.374	0.262	0.006
13.025	0.412	0.010	0.035	0.026	1.356	0.394	0.002	-0.011	0.018	0.585	0.389	0.021	-0.022	0.053	0.413	0.398	0.006
14.165	0.582	0.011	0.027	0.020	1.333	0.562	0.003	-0.008	0.014	0.582	0.559	0.017	-0.013	0.031	0.407	0.566	0.007

Table 46. Relative DoE for SiC at 250 °C.

	LNE					NIST					PTB					INRIM						
CWL, µm	Em	U_{Em}	D_i	U_i	E	Em	U_{Em}	D_i	U_i	E	Em	U_{Em}	D_i	U_i	E	Em	U_{Em}	D_i	U_i	E	ε_{CRV}	$U_{cut\text{-}off}$
1.997																						
2.253																						
2.500																						
3.026																						
3.615						0.824	0.008	0.003	0.022	0.137	0.816	0.031	-0.007	0.039	0.178	0.816	0.022	-0.007	0.029	0.228	0.822	0.015
3.965	0.856	0.024	0.029	0.030	0.951	0.826	0.008	-0.007	0.020	0.375	0.823	0.026	-0.010	0.033	0.318	0.829	0.021	-0.004	0.027	0.160	0.832	0.014
4.530	0.855	0.021	0.025	0.031	0.803	0.829	0.008	-0.007	0.023	0.289	0.825	0.019	-0.012	0.028	0.406	0.831	0.020	-0.005	0.029	0.158	0.835	0.013
5.026	0.858	0.020	0.023	0.028	0.823	0.833	0.008	-0.006	0.020	0.326	0.836	0.016	-0.002	0.023	0.101	0.836	0.020	-0.003	0.027	0.119	0.838	0.012
5.265	0.856	0.019	0.020	0.026	0.788	0.834	0.008	-0.006	0.017	0.372	0.842	0.014	0.004	0.020	0.183	0.836	0.020	-0.004	0.026	0.140	0.839	0.011
6.019	0.847	0.018	0.003	0.025	0.121	0.843	0.008	-0.001	0.018	0.067	0.844	0.012	-0.001	0.020	0.030	0.846	0.020	0.002	0.027	0.067	0.844	0.010
6.395	0.851	0.017	0.003	0.024	0.106	0.848	0.008	0.000	0.017	0.018	0.845	0.012	-0.004	0.019	0.230	0.853	0.022	0.005	0.029	0.185	0.849	0.010
7.026	0.868	0.017	0.010	0.022	0.435	0.858	0.008	-0.002	0.015	0.146	0.857	0.010	-0.003	0.015	0.223	0.866	0.022	0.007	0.027	0.249	0.860	0.009
7.518	0.885	0.016	0.015	0.021	0.696	0.870	0.008	-0.003	0.014	0.245	0.871	0.009	-0.001	0.014	0.107	0.873	0.022	0.001	0.026	0.025	0.873	0.009
8.040	0.899	0.016	0.015	0.020	0.736	0.882	0.008	-0.003	0.013	0.253	0.884	0.009	-0.001	0.013	0.088	0.885	0.022	0.000	0.026	0.016	0.885	0.009
8.479	0.912	0.016	0.015	0.020	0.721	0.896	0.009	-0.003	0.014	0.214	0.897	0.009	-0.002	0.014	0.124						0.899	0.009
9.034	0.922	0.016	0.012	0.020	0.623	0.909	0.009	-0.002	0.014	0.148	0.910	0.008	-0.001	0.013	0.102	0.907	0.022	-0.004	0.026	0.161	0.911	0.008
9.479	0.947	0.016	0.016	0.019	0.801	0.931	0.009	-0.002	0.014	0.177	0.930	0.008	-0.003	0.013	0.255	0.935	0.024	0.002	0.028	0.084	0.933	0.009
9.927	0.891	0.015	0.024	0.020	1.208	0.869	0.008	-0.002	0.014	0.154	0.864	0.008	-0.008	0.014	0.589	0.862	0.024	-0.010	0.029	0.334	0.871	0.008
10.966	0.222	0.009	0.072	0.060	1.199	0.203	0.002	-0.021	0.050	0.423	0.197	0.015	-0.047	0.082	0.570	0.202	0.015	-0.026	0.081	0.323	0.207	0.005
12.058	0.156	0.009	0.040	0.073	0.544	0.147	0.001	-0.016	0.058	0.279	0.144	0.018	-0.036	0.130	0.278	0.159	0.022	0.064	0.151	0.421	0.150	0.005
12.565	0.269	0.009	0.041	0.042	0.995	0.254	0.002	-0.016	0.033	0.472	0.250	0.017	-0.033	0.071	0.474						0.258	0.006
13.025	0.403	0.010	0.022	0.030	0.722	0.391	0.004	-0.009	0.025	0.372	0.386	0.015	-0.023	0.042	0.536						0.395	0.007
14.165	0.578	0.011	0.018	0.023	0.812	0.562	0.005	-0.009	0.019	0.460	0.558	0.013	-0.015	0.026	0.591						0.567	0.008

Table 47. Relative DoE for SiC at 300 °C.

	LNE					NIST					INRIM						
CWL, µm	Em	U_{Em}	D_i	U_i	E	Em	U_{Em}	D_i	U_i	E	Em	U_{Em}	D_i	U_i	E	ε_{CRV}	$U_{cut\text{-}off}$
1.997																	
2.253																	
2.500																	
3.026																	
3.615	0.852	0.023	0.027	0.029	0.902	0.822	0.008	-0.010	0.021	0.476	0.827	0.024	-0.004	0.031	0.139	0.830	0.016
3.965	0.850	0.022	0.023	0.028	0.835	0.823	0.008	-0.009	0.020	0.470	0.830	0.021	-0.002	0.027	0.057	0.831	0.014
4.530	0.854	0.020	0.024	0.026	0.912	0.827	0.008	-0.008	0.020	0.409	0.828	0.020	-0.007	0.026	0.279	0.834	0.014
5.026	0.855	0.018	0.021	0.024	0.842	0.831	0.008	-0.007	0.019	0.366	0.831	0.020	-0.008	0.026	0.308	0.837	0.013
5.265	0.854	0.018	0.018	0.024	0.741	0.833	0.008	-0.008	0.020	0.385	0.835	0.020	-0.005	0.026	0.171	0.839	0.013
6.019	0.842	0.016	-0.005	0.024	0.198	0.845	0.008	-0.001	0.020	0.051	0.855	0.022	0.011	0.029	0.388	0.846	0.012
6.395	0.846	0.016	-0.003	0.026	0.126	0.850	0.008	0.001	0.023	0.064	0.850	0.022	0.001	0.031	0.040	0.849	0.012
7.026	0.868	0.016	0.005	0.027	0.196	0.860	0.008	-0.003	0.025	0.138	0.864	0.022	0.001	0.032	0.029	0.863	0.012
7.518	0.884	0.015	0.010	0.027	0.376	0.871	0.008	-0.005	0.024	0.210	0.873	0.022	-0.003	0.032	0.091	0.875	0.012
8.040	0.895	0.015	0.009	0.022	0.389	0.884	0.008	-0.004	0.020	0.215	0.884	0.022	-0.004	0.028	0.126	0.887	0.012
8.479	0.911	0.015	0.011	0.021	0.518	0.897	0.009	-0.004	0.016	0.224						0.901	0.009
9.034	0.923	0.015	0.008	0.022	0.389	0.911	0.009	-0.004	0.020	0.210	0.911	0.022	-0.004	0.028	0.155	0.915	0.012
9.479	0.947	0.015	0.010	0.023	0.454	0.932	0.009	-0.006	0.021	0.302	0.936	0.024	-0.002	0.030	0.053	0.938	0.012
9.927	0.899	0.014	0.018	0.020	0.907	0.876	0.008	-0.009	0.017	0.494	0.872	0.024	-0.013	0.030	0.437	0.883	0.011
10.966	0.234	0.009	0.059	0.063	0.945	0.217	0.002	-0.018	0.055	0.318	0.216	0.013	-0.025	0.075	0.331	0.221	0.006
12.058	0.153	0.009	0.018	0.071	0.254	0.149	0.001	-0.011	0.057	0.199	0.161	0.018	0.068	0.129	0.527	0.151	0.005
12.565	0.263	0.009	0.038	0.046	0.819	0.253	0.002	-0.003	0.030	0.089						0.253	0.002
13.025	0.397	0.010	0.019	0.033	0.579	0.389	0.004	-0.003	0.024	0.120						0.390	0.004
14.165	0.574	0.011	0.018	0.024	0.738	0.561	0.005	-0.005	0.018	0.258						0.564	0.005

Table 48. Relative DoE for SiC at 350 °C.

	LNE					NIST					INRIM						
CWL, µm	Em	U_{Em}	D_i	U_i	E	Em	U_{Em}	D_i	U_i	E	Em	U_{Em}	D_i	U_i	E	ε_{CRV}	$U_{cut\text{-}off}$
1.997																	
2.253																	
2.500																	
3.026																	
3.615	0.851	0.023	0.027	0.036	0.748	0.822	0.008	-0.009	0.030	0.290	0.823	0.022	-0.007	0.035	0.195	0.829	0.015
3.965	0.850	0.021	0.023	0.034	0.681	0.824	0.008	-0.008	0.028	0.291	0.827	0.021	-0.004	0.033	0.133	0.830	0.014
4.530	0.850	0.019	0.020	0.032	0.638	0.827	0.008	-0.006	0.027	0.239	0.827	0.020	-0.007	0.032	0.231	0.833	0.014
5.026	0.853	0.018	0.018	0.030	0.606	0.832	0.008	-0.007	0.026	0.271	0.833	0.020	-0.005	0.031	0.170	0.838	0.013
5.265	0.850	0.018	0.014	0.031	0.467	0.833	0.008	-0.006	0.027	0.215	0.834	0.020	-0.004	0.032	0.126	0.838	0.013
6.019	0.844	0.016	-0.002	0.031	0.070	0.844	0.008	-0.002	0.028	0.079	0.855	0.022	0.011	0.035	0.305	0.846	0.012
6.395	0.847	0.016	-0.002	0.030	0.078	0.849	0.008	0.000	0.028	0.008	0.854	0.022	0.005	0.035	0.145	0.849	0.012
7.026	0.867	0.015	0.005	0.032	0.172	0.860	0.008	-0.003	0.029	0.107	0.862	0.022	-1E-04	0.036	0.003	0.862	0.012
7.518	0.884	0.015	0.011	0.031	0.353	0.871	0.008	-0.004	0.029	0.131	0.866	0.022	-0.009	0.036	0.260	0.875	0.012
8.040	0.897	0.015	0.009	0.027	0.342	0.884	0.008	-0.006	0.025	0.218	0.888	0.022	-0.001	0.032	0.020	0.889	0.012
8.479	0.907	0.015	0.008	0.027	0.294	0.897	0.009	-0.003	0.024	0.114						0.900	0.009
9.034	0.923	0.015	0.008	0.028	0.288	0.911	0.009	-0.004	0.026	0.168	0.913	0.022	-0.002	0.033	0.075	0.915	0.012
9.479	0.942	0.015	0.006	0.029	0.219	0.932	0.009	-0.005	0.028	0.177	0.939	0.024	0.003	0.036	0.089	0.936	0.012
9.927	0.904	0.014	0.016	0.026	0.605	0.882	0.008	-0.008	0.024	0.339	0.882	0.024	-0.009	0.034	0.249	0.890	0.011
10.966	0.248	0.009	0.054	0.076	0.708	0.233	0.002	-0.011	0.069	0.162	0.228	0.011	-0.034	0.080	0.424	0.236	0.006
12.058	0.153	0.009	0.012	0.083	0.148	0.149	0.001	-0.019	0.069	0.276	0.165	0.013	0.087	0.102	0.860	0.152	0.005
12.565	0.256	0.009	0.030	0.053	0.564	0.248	0.002	-0.002	0.038	0.050						0.248	0.002
13.025	0.391	0.010	0.016	0.039	0.416	0.383	0.004	-0.002	0.031	0.072						0.384	0.004
14.165	0.571	0.011	0.017	0.030	0.555	0.559	0.005	-0.004	0.025	0.162						0.561	0.005

Table 49. Relative DoE for SiC at 400 °C.

	LNE					NIST					INRIM						
CWL, µm	Em	U_{Em}	D_i	U_i	E	Em	U_{Em}	D_i	U_i	E	Em	U_{Em}	D_i	U_i	E	ε_{CRV}	$U_{cut\text{-}off}$
1.997																	
2.253																	
2.500																	
3.026	0.846	0.026	0.025	0.032	0.773	0.819	0.008	-0.008	0.021	0.371	0.825	0.022	-0.001	0.028	0.044	0.826	0.015
3.615	0.843	0.022	0.020	0.029	0.672	0.822	0.008	-0.006	0.021	0.288	0.823	0.021	-0.004	0.027	0.152	0.826	0.014
3.965	0.844	0.021	0.018	0.027	0.652	0.823	0.008	-0.008	0.020	0.385	0.829	0.021	-0.001	0.027	0.037	0.829	0.014
4.530	0.845	0.019	0.015	0.025	0.622	0.827	0.008	-0.006	0.019	0.328	0.830	0.020	-0.003	0.026	0.127	0.832	0.014
5.026	0.849	0.018	0.015	0.024	0.624	0.831	0.008	-0.006	0.019	0.316	0.833	0.020	-0.004	0.026	0.163	0.836	0.013
5.265	0.848	0.017	0.012	0.025	0.474	0.833	0.008	-0.006	0.020	0.280	0.837	0.020	-0.001	0.027	0.050	0.838	0.013
6.019	0.844	0.016	-0.002	0.025	0.086	0.844	0.008	-0.002	0.022	0.085	0.854	0.022	0.010	0.030	0.321	0.846	0.012
6.395	0.845	0.016	-0.004	0.026	0.146	0.850	0.008	0.002	0.024	0.064	0.850	0.022	0.002	0.032	0.075	0.848	0.012
7.026	0.866	0.015	0.004	0.026	0.135	0.860	0.008	-0.003	0.024	0.120	0.865	0.022	0.003	0.032	0.080	0.863	0.012
7.518	0.882	0.015	0.007	0.025	0.297	0.872	0.008	-0.004	0.022	0.182	0.874	0.022	-0.001	0.030	0.042	0.875	0.012
8.040	0.893	0.015	0.005	0.023	0.222	0.885	0.008	-0.004	0.021	0.172	0.889	0.022	0.001	0.029	0.045	0.888	0.012
8.479	0.905	0.015	0.005	0.023	0.226	0.899	0.009	-0.002	0.018	0.096						0.901	0.009
9.034	0.920	0.015	0.005	0.024	0.195	0.913	0.009	-0.003	0.022	0.117	0.914	0.022	-0.001	0.029	0.049	0.916	0.012
9.479	0.941	0.015	0.004	0.025	0.169	0.933	0.009	-0.004	0.024	0.157	0.940	0.024	0.004	0.033	0.120	0.937	0.012
9.927	0.908	0.014	0.013	0.022	0.613	0.890	0.009	-0.007	0.020	0.350	0.889	0.024	-0.008	0.031	0.250	0.896	0.011
10.966	0.265	0.010	0.056	0.082	0.680	0.250	0.002	-0.002	0.077	0.030	0.241	0.008	-0.039	0.081	0.482	0.251	0.005
12.058	0.160	0.009	0.047	0.071	0.657	0.150	0.001	-0.015	0.054	0.284	0.153	0.013	-0.001	0.092	0.007	0.153	0.005
12.565	0.246	0.009	0.005	0.056	0.086	0.245	0.002	-3E-04	0.042	0.007						0.245	0.002
13.025	0.383	0.010	0.010	0.037	0.269	0.379	0.004	-0.001	0.027	0.048						0.379	0.004
14.165	0.568	0.011	0.017	0.025	0.674	0.557	0.005	-0.004	0.018	0.223						0.559	0.005

Table 50. Relative DoE for SiC at 450 °C.

	LNE					NIST					INRIM						
CWL, µm	Em	U_{Em}	D_i	U_i	E	Em	U_{Em}	D_i	U_i	E	Em	U_{Em}	D_i	U_i	E	ε_{CRV}	$U_{cut\text{-}off}$
1.997																	
2.253																	
2.500																	
3.026																	
3.615	0.843	0.020	0.019	0.027	0.699	0.821	0.008	-0.008	0.020	0.378	0.825	0.021	-0.003	0.027	0.104	0.827	0.014
3.965	0.841	0.019	0.016	0.026	0.623	0.823	0.008	-0.007	0.020	0.342	0.826	0.021	-0.003	0.027	0.099	0.828	0.014
4.530	0.845	0.018	0.015	0.024	0.655	0.827	0.008	-0.006	0.019	0.344	0.829	0.020	-0.004	0.026	0.158	0.832	0.013
5.026	0.846	0.017	0.012	0.023	0.540	0.831	0.008	-0.006	0.018	0.312	0.834	0.020	-0.002	0.026	0.093	0.836	0.012
5.265	0.847	0.016	0.011	0.024	0.459	0.833	0.008	-0.005	0.020	0.266	0.836	0.020	-0.002	0.027	0.069	0.837	0.012
6.019	0.842	0.015	-0.004	0.025	0.158	0.845	0.008	-4E-04	0.022	0.021	0.853	0.022	0.009	0.031	0.307	0.845	0.012
6.395	0.847	0.015	-0.003	0.024	0.131	0.850	0.008	0.001	0.022	0.044	0.852	0.022	0.003	0.031	0.109	0.849	0.011
7.026	0.863	0.014	0.001	0.027	0.027	0.861	0.008	-0.002	0.025	0.063	0.866	0.022	0.004	0.033	0.125	0.862	0.011
7.518	0.879	0.014	0.004	0.028	0.161	0.872	0.008	-0.003	0.026	0.112	0.875	0.022	4E-04	0.033	0.011	0.875	0.011
8.040	0.892	0.014	0.004	0.023	0.190	0.885	0.008	-0.003	0.021	0.135	0.888	0.022	-3E-05	0.030	0.001	0.888	0.011
8.479	0.905	0.014	0.005	0.022	0.220	0.899	0.009	-0.002	0.018	0.106						0.901	0.009
9.034	0.920	0.013	0.005	0.024	0.196	0.913	0.009	-0.002	0.022	0.110	0.913	0.022	-0.003	0.030	0.094	0.915	0.011
9.479	0.941	0.013	0.004	0.025	0.154	0.933	0.009	-0.004	0.024	0.176	0.944	0.024	0.007	0.033	0.216	0.937	0.011
9.927	0.911	0.013	0.011	0.022	0.506	0.896	0.009	-0.006	0.021	0.292	0.893	0.024	-0.008	0.032	0.266	0.901	0.011
10.966	0.280	0.009	0.048	0.092	0.520	0.266	0.002	-0.004	0.088	0.048	0.258	0.008	-0.034	0.091	0.372	0.267	0.005
12.058	0.164	0.009	0.065	0.067	0.975	0.150	0.001	-0.026	0.052	0.501	0.156	0.010	0.015	0.075	0.202	0.154	0.005
12.565	0.246	0.009	0.025	0.049	0.502	0.240	0.002	-0.002	0.034	0.050						0.240	0.002
13.025	0.373	0.009	-1E-05	0.038	3E-04	0.373	0.004	2E-06	0.031	6E-05						0.373	0.004
14.165	0.565	0.010	0.017	0.023	0.717	0.553	0.005	-0.005	0.018	0.265						0.556	0.005

Table 51. Relative DoE for SiC at 500 °C.

	LNE					NIST					INRIM						
CWL, µm	Em	U_{Em}	D_i	U_i	E	Em	U_{Em}	D_i	U_i	E	Em	U_{Em}	D_i	U_i	E	ε_{CRV}	$U_{cut\text{-}off}$
1.997																	
2.253																	
2.500																	
3.026	0.840	0.021	0.019	0.027	0.714	0.819	0.008	-0.006	0.019	0.317	0.820	0.020	-0.004	0.026	0.173	0.824	0.014
3.615	0.841	0.019	0.018	0.025	0.699	0.821	0.008	-0.006	0.020	0.309	0.821	0.020	-0.006	0.027	0.235	0.826	0.013
3.965	0.840	0.017	0.014	0.024	0.596	0.823	0.008	-0.006	0.019	0.332	0.826	0.020	-0.003	0.026	0.109	0.828	0.013
4.530	0.843	0.016	0.013	0.022	0.612	0.827	0.008	-0.006	0.018	0.328	0.828	0.019	-0.004	0.025	0.160	0.832	0.012
5.026	0.845	0.015	0.011	0.022	0.515	0.832	0.008	-0.005	0.018	0.284	0.833	0.019	-0.003	0.025	0.134	0.836	0.012
5.265	0.845	0.015	0.010	0.023	0.417	0.834	0.008	-0.005	0.020	0.227	0.835	0.019	-0.003	0.027	0.109	0.837	0.012
6.019	0.840	0.014	-0.006	0.024	0.234	0.846	0.008	0.001	0.021	0.026	0.852	0.019	0.008	0.028	0.295	0.845	0.011
6.395	0.846	0.014	-0.004	0.024	0.146	0.851	0.008	0.002	0.022	0.096	0.849	0.021	4E-04	0.030	0.012	0.849	0.011
7.026	0.862	0.014	-0.001	0.027	0.020	0.861	0.008	-0.001	0.026	0.035	0.866	0.021	0.005	0.033	0.139	0.862	0.011
7.518	0.878	0.013	0.003	0.028	0.110	0.873	0.008	-0.002	0.026	0.086	0.876	0.021	0.001	0.033	0.029	0.875	0.011
8.040	0.891	0.013	0.003	0.022	0.155	0.886	0.009	-0.003	0.020	0.125	0.889	0.021	0.001	0.029	0.026	0.888	0.011
8.479	0.903	0.013	0.003	0.022	0.126	0.900	0.009	-0.001	0.019	0.066						0.901	0.009
9.034	0.916	0.013	0.001	0.024	0.035	0.915	0.009	-0.001	0.023	0.024	0.915	0.021	-2E-04	0.030	0.006	0.915	0.011
9.479	0.940	0.013	0.003	0.026	0.100	0.934	0.009	-0.003	0.025	0.114	0.941	0.023	0.005	0.034	0.135	0.937	0.011
9.927	0.914	0.012	0.008	0.022	0.356	0.903	0.009	-0.004	0.021	0.200	0.900	0.023	-0.007	0.031	0.235	0.907	0.011
10.966	0.301	0.009	0.062	0.099	0.629	0.284	0.003	0.004	0.095	0.038	0.274	0.006	-0.032	0.096	0.337	0.283	0.004
12.058	0.163	0.008	0.049	0.066	0.751	0.151	0.001	-0.028	0.050	0.549	0.160	0.008	0.031	0.066	0.474	0.155	0.005
12.565	0.241	0.009	0.020	0.050	0.402	0.236	0.002	-0.001	0.036	0.039						0.236	0.002
13.025	0.369	0.009	0.001	0.038	0.023	0.369	0.004	-1E-04	0.030	0.004						0.369	0.004
14.165	0.561	0.010	0.014	0.024	0.590	0.551	0.005	-0.004	0.018	0.220						0.553	0.005

Table 52. Relative DoE for SiC at 550 °C.

	LNE					NIST					INRIM						
CWL, µm	Em	U_{Em}	D_i	U_i	E	Em	U_{Em}	D_i	U_i	E	Em	U_{Em}	D_i	U_i	E	ε_{CRV}	$U_{cut\text{-}off}$
1.997	0.836	0.027	0.022	0.035	0.619						0.807	0.022	-0.014	0.029	0.479	0.819	0.022
2.253	0.840	0.025	0.026	0.033	0.782	0.817	0.008	-0.003	0.016	0.161						0.819	0.008
2.500	0.837	0.022	0.019	0.029	0.669	0.817	0.008	-0.005	0.020	0.264	0.817	0.021	-0.005	0.027	0.194	0.821	0.014
3.026	0.838	0.019	0.019	0.028	0.692	0.817	0.008	-0.007	0.022	0.304	0.818	0.020	-0.006	0.028	0.204	0.822	0.014
3.615	0.839	0.017	0.017	0.024	0.701	0.820	0.008	-0.006	0.019	0.325	0.820	0.020	-0.006	0.027	0.242	0.825	0.013
3.965	0.838	0.016	0.014	0.023	0.622	0.822	0.008	-0.006	0.018	0.341	0.824	0.020	-0.004	0.026	0.146	0.827	0.012
4.530	0.841	0.015	0.013	0.021	0.614	0.826	0.008	-0.006	0.017	0.324	0.827	0.019	-0.005	0.025	0.195	0.831	0.012
5.026	0.841	0.014	0.008	0.021	0.391	0.831	0.008	-0.004	0.018	0.224	0.832	0.019	-0.003	0.026	0.099	0.834	0.011
5.265	0.844	0.014	0.009	0.022	0.397	0.833	0.008	-0.005	0.020	0.238	0.835	0.019	-0.002	0.027	0.078	0.837	0.011
6.019	0.840	0.013	-0.005	0.023	0.233	0.845	0.008	0.001	0.021	0.043	0.851	0.019	0.008	0.028	0.284	0.844	0.011
6.395	0.844	0.013	-0.005	0.023	0.205	0.850	0.008	0.003	0.022	0.124	0.849	0.021	0.002	0.030	0.058	0.848	0.011
7.026	0.861	0.013	-2E-04	0.027	0.008	0.861	0.008	-0.001	0.026	0.025	0.864	0.021	0.003	0.033	0.091	0.861	0.011
7.518	0.877	0.013	0.003	0.028	0.118	0.872	0.008	-0.002	0.027	0.078	0.874	0.021	-0.001	0.034	0.019	0.874	0.011
8.040	0.890	0.013	0.003	0.022	0.152	0.885	0.008	-0.002	0.021	0.107	0.886	0.021	-0.001	0.029	0.021	0.887	0.011
8.479	0.902	0.012	0.003	0.021	0.136	0.898	0.009	-0.001	0.019	0.074						0.900	0.009
9.034	0.915	0.012	0.002	0.025	0.065	0.913	0.009	-1E-04	0.024	0.005	0.910	0.021	-0.004	0.031	0.132	0.913	0.011
9.479	0.937	0.012	0.003	0.026	0.106	0.932	0.009	-0.003	0.025	0.102	0.937	0.023	0.002	0.034	0.074	0.935	0.011
9.927	0.917	0.012	0.008	0.023	0.339	0.906	0.009	-0.004	0.022	0.198	0.903	0.024	-0.007	0.032	0.228	0.910	0.010
10.966	0.318	0.009	0.054	0.117	0.461	0.305	0.003	0.010	0.115	0.086	0.290	0.006	-0.040	0.115	0.346	0.302	0.004
12.058	0.163	0.008	0.043	0.069	0.629	0.155	0.001	-0.008	0.052	0.145	0.155	0.007	-0.011	0.063	0.168	0.156	0.004
12.565	0.243	0.009	0.029	0.048	0.600	0.235	0.002	-0.002	0.033	0.061						0.236	0.002
13.025	0.366	0.009	-0.002	0.039	0.042	0.367	0.004	2E-04	0.031	0.008						0.367	0.004
14.165	0.557	0.010	0.011	0.024	0.451	0.549	0.005	-0.003	0.019	0.167						0.551	0.005

Table 53. Relative DoE for SiC at 600 °C.

	LNE					NIST					INRIM						
CWL, µm	Em	U_{Em}	D_i	U_i	E	Em	U_{Em}	D_i	U_i	E	Em	U_{Em}	D_i	U_i	E	ε_{CRV}	$U_{cut\text{-}off}$
1.997																	
2.253																	
2.500																	
3.026	0.836	0.019	0.018	0.026	0.686	0.815	0.008	-0.007	0.021	0.347	0.818	0.020	-0.004	0.027	0.145	0.821	0.013
3.615	0.834	0.017	0.014	0.024	0.570	0.818	0.008	-0.006	0.020	0.316	0.821	0.020	-0.003	0.027	0.110	0.823	0.012
3.965	0.834	0.016	0.012	0.022	0.527	0.820	0.008	-0.005	0.019	0.282	0.821	0.020	-0.004	0.027	0.146	0.825	0.012
4.530	0.837	0.015	0.011	0.021	0.514	0.825	0.008	-0.005	0.017	0.263	0.825	0.019	-0.005	0.025	0.190	0.829	0.011
5.026	0.839	0.014	0.008	0.021	0.385	0.830	0.008	-0.003	0.018	0.174	0.828	0.019	-0.005	0.026	0.208	0.832	0.011
5.265	0.840	0.014	0.006	0.023	0.257	0.832	0.008	-0.003	0.021	0.167	0.834	0.019	-0.001	0.028	0.027	0.835	0.011
6.019	0.838	0.013	-0.007	0.023	0.299	0.845	0.008	0.001	0.021	0.067	0.854	0.021	0.012	0.030	0.407	0.843	0.011
6.395	0.842	0.013	-0.006	0.024	0.266	0.850	0.008	0.003	0.022	0.140	0.851	0.021	0.005	0.031	0.150	0.847	0.010
7.026	0.859	0.013	-0.002	0.027	0.059	0.860	0.008	-2E-04	0.025	0.008	0.865	0.021	0.005	0.033	0.158	0.860	0.010
7.518	0.876	0.012	0.002	0.027	0.085	0.872	0.008	-0.002	0.026	0.085	0.876	0.021	0.002	0.033	0.074	0.874	0.010
8.040	0.885	0.012	0.000	0.023	0.009	0.884	0.008	-0.001	0.021	0.044	0.888	0.021	0.003	0.030	0.109	0.885	0.010
8.479	0.897	0.012	-0.001	0.022	0.065	0.898	0.009	1E-04	0.021	0.005	0.901	0.021	0.004	0.029	0.129	0.898	0.010
9.034	0.913	0.012	-0.001	0.023	0.030	0.913	0.009	-2E-04	0.022	0.009	0.916	0.021	0.003	0.030	0.098	0.913	0.010
9.479	0.936	0.012	0.002	0.025	0.083	0.932	0.009	-0.002	0.024	0.100	0.938	0.023	0.004	0.033	0.128	0.934	0.011
9.927	0.920	0.012	0.006	0.023	0.264	0.911	0.009	-0.003	0.022	0.151	0.909	0.023	-0.006	0.032	0.194	0.914	0.010
10.966	0.339	0.009	0.047	0.136	0.348	0.326	0.003	0.007	0.134	0.051	0.314	0.006	-0.031	0.135	0.230	0.324	0.004
12.058	0.165	0.008	0.036	0.077	0.463	0.159	0.002	-0.004	0.064	0.060	0.157	0.007	-0.016	0.072	0.215	0.160	0.004
12.565	0.240	0.009	0.023	0.050	0.461	0.234	0.002	-0.002	0.035	0.045						0.234	0.002
13.025	0.360	0.009	-0.009	0.041	0.219	0.363	0.003	0.001	0.034	0.040						0.363	0.003
14.165	0.553	0.010	0.009	0.025	0.365	0.546	0.005	-0.003	0.020	0.134						0.548	0.005

Table 54. Relative DoE for SiC at 700 °C.

	LNE					NIST					INRIM						
CWL, µm	Em	U_{Em}	D_i	U_i	E	Em	U_{Em}	D_i	U_i	E	Em	U_{Em}	D_i	U_i	E	ε_{CRV}	$U_{cut\text{-}off}$
1.997																	
2.253																	
2.500																	
3.026																	
3.615	0.830	0.015	0.010	0.024	0.423	0.819	0.008	-0.004	0.020	0.209	0.819	0.020	-0.004	0.028	0.153	0.822	0.012
3.965	0.831	0.015	0.008	0.021	0.386	0.821	0.008	-0.004	0.018	0.215	0.821	0.020	-0.003	0.027	0.111	0.824	0.011
4.530	0.835	0.014	0.008	0.020	0.377	0.825	0.008	-0.004	0.017	0.240	0.827	0.019	-0.002	0.025	0.065	0.829	0.011
5.026	0.838	0.013	0.006	0.020	0.313	0.830	0.008	-0.003	0.017	0.195	0.831	0.019	-0.002	0.026	0.078	0.833	0.010
5.265	0.838	0.013	0.004	0.023	0.169	0.833	0.008	-0.003	0.021	0.125	0.835	0.019	0.000	0.028	0.010	0.835	0.010
6.019	0.833	0.012	-0.010	0.025	0.404	0.844	0.008	0.004	0.023	0.166	0.852	0.021	0.013	0.032	0.399	0.841	0.010
6.395	0.837	0.012	-0.010	0.026	0.399	0.850	0.008	0.005	0.024	0.210	0.853	0.021	0.009	0.033	0.268	0.845	0.010
7.026	0.857	0.012	-0.003	0.027	0.103	0.860	0.008	0.001	0.026	0.026	0.864	0.021	0.006	0.034	0.167	0.860	0.010
7.518	0.874	0.012	0.001	0.028	0.032	0.872	0.008	-0.001	0.028	0.042	0.875	0.021	0.002	0.035	0.061	0.873	0.010
8.040	0.882	0.012	-0.001	0.024	0.062	0.884	0.008	-3E-05	0.023	0.001	0.888	0.021	0.005	0.031	0.153	0.884	0.010
8.479	0.896	0.012	2E-04	0.022	0.010	0.896	0.009	-1E-04	0.020	0.006						0.896	0.009
9.034	0.910	0.012	-3E-04	0.026	0.010	0.910	0.009	4E-04	0.026	0.015	0.909	0.021	-0.001	0.033	0.021	0.910	0.010
9.479	0.927	0.012	-0.002	0.028	0.063	0.928	0.009	-0.001	0.027	0.020	0.936	0.022	0.008	0.034	0.246	0.929	0.010
9.927	0.923	0.012	0.004	0.024	0.158	0.918	0.009	-0.002	0.023	0.095	0.916	0.023	-0.004	0.033	0.115	0.920	0.010
10.966	0.375	0.009	0.040	0.181	0.221	0.364	0.003	0.009	0.180	0.050	0.345	0.007	-0.043	0.180	0.238	0.361	0.005
12.058	0.164	0.008	0.022	0.078	0.277	0.160	0.002	-0.003	0.063	0.052	0.161	0.006	-0.002	0.068	0.024	0.161	0.004
12.565	0.226	0.009	0.007	0.054	0.137	0.224	0.002	-5E-04	0.040	0.012						0.224	0.002
13.025	0.351	0.009	-0.001	0.038	0.034	0.352	0.003	2E-04	0.031	0.006						0.352	0.003
14.165	0.548	0.009	0.010	0.024	0.419	0.540	0.005	-0.003	0.020	0.156						0.542	0.005

Table 55. Relative DoE for SiC at 800 °C.

	NIST					INRIM						
CWL, µm	Em	U_{Em}	D_i	U_i	E	Em	U_{Em}	D_i	U_i	E	ε_{CRV}	$U_{cut\text{-}off}$
1.997	0.815	0.008	1E-04	0.016	0.007	0.814	0.022	-0.001	0.029	0.029	0.815	0.008
2.253												
2.500	0.816	0.008	-0.001	0.016	0.058	0.822	0.021	0.006	0.028	0.228	0.816	0.008
3.026	0.816	0.008	-3E-04	0.016	0.020	0.818	0.020	0.002	0.027	0.074	0.816	0.008
3.615	0.819	0.008	1E-04	0.016	0.008	0.818	0.020	-0.001	0.027	0.030	0.819	0.008
3.965	0.821	0.008	-2E-04	0.016	0.011	0.822	0.020	0.001	0.027	0.039	0.821	0.008
4.530	0.826	0.008	-3E-04	0.016	0.020	0.828	0.019	0.002	0.026	0.069	0.826	0.008
5.026	0.831	0.008	-1E-04	0.016	0.007	0.831	0.019	0.001	0.026	0.023	0.831	0.008
5.265	0.833	0.008	-4E-04	0.017	0.023	0.835	0.019	0.002	0.027	0.083	0.833	0.008
6.019	0.845	0.008	-0.001	0.019	0.061	0.851	0.019	0.006	0.028	0.230	0.846	0.008
6.395	0.850	0.008	-3E-04	0.020	0.016	0.852	0.021	0.002	0.030	0.071	0.850	0.008
7.026	0.859	0.008	-0.001	0.023	0.023	0.863	0.021	0.003	0.032	0.108	0.860	0.008
7.518	0.871	0.008	-3E-04	0.024	0.012	0.873	0.021	0.002	0.033	0.056	0.871	0.008
8.040	0.881	0.008	-5E-04	0.021	0.023	0.884	0.021	0.003	0.030	0.098	0.882	0.008
8.479												
9.034	0.905	0.009	0.001	0.020	0.029	0.902	0.021	-0.003	0.029	0.116	0.905	0.009
9.479	0.922	0.009	-0.001	0.022	0.030	0.927	0.022	0.004	0.030	0.129	0.923	0.009
9.927	0.922	0.009	3E-04	0.017	0.015	0.920	0.024	-0.002	0.030	0.065	0.922	0.009
10.966	0.411	0.004	0.011	0.282	0.040	0.391	0.007	-0.038	0.282	0.134	0.406	0.004
12.058	0.170	0.002	0.002	0.082	0.028	0.165	0.006	-0.027	0.088	0.310	0.169	0.002
12.565												
13.025												
14.165												

Appendix B
CCT-S1 Supplementary Comparison

Spectral Normal Emittance/Emissivity

Technical Protocol

Contents

1. Introduction

Under the Mutual Recognition Arrangement (MRA) [1] the metrology equivalence of national measurement standards will be determined by a set of key comparisons chosen and organized by the Consultative Committees of the CIPM working closely with the Regional Metrology Organizations (RMOs).

In May 2003 the Consultative Committee for Thermometry (CCT), formed a new Working Group 9 (WG-9) for Thermophysical Quantities, which was tasked to determine the need for key comparisons in the field of thermophysical quantities.

At its meeting in June 2005 CCT-WG-9 identified a need for comparisons of three critical quantities: emittance, thermal conductivity, and thermal diffusivity. It was decided to initiate three supplementary comparisons of these quantities as a preliminary step to eventual key comparisons. In particular, a supplementary comparison of spectral normal emittance (emissivity) was initiated, and NPL (United Kingdom) was appointed as the pilot laboratory. The supplementary comparison was accepted by the CIPM and assigned the identifier CCT-S1.

Ten NMIs were contacted by May of 2006, based on the CCT database of NMI measurement capabilities and invited to participate. Five NMIs initially agreed to participate: INRIM, LNE, NIST, NMIJ, and NPL. In December of 2006, NPL, due to internal descisions, had to resign from the comparison. Also, in early 2007, PTB joined as a replacement fifth participant. In May of 2007, NIST was assigned to be the new pilot laboratory.

The procedures outlined in this document cover the technical procedure to be followed during the measurements of the transfer samples. The procedure follows the guidelines established by the BIPM [1].

2 Organization

2.1 Participants

The list of participants was agreed to via email correspondence beginning in May of 2006 through March of 2007.

In accordance with the guidelines established at the CCT, participants must be members of CCT, and have made an independent realisation of their emittance scale.

By their declared intention to participate in this supplementary comparison, the laboratories accept the general instructions and the technical protocols written in this document and commit themselves to follow the procedures strictly.

Once the protocol and list of participants has been agreed to, no change to the protocol or list of participants may be made without prior agreement of all participants.

2.2 Participants' details

NIST	Leonard Hanssen and Boris Wilthan National Institute of Standards and Technology 100 Bureau Drive Gaithersburg, MD 20899-8442 USA	Phone/email: + 1 301 975 2344 hanssen@nist.gov + 1 303 497 3690 boris.wilthan@nist.gov
LNE	Jean-Remy Filtz and Jacques Hameury Laboratoire National de Métrologie et d'Essais Division Thermique et Optique, 29, Avenue Roger Hennequin F-78197 Trappes, FRANCE	Phone/email: +33 1 30 69 10 00 Jean-Remy.Filtz@lne.fr Jacques.Hameury@lne.fr
INRIM	Ferruccio Girard and Mauro Battuello Instituto Nazionale di Ricerca Metrologica Divisione Termodinamica Strada delle Cacce, 91 - 10135 Turin ITALY	Phone/email: +39 011 3919749 f.girard@inrim.it +39 011 3919738 m.battuello@inrim.it
NMIJ	Juntaro Ishii Radiation Thermometry Section National Metrology Institute of Japan AIST-3, 1-1-1, Umezono, Tsukuba Ibaraki 305-8563 JAPAN	Phone/email: +81 29 861 4031 j-ishii@aist.go.jp
PTB	Jörg Hollandt and Christian Monte Physikalisch-Technische Bundesanstalt FB 7.3 Detektorradiometrie und Strahlungsthermometrie Abbestraße 2-12 10587 Berlin GERMANY	Phone/email: +49 30 3481 7369 Joerg.Hollandt@ptb.de +49 30 3481 7246 christian.monte@ptb.de

2.3 Form of comparison

The comparison will be carried out through the measurements of transfer standard artefacts. Each participant will acquire a separate set of 3 artefacts to accommodate the varied measurement instrument requirements, except for PTB. (PTB will obtain 1 of the 3 artefacts for itself only, and the other two artefacts from NMIJ after its measurements are completed. This is because PTB joined the comparison after NPL had already produced the initial sets of two artefacts, and because PTB is able to accommodate the artefacts (size) made for NMIJ.

A full description of the transfer standard samples is given in Section 3 of this protocol.

The comparison will have the following steps:

Step 1. The samples will initially be measured at room temperature by the pilot laboratory.

Step 2. The samples will then be distributed to participants who will perform the measurements at the assigned sample temperatures.

Step 3. The samples will be returned to the pilot laboratory to carry out a repeat measurements at room temperature.

Each laboratory will have 1 year for measurements and transportation. In step 2, the deadline for returning the artefacts will be advised when the samples are shipped to the participants.

Final results must be submitted directly to the pilot laboratory within three months of completion of each round of measurements by each participating laboratory.

If for some reason, the NMI is not ready or customs clearance takes too much time in a country, the participant laboratory must contact the pilot laboratory. Exclusion of a participant's results from the report may occur if the results are not available in time to prepare the draft report.

2.4 Timetable

Activity	**Date**
Invitations to participate	December 2005 and May 2006
Receipt of request to participate	September 2006
Technical protocol sent to participants	February 2007
Technical protocol approved by participants	May 2007
First measurement by Pilot Laboratory (Step 1)	June 2007
Artefacts sent to participants	September 2007
First measurement by participants (Step 2)	November 2007
Artefacts returned to Pilot Laboratory	June 2008
Results of first measurement submitted to Pilot	September 2008
Second measurement by Pilot laboratory (Step 3)	February 2009
Pre-Draft A process starts	May 2010
Draft A comparison report circulated	May 2014
Draft B comparison report submitted to CCT	September 2014

2.5 Handling of the artefacts

During step 2 of Section 2.3 the standard artefacts should be examined immediately upon receipt at final destination. The condition of the artefacts and associated packaging should be examined and if any problems noted, communicated to the pilot laboratory.

The artefacts should only be handled by authorized persons wearing powder-free gloves and stored in such a way as to prevent damage.

Cleaning should not be carried out unless there is clear evidence of contamination. Dust could be removed with a stream of dry gas (avoid cans with liquid propellants). Should further cleaning be required, the laboratory should consult with the pilot laboratory. If cleaning is approved, then

- make a measurement before cleaning
- use their own standard cleaning method, which must be described in their measurement report.
- make a measurement after cleaning
- If an artefact appears damaged it should be returned to the pilot laboratory and a replacement should be requested.

After the measurements of each step of Section 4.3 artefacts should be packaged in their original transit cases for transportation (steps 1, 2, and 3) to the pilot laboratory (or to PTB in the case of NMIJ for BN and OxIn). Ensure that the content of the package is complete and that the container has been properly packed before sealing and shipment.

2.6 Transport of the artefacts

It is of the utmost importance that the artefacts be transported in a manner in which they will not be lost, damaged or handled by unauthorised persons.

Artefacts should be marked as “fragile”.

If required participants may request that the pilot laboratory arrange for a customs carnet to accompany the artefacts. If a carnet is not used, then the artefacts should be accompanied by documentation identifying the items uniquely.

The pilot laboratory covers the costs for transportation to the participant laboratory. Arrangement of the transportation back to the pilot laboratory is each participant laboratory’s responsibility. Each participating laboratory covers the costs for its own measurements, transportation and any customs charges as well as for any damage that may have occurred within its country. The pilot laboratory has limited insurance for any loss of or damage to the artefacts during transportation. If damage occurs in the USA or in transit from the pilot laboratory to the participant then the pilot laboratory will replace the set of artefacts at its own cost.

3 Description of the artefacts

The standard artefact set used by the CCT-S1 participants to check the spectral emittance scale consists of 3 different artefacts: boron nitride (BN) and oxidized Inconel (OxIn) provided by NPL, and silicon carbide (SiC) provided by NIST. The sizes of the artefact sets are as follows:

- NMIJ 45 mm dia. x 2 mm thick
- LNE 25 mm dia. x 10 mm thick
- NIST 18.5 mm dia. x 5 mm thick
- INRIM 16 mm dia. x 2 mm thick
- PTB 45 mm dia. x 2 mm thick

Since the BN and OxIn artefacts were produced prior to the addition of PTB, only a single 45 mm artefact is available and is shared by NMIJ and PTB.

The LNE artefacts have two 1.1 mm dia. x 7 mm deep holes drilled into the side [located orthogonal to each other when viewing the front (to be measured) surface] approximately 2 mm from the top surface and 1.25 mm from the bottom surface, respectively, and the NIST artefacts have a single 0.9 mm dia. x 7 mm deep hole centered on the side, for accommodating thermocouple sensors for temperature monitoring.

All artefacts have been heat treated in air for extended periods of time at temperatures slightly higher than the highest temperatures required for measurement. Previous experience and intervening measurements have indicated the relative stability of the artefacts after the baking process. The sets and heat treatments performed in air, are as follows:

- Boron Nitride 600 °C for 30 hrs
- Oxidized Inconel 980 °C for 30 hrs
- Silicon Carbide 900 °C for 20 hrs

The front side (to be measured) is indicated by markings on the artefact edge.

4 Measurement instructions

4.1 Traceability

Temperature measurements should be made using the International Temperature Scale of 1990 (ITS-90).

4.2 Measurand

The measurand is the spectral normal emittance (emissivity).

The emittance can be obtained through either a relative spectral radiance measurement, or through a spectral reflectance measurement and employing energy conservation and Kirchhof's law,

- over as large a spectral range as feasible with at least a minimum wavelength between 2 μm and 5 μm, and a maximum wavelength between 10 μm and 16 μm,
- at artefact temperatures of as large a subset as feasible of 23 °C, 50 °C, 100 °C, 150 °C, 200 °C, 250 °C, 300 °C, 350 °C, 400 °C, 450 °C, 500 °C, 550 °C, 600 °C, 700 °C, and 800 °C, and
- under either vacuum or "clean air" or other gas purge conditions absent CO2 and H2O vapor.

4.3 Measurement instructions

Before measurement each artefact should be inspected for damage or contamination. Any initial or subsequent damage or cleaning should be documented and communicated to the pilot laboratory.

The artefact emittance must be measured independently several times. The number of measurements should be that normally used by the participating laboratory to obtain the appropriate accuracy of their specific measurement facility. Only the mean or final declared value of each artefact of the set is required to be included in the report to the pilot laboratory.

The measurement of interest in this comparison is the average emittance of each artefact over a circular area of at least several millimeters in diameter centered on the middle of the artefact as determined from the edges of the artefact. Should the participant laboratory observe spatial variation of the emittance, it should incorporate an uncertainty to account for this variability.

The viewing geometry shall be as close as possible to that of a parallel beam with normal angle of viewing (or incidence in the case of a reflectance measurement), taking into consideration the needs for a reasonable signal-to-noise ratio (parallel beam) and avoidance of inter-reflection and background reflection issues (normal incidence). Deviation from these conditions should be reported. Any influence on emittance as described by 4.2 caused such by deviations should be handled as either a correction with an associated uncertainty or solely as an uncertainty, whichever is the participant laboratory's regular practice.

The spectral bandwidth for the measurements should be reported to the pilot laboratory.

No information relating to the comparison, such as measurement results, obtained by a participant during the course of the comparison shall be communicated to any party other than the pilot laboratory. The pilot laboratory will be responsible for disseminating information to other participants and any other release of information. In the latter case the pilot laboratory will seek permission of all the participants before releasing information.

5 Measurement uncertainty

Measurement uncertainty shall be estimated according to the ISO Guide to the Expression of Uncertainty in Measurement [2]. Due to the wide variety of measurement instrumentation used by the participants in this comparison, including 3 distinct spectrometer types, the sources of measurement error and their associated uncertainty components will not be the same. The participant laboratories should provide a list of the major uncertainty components for their measurements along with one or more examples for individual data points.

Due to the large number of individual data points in the spectral measurements, the participant laboratories are only required to provide the final expanded (k=2) uncertainty values along with the emittance for every data point. Reporting the separation of the uncertainty into type A and type B components is also encouraged.

Type A uncertainty components may include the following:

- reproducibility of the measurement result,
- repeatability of the measured result,
- noise of the emittance spectra.

Type B uncertainty components may include the following:

- temperature of the sample, including temperature uniformity and stability w/ time,
- temperature difference (or correction) between sample surface and temperature sensor,
- temperature of reference blackbodies, including absolute temperature, uniformity and stability,
- effective emissivity of reference blackbodies,
- size of source effect,
- correction for reflected background radiation,
- alignment changes between the sample and reference measurements,
- polarisation of the light (for off-normal measurements),
- diffraction effects
- drift of the sources during the measurements,
- wavelegth (or wavenumber) scale
- spectral bandwidth,
- uncertainty components specific to the apparatus used for the measurements, including the spectrometer and detectors used.

5.1 Additional type B uncertainty components for reflectometer measurements may include the following:

- reference sample reflectance,
- variation of reflectometer responsivity (throughput) between sample and reference measurements,
- inter-reflection between sample and detector (or source),
- overfilling of the sample and reference with the input beam due to diffraction and scattering

6 Reporting of results

The final results should be submitted to the pilot laboratory at the latest within three months from completion of measurements in step 2. The results should be submitted in the spreadsheet form, which is distributed to the particpants by the pilot laboratory. The form requires entry of the emittance values and the associated final uncertainty values. The uncertainties should be either the combined standard uncertainty (k=1) or expanded uncertainty (k=2), with an indication of which is used. The emittance spectral data is to be presented in two forms: one at the actual wavelengths as measured, and a second interpolated against a wavelength scale with 0.1 μm increments, for direct comparison purposes.

In completing the description of the participant's measurement facility, descriptions, including schematics of the measurement systems should be provided. Copies of reference publications are acceptable.

Following receipt of all measurement reports from the participating laboratories, the pilot laboratory will follow the procedure outlined in the Guidelines for CCPR Comparison Report Preparation [3].

7 Analysis of Comparison Results

7.1 Introduction

In the Technical Supplement to the Mutual Recognition Arrangement (MRA) [4], key comparisons are identified as the technical basis for the arrangement. One primary goal of this supplementary comparison CCT-S1, is to follow the process of a key comparison as closely as possilbe, including the technical deliverables, which are outlined as:

(a) reference values, known as comparison reference values (CRV) and

(b) the unilateral degree of equivalence (DOE) of each national measurement standard, both its deviation from the CRV and the uncertainty of that deviation at the 95 % level of confidence.

The bilateral degrees of equivalence between pairs of national measurement standards are also defined in the Technical Supplement; it has been determined to be optional however, by some of the CC's including the CCPR and CCT in the key and supplementary comparison reports [5].

As the key comparisons are the technical basis for the MRA, the results reported should be the basis upon which CMCs are validated and subsequently evaluated. For instance, the CCPR Guidelines state that all participants should be able to "check the consistency of their CMCs with the KC results" ([3], §8.1). This means that the comparison should

determine the value of each participant's bias (DOE) and the uncertainty associated with that value in order to give some indication as to whether a participant has adequately estimated the likely magnitude of that bias.

7.2 Data processing by the pilot laboratory

In order to perform a valid comparison between the laboratories' results, several differences between the participants' artefacts and measurement process need to be compensated for. These are: 1) non-uniformity of the artefact spectral emittance of a single type (seen by the pilot laboratory in preparation for the comparison); 2) anticipated potential drift in the artefact emittance values due to oxidation or effects of heating the artefacts to elevated temperatures; 3) differences in the spectral resolution between the participants; 4) potential differences in the spectral spacing of the actual data as will be measured. Both 3) and 4) are related to the participants' measurement instrumentation and methods.

The average spectral emittance of the artefacts for each material is determined at room temperature by the pilot laboratory. Corrections for the deviations from the average are to be applied to all of the results from the participants. An uncertainty component for these measurements at temperatures above room temperature is also generated.

The main difference in spectral resolution is between the filter-based measurements of LNE and the Fourier-transform-interferometer- and monochromator-based measurements of the other NMIs. Hence, the spectral data of NMIJ, NIST and PTB will be converted into equivalent filter-resolved data using filter transmittance spectra provided by LNE.

Detailed descriptions of all data processing by the pilot laboratory will be provided in the comparison report.

7.3 Data analysis

After processing to make the participant's results directly comparable, we will employ weighted mean averaging with cut-off to obtain a nominal comparison reference value (CRV) for each LNE nominal filter wavelength and temperature. In the weighted mean calculation, each participant's values are weighted by their quoted standard uncertainties up to a cut-off point, which is given by the average of the standard uncertainties below the median of all the standard uncertainties [6].

The individual participant's results will then be compared to the CRVs. The relative deviations and their uncertainties are the unilateral relative Degrees of Equivalence (DoE). The difference between the unilateral relative DoE values of two participants will be the bilateral relative DoE. To determine whether any of the results can be considered outliers, the error function will be calculated and presented.

References

[1] MRA, Mutual Recognition Arrangement, BIPM, 1999. T.J. Quinn, "Guidelines for CIPM key comparisons" BIPM, Paris, (1999, modified 2003).

[2] BIPM IEC IFCC ILAC ISO IUPAC IUPAP and OIML 2008 *Guide to the Expression of Uncertainty in Measurement* (Geneva: International Organization for Standardization) available at http://www.bipm.org/utils/common/documents/jcgm/JCGM_100_2008_E.pdf.

[3] Consultative Committee on Photometry and Radiometry Key Comparison Working Group, Guidelines for CCPR Comparison Report Preparation, 2009 available at http://www.bipm.org/utils/common/pdf/Guidelines_for_CCPR_KC_Reports.pdf.

[4] International Committee for Weights and Measures, 2003, Mutual Recognition of National Measurement Standards and of Calibration and Measurement Certificates Issued by National Measurement Institutes (Paris: Comité International des Poids et Mesures), available at http://www.bipm.org/utils/en/pdf/mra_2003.pdf .

[5] CCPR 2009 *20th CCPR Meeting, Draft Report* Decision D8.

[6] CCPR-G2 Rev.3, 2013 *Guidelines for CCPR Key Comparison Report Preparation.*